A Study of Tensile and Microhardness Properties of m-LLDPE/LDPE Blends

By

MOHAMMAD FAHEEM

A Thesis presented to the

DEANSHIP OF GRADUATE STUDIES

In Partial Fulfillment of the Requirements
for the degree

MASTER OF SCIENCE

IN

MECHANICAL ENGINEERING

KING FAHD UNIVERSITY
OF PETROLEUM AND MINERALS

Dhahran, Saudi Arabia

June 2003

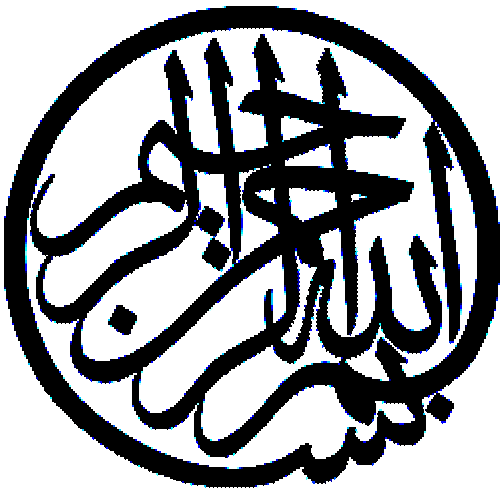

In the Name of Allah, Most Gracious, Most Merciful.

KING FAHD UNIVERSITY OF PETROLEUM AND MINERALS
DHAHRAN 31261, SAUDI ARABIA

DEANSHIP OF GRADUATE STUDIES

This thesis, written by **MOHAMMAD FAHEEM** under the direction of his Thesis Advisor and approved by his Thesis Committee, has been presented to and accepted by the Dean of Graduate Studies, in partial fulfillment of the requirements for the degree of **MASTER OF SCIENCE IN MECHANICAL ENGINEERING.**

Thesis Committee

_____
Dr. Khaled Mezghani (Advisor)

_____
Dr. Nesar Merah (Member)

_____
Dr. Ibnelwaleed A Hussein (Member)

_____
Dr.Faleh Al-.Sulaiman
Department Chairman

_____
Prof. Osama A. Jannadi
Dean of Graduate Studies

_____
Date

Dedicated to My Beloved Parents and Family Members
whose constant prayers, sacrifice and inspiration led to this
wonderful accomplishment

ACKNOWLEDGEMENTS

All praises and thanks are due to Allah (subhana wa taala) for bestowing me with health, knowledge and patience to complete this work. Thereafter, acknowledgement is due to KFUPM for the support given to this research through its tremendous facilities and for granting me the opportunity to pursue graduate studies with financial support.

I acknowledge, with deep gratitude and appreciation, the inspiration, encouragement, valuable time and guidance given to me by my Committee Chairman, Dr. Khaled Mezghani.

I am grateful to my Committee members, Dr. Nesar Merah and Dr. Ibnelwaleed A Hussein for their constructive guidance and technical support. I also acknowledge the sincere and untiring efforts of Engr. Mr. Latif Hashmi in preparing the experimental program and set-ups utilized in this study. Thanks are also due to the laboratory personnel, Mr. Othman Al-Thubaiti, Mr.Saleh and Mr.Zain who assisted me in the experimental work and the Department secretaries, Mr. Lateef and Mr.Jameel for their help and assistance.

Special thanks are due to my senior colleagues at the University, Mujtaba Hussain, Salman A Gaffar, Abdul Baseer, Mohammad Ahsan, Ahmed Jamal, Ghulam Arshed, Abdus Samad and Irfan S Hussaini who were always there to help me in my work. I would also like to thank my friends Aurifullah Vantala, Syed Imran, Sohail Anwar, Hameed Tayyab, Aurifusalam, Abdullah, Ali, Anwar, Omar Farooq, Fasi, Zahed, Ameer, Hameeduddin, Jalal Shah, Majid, Abbas, Mujahid, Bilal, Hassan and all others who provided wonderful company and good memories that will last a life time.

Finally, thanks are due to my dearest mother, late father, and all my family members for their emotional and moral support throughout my academic career and also for their love, patience, encouragement and prayers.

TABLE OF CONTENTS

LIST OF TABLES

LIST OF FIGURES

THESIS ABSTRACT

NAME: **MOHAMMAD FAHEEM**

TITLE: **A STUDY OF TENSILE AND MICROHARDNESS PROPERTIES OF m-LLDPE/LDPE BLENDS**

DEPARTMENT: **MECHANICAL ENGINEERING**

DATE: **4 JUNE, 2003**

Polyethylene (PE) is the largest produced thermoplastic polymer and is highly used in packaging applications. There exist different types of PE polymers depending on the molecular architecture. The most common types are: Low-Density Polyethylene (LDPE); Linear Low-Density Polyethylene (LLDPE); and High-Density Polyethylene (HDPE). LDPE is produced from free-radical polymerization of ethylene, and it has broad molecular distribution and good processability but lower mechanical properties. LLDPE is produced from co-polymerization of ethylene and α-olefin (butene, hexene or octene) using metallocene catalyst, and it possesses better mechanical properties but lower processability. Usually, for a packaging application, LLDPE is favored for its mechanical properties; however, its processability is a disadvantage. An approach to over come this problem is to blend LLDPE with LDPE.

The main objective of this study is to investigate the influence of branch type (butene, hexene and octene) of LLDPE on the mechanical properties of its blends with LDPE. Three blend systems: B-type (B-LLDPE/LDPE), H-type (H-LLDPE/LDPE) and O-type (O-LLDPE/LDPE) were studied for tensile and microhardness. The results show that an addition of small amount (10%) of LDPE to LLDPE polymers produced a negligible effect on modulus of elasticity, yield and tensile strengths, and ductility of the blends. Whereas, the effect of the addition of small amount of LLDPE to LDPE depends on the type of blends and varies from one mechanical property to another. The correlation of Vickers hardness numbers with yield strength values was found to follow Tabor's relationship for most of the blend systems. The mechanical properties and the microhardness results are well correlated with the amount of crystallinity in the studied samples.

MASTER OF SCIENCE DEGREE

KING FAHD UNIVERSITY OF PETROLEUM AND MINERALS

Dhahran, Saudi Arabia

رسالة الماجستير

الاسم : محمد فهيم

العنوان: دراسة خواص مقاومة الشد و القساوة المصغرة للخلائط m-LLDPE/LDPE

قسم : الهندسة الميكانيكية

التاريخ: 4-جوليو-2003

بولي اتيلين هوالبوليمر الاكثر انتاجا في العالم و اكثر استخداماته هي في عملية التغليف.يوجد انواع مختلفة من البولي اتيلين وذلك بحسب التركيب الكيميائي .والانواع الاكثر استخداما هي :البولي اتيلين المنخفض الكثافة (LDPE), البولي اتيلين المنخفض الكثافة الخطي(LLDPE) و البولي اتيلين ذو الكثافة العالية (HDPE) . LDPE ينتج من عملية البلمرة الراديكالية الحرة للاتيلين وهذه العملية تتميز بتوزيع ذري واسع ,وتصنيع سهل, لكن خصائصه الميكانيكية ضعيفة .LLDPE ينتج من عملية البلمرة الراديكالية الحرة للاتيلين و الفا- اولفين(بيوتين ,هيكسين ,او الاوكتين) ياستخدام المتلوسين كمحفز,و لل LLDPE خواص ميكانيكية افضل لكن عملية تصنيعه اصعب .يالعادة يشتخدم LLDPE ,لطتبيقات التغليف رغم صعوبة تصنيعه .وكطريقة للتغلب على هذه السيئة هي خلط LLDPE مع LDPE.الهدف الرئيسي من هذه الدراسة هو بحث تاثير انواع LLDPE (بيوتين ,هيكسين و الاوكتين) على الخواص الميكانيكية لخلائطه مع LDPE .

وقد درست خواص مقاومة الشد و القساوة المصغرة ثلاث خلائط:النوع B (B-LLDPE/LDPE), النوع H- H) (LLDPE/LDPE, النوع O (O-LLDPE/LDPE), والنتيجة اظهرت ان في حال اضافة كمية صغيرة (10%) من LDPE الى LLDPE هذا سينتج تاثير قليل جدا على معامل اللدونة ,والمطاوعة و مقاومة الشد وقابلية السحب للخلائط .بينما عند اضافة LLDPE الىLDPE فان النتيجة ستتعلق بنوع الخلائط المستخدمة وتتغير الخواص الميكانيكية من خلطة الى اخرى .وقد وجد ان العلاقة بين رقم قساوة فيكرز و قيم اجهاد الخضوع تتبع علاقة تابور لمعظم الخلائط . نتائج خواص مقاومة الشد و القساوة المصغرة تتعلق بشكل كبير بمدى البللورة في العينة المدروسة .

هذه الدراسة اعدت لنيل درجة الماجستير في العلوم
في جامعة الملك فهد للبترول والمعادن
الظهران 31261
المملكة العربية السعودية

CHAPTER 1

INTRODUCTION

1.1 BACKGROUND

A polymer is a long molecule, which contains a chain of atoms held together by covalent bonds. It is produced through a process known as polymerization whereby monomer molecules react together chemically to form either linear chains or a three dimensional network of polymer chains. If one type of monomer is employed to form the polymer the resulting molecule is called a homopolymer. A copolymer is obtained by using different types of monomer species.

Polymers can be separated into three groups; thermoplastics, rubbers and thermosets. In addition, thermoplastics are separated into crystalline and amorphous polymers. The ability of polymers to crystallize depends upon many factors such as the degree of branching and the regularity of molecules. However, crystalline thermoplastics are in general only semi-crystalline and do not crystallize completely when cooled from the melt. Thermosets are heavily cross-linked polymers, which are normally rigid and intractable. They consist of a dense three-dimensional molecular network and, like rubbers, degrade rather than melt on the application of heat.

On the basis of structure of molecular chains, polymer structures can be classified under three categories; linear, branched or cross-linked polymers. Linear polymers are those in which the mer units are joined together end to end in single chains. In branched polymers, the side-branch chains are connected to the backbone of the polymer chain. The chain packing efficiency is reduced with the formation of side chain branches, which results in a lowering of polymer density. In cross-linked polymers, adjacent linear chains are joined to each other at various positions by covalent bonds. The process of cross-linking is achieved either during synthesis or by a non- reversible chemical reaction that is usually carried out at an elevated temperature. Polyethylene (PE) is the largest produced thermoplastic polymer in the world. Ethylene may be polymerized by a number of processes to produce different varieties of polyethylene. Packaging applications, which require several performance criteria, dominate the utilization of polyethylene film. In its simplest form a polyethylene molecule consists of a long backbone of an even number of covalently linked carbon atoms with a pair of hydrogen atoms attached to each carbon; chain ends are terminated by methyl groups. This structure is shown schematically in Figure 1.1. Chemically pure polyethylene resins consist of alkanes with the formula C2nH4n+2, where ‘n’ is the degree of polymerization, i.e. the number of ethylene monomers polymerized to form the chain. While the basic structure of polyethylene molecules, i.e. the repeat unit, is the same in all molecules, they can be assembled differently; for example, branches can be present in the main chain (called backbone). There may be short-branches (SCB) (2-6 carbons) or long branches (LCB) (more than 8 carbons) depending on the polymerization process and conditions (e.g. temperature and pressure). Depending on the branch type and content, different types of polyethylenes

are available: (i) low-density polyethylene (LDPE); (ii) high-density polyethylene (HDPE); (iii) linear low-density polyethylene (LLDPE). Also, ultra high-molecular weight polyethylene (UHMWPE) exists for special applications.

The first commercial ethylene polymer (1939) was low-density, low-crystalline (branched) polyethylene (LDPE), which is the largest of the thermoplastics produced in the world. LDPE is produced by free radical bulk polymerization using traces of oxygen or peroxide (benzoyl or diethyl) and sometimes hydroperoxide and azo compounds as the initiator. This results in the production of branched polymer molecules. LDPE is a partially crystalline solid with melting temperature range of 100 to 120˚C, densities around 0.910-0.935 g/cm^3 with crystallinities of 40-60 %. Branches act as defects, and as such the level of side chain branching determines the degree of crystallinity, which in turn affects polymer properties [2-7]. The number of branches in LDPE may be as high as 20 per 1000 carbon atoms. The first and predominant type of branching, which arises from intermolecular chain transfer, consists of ethyl short-chain alkyl groups such as ethyl or butyl. The second type of chain branching is produced by intermolecular chain transfer. This leads to long chain branches that, on the average, may be as long as the main chain. The physical properties of LDPE depend on three structural factors. These are the degree of crystallinity (density), molecular weight (MW), and the molecular weight distribution (MWD). The degree of crystallinity and therefore, density of polyethylene is dictated primarily by the amount of short-chain branching. In the solid state, branches and other defects in the regular chain structure limit the crystallinity level. As the packing of crystalline regions is better than that of noncrystalline regions, the overall density of a polyethylene resin will increase as the degree of crystallinity rises.

Generally, the higher the concentration of branches, the lower the density of the solid. The principal classes of polyethylene are illustrated schematically in Figure 1.2.

The weight average molecular weight (Mw) of LDPE is typically in the range of 6000 to 40000 g/mol. Polyethylene with limited branching, that is, linear or high-density polyethylene (HDPE), can be produced by the polymerization of ethylene with supported metal-oxide catalysts or in the presence of co-ordination catalysts. They are highly crystalline, with a melting point over 127˚C (usually about 135˚C), densities in the 0.94-0.97 range and crystallinity about 70-90%. The third and most recently discovered PEs is the linear low-density polyethylene (LLDPE). It is produced by co-polymerizing ethylene with α-olefin such as 1-octene, 1-hexene or 1-butene. They can have wide range of branch contents depending on the incorporation of the comonomer. Typical densities range from as high as 0.90 g/cm^3 to 0.94 g/cm^3. LLDPE was first produced by Ziegler-Natta type of catalysts. However this produced LLDPEs with broad molecular weight distribution and a non-uniform distribution of branches along the backbone chain on account of multi-site nature of the catalyst. Recently, metallocene LLDPE (m-LLDPE) were developed. The single site nature of metallocene catalysts allows scientists to design polymers with narrow molecular weight distributions and uniform branches. While the metallocene polymers give better physical and mechanical properties than their Ziegler-Natta counterparts with the same average molecular weights, they often have poor processibilities due to high viscosities. Applications of metallocene linear low-density polyethylene are in coatings, tie layers, and seal layers in multiplayer film packaging.

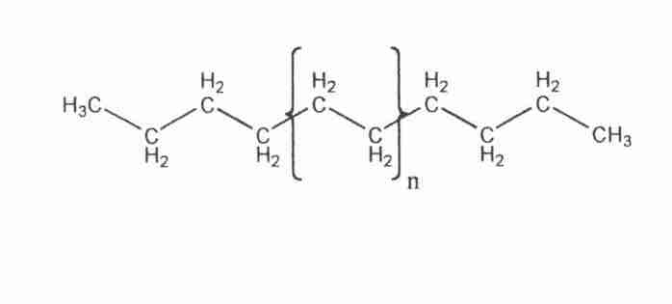

Figure 1.1: Chemical Structure of pure polyethylene [1]

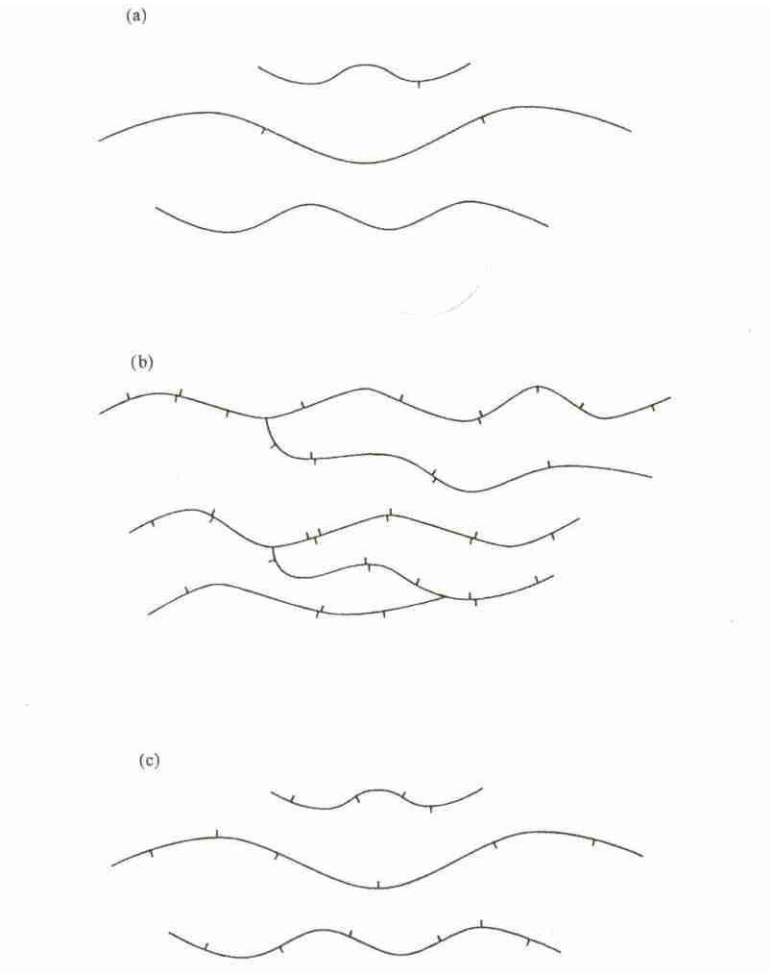

Figure 1.2: Schematic representations of different classes of polyethylene. (a) High-density polyethylene (b) Low-density polyethylene (c) Linear low-density polyethylene [1]

PE is a semi-crystalline polymer whose properties are greatly influenced by its crystallinity and relative amounts of amorphous phases. When grown from melts, polyethylene molecules crystallize as lamellae where there will be some folding of the molecules to allow re-entry into the crystallite but some molecules will link or 'tie' separate lamellae across amorphous regions which is shown schematically in the Figures 1.3 and 1.4.

The crystalline morphology consists of chain-folded lamellae (Figure 1.5) joined in supermolecular structures called spherulites (Figure 1.6). In the case of semi-crystalline polymers, regular crystalline units are linked by unoriented, random-conformation of chains that constitute amorphous regions (Figure 1.7). The crystalline regions are usually denser (about 10%) and harder than the amorphous polymer. Schematic representation of the phases present in the solid polyethylene is clearly illustrated in Figure 1.8. The presence of crystalline structure has a significant influence on the physical, thermal and mechanical properties of polymer. The amorphous part provides the flexibility and high impact strength.

1.2 POLYETHYLENE BLENDS

Polymer blends are of interest for generating mechanical properties that cannot be obtained from single component materials. This field is driven commercially by the demand for ever-increasing physical, mechanical, thermal and other properties. Faced with this situation, there are two general responses. The first would be to synthesize a new polymer to meet the desired specifications. This approach has two major drawbacks.

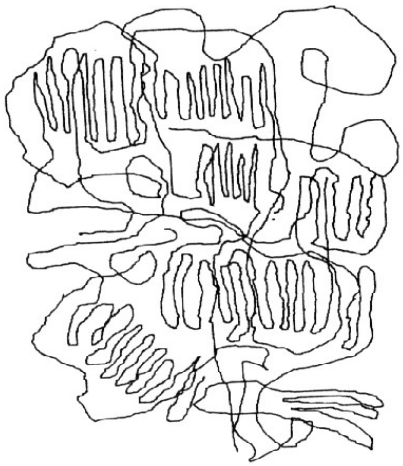

Figure 1.3: Schematic illustration of a semi-crystalline structure showing lamellae linked by ‘tie’ molecules through amorphous regions [2]

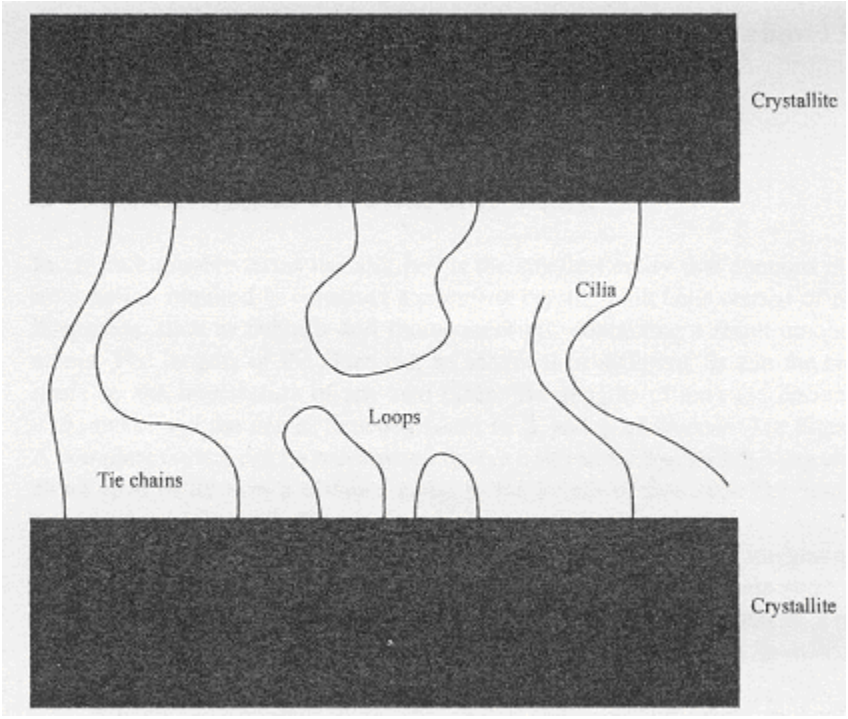

Figure 1.4: Tie chains and loops in the non-crystalline phases of polyethylene [1]

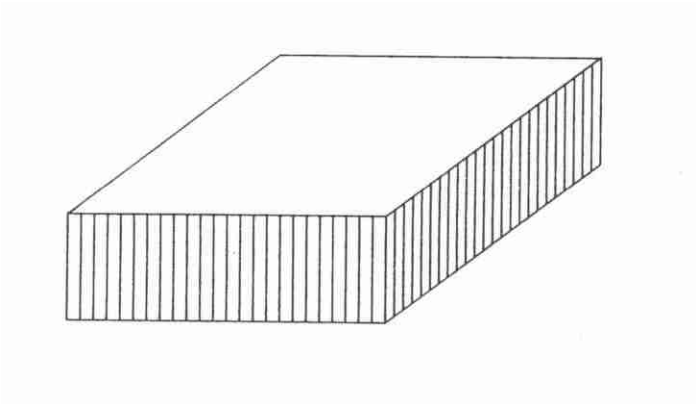

Figure 1.5: Idealized representation of a polyethylene lamella [1]

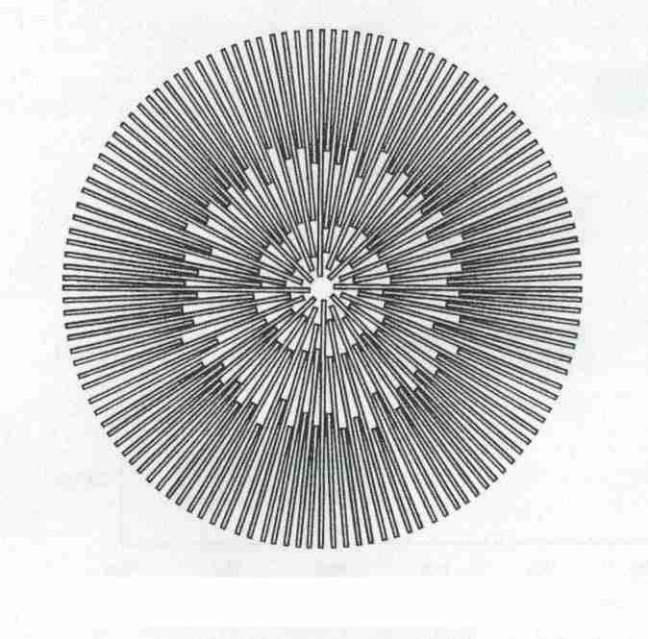

Figure 1.6: Schematic representation of a spherulite [1]

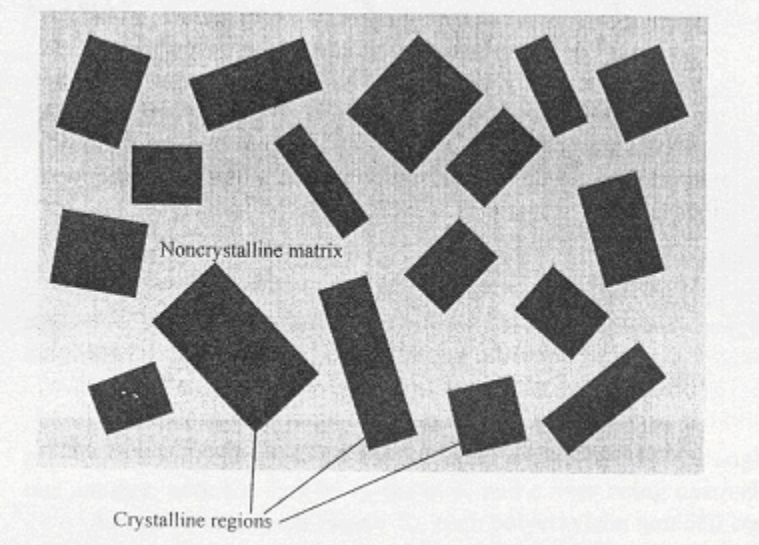

Figure 1.7: Generic illustration of semi crystalline morphology [1]

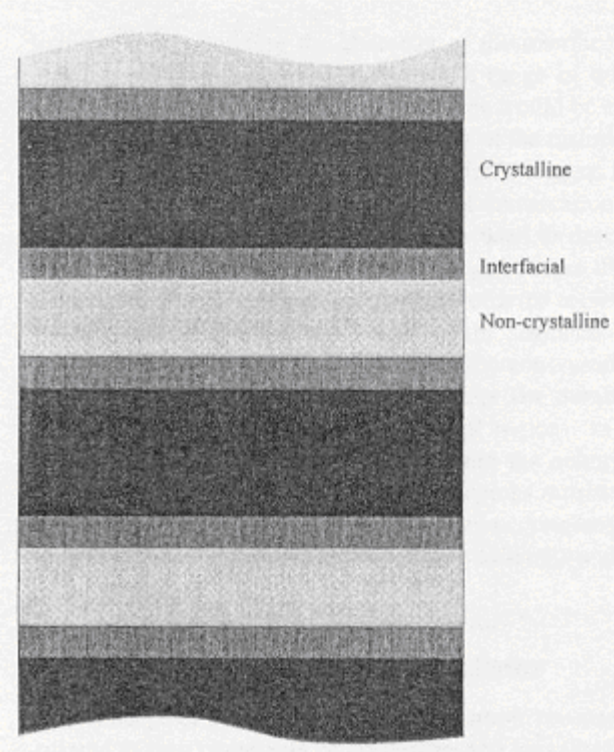

Figure 1.8: Schematic representations of the phases present in solid polyethylene [1]

Firstly, polymer science has yet to reach the state of maturity that allows the design and synthesis of materials with prescribed properties. The other problem is that the cost of developing and manufacturing a new polymer from scratch is very high. The second approach, which is less expensive, is to blend polymers, usually not more than two, which provide the desired properties.

Polymer blends can be miscible, immiscible or partially miscible. The term compatible is used to describe polymer blends that have useful practical properties, regardless of whether they are miscible or immiscible whereas the term miscible is used to describe polymer blends that have thermodynamic miscibility down to the segmental level. For the components to be miscible, a necessary, but not sufficient condition is that Gibbs free energy of mixing, ΔG_{mix} in the following equation must be negative.

$$\Delta G_{mix} = \Delta H_{mix} - T \Delta S_{mix} \tag{1.1}$$

For polymers, enthalpy of the mixing, ΔH_{mix} is generally positive. The pair of polymers is immiscible as the positive ΔH_{mix} term usually dominates the entropy of mixing, $T\Delta S_{mix}$ term.

1.3 CRYSTALLINITY DETERMINATION

The three most popular methods for determining crystallinity are by density measurements, thermal analysis, and X-ray methods. The different techniques do not give necessarily the same value for the crystallinity since all three depend on different

properties of the pure crystalline polymer and these are often difficult to determine exactly because of the difficulty in obtaining fully crystalline material.

1.3.1 Density measurements

The density of a semi-crystalline polymer will be between that of a fully crystalline and amorphous sample. The basis of the density measurement is therefore to measure the density of sample of interest and compare that with the published densities of fully crystalline and amorphous samples. Defining 'ρ' as the measured density 'ρ_a' as the fully amorphous density and 'ρ_c' as the fully crystalline density leads to an expression for W_c the weight fraction degree of crystallinity [2]

$$W_c = \frac{\frac{1}{\rho} - \frac{1}{\rho_a}}{\frac{1}{\rho_c} - \frac{1}{\rho_a}} = \frac{\rho_c\,(\rho - \rho_a)}{\rho\,(\rho_c - \rho_a)} \tag{1.2}$$

1.3.2 Thermal methods

The thermal method depends on measurements of the heat of fusion ΔH of the polymer of interest and a comparison of this value with the fully crystalline heat of fusion ΔH_C. The weight fraction crystallinity W_c [2] is then given by

$$W_c = \frac{\Delta H}{\Delta H_c} \tag{1.3}$$

The heat of fusion is measured directly from a differential scanning calorimetry (DSC), which involves heating a sample at a constant heat rate in the range of 5-

20°C/min and integrating under the heat flow rate against temperature curve to obtain the heat of fusion.

1.3.3 X-ray methods

A crystalline sample will produce a sharp pattern with sharp well-defined peaks and an amorphous sample broad diffraction 'halos' centered on the most probable atomic spacings. The measured pattern is decomposed into amorphous and crystalline components by comparison with a diffraction pattern taken from a fully amorphous sample. The fractional crystallinity may be estimated from the expression

$$W_c = \frac{I_{total} - I_A}{I_{total}} \tag{1.4}$$

Where 'W_c' is the fractional crystallinity and 'I_A' the fully amorphous intensity, and 'I_{total}' is the measured sample intensity [2].

1.3.4 Other methods

Infra-red (IR) and Raman Spectroscopy can be adapted to determine crystallinity. Nuclear Magnetic Spectroscopy (NMR) can in principle be used to measure crystallinity but is rarely used.

1.4 THERMAL PROPERTIES

Semicrystalline polymers in general differ from most crystalline solids in that they display a melting range rather than a discrete melting point. The melting range is a consequence of the inevitable distribution of lamellar thickness in the solid state.

1.4.1 Melting Range

Polyethylene undergoes a transition from the semicrystalline to the molten state that takes place over a temperature range that can span from less than 10°C up to 70°C. As it passes through this transition the semicrystalline morphology gradually takes on more of the characteristics of the amorphous state at the expense of the crystalline regions. The melting range is broad because it consists of a series of overlapping melting points that correspond to the melting of lamellae of various thicknesses. A dispersion of lamellar thicknesses is a natural consequence of entanglements and chain branching that divides chain backbones into a series of discrete crystallizable sequences with a distribution of lengths. The broadest melting ranges occur in branched samples crystallized during rapid cooling.

The melting characteristics of polymers are commonly investigated by means of differential Scanning Caloriemetry (DSC). DSC provides a trace, called a thermogram that consists of the instantaneous heat capacity of a specimen plotted as a function of temperature. The greater the volume of crystallites that melt at a given temperature, the higher the sample's instantaneous heat capacity. There is an approximately inverse relationship between the position of the peak maximum and the overall breadth of the melting peak. Samples with lower molecular weights, lower levels of branching, and slower crystallization rates tend to have narrower melting distributions and elevated peak melting temperatures. The normalized area under the peak, which is a measure of degree of crystallinity, can be approximately correlated with the temperature of the peak maximum and the sharpness of the melting range.

1.4.2 Heat of Fusion

The heat of fusion (ΔH_f) of a sample is a measure of the amount of heat that must be introduced to convert its crystalline fraction to the disordered state. It is thus uniquely dependent upon the degree of crystallinity of the sample and the theoretical heat of fusion of a 100% crystalline sample. The heat of fusion (ΔH) of 100% crystalline polyethylene sample has been calculated to be 293.6 J/g.

$$\% \, Crystallinity = \frac{\Delta H_f}{\Delta H} \times 100 \tag{1.5}$$

The factors that determine the actual degree of ordering realized, and hence the heat of fusion, are principally the rate of crystallization and the degree of orientation. The slower the crystallization process or the higher the degree of orientation, the greater will be the heat of fusion.

1.5 MECHANICAL PROPERTIES

The mechanical properties of a polyethylene specimen can be defined as those attributes that involve the physical rearrangement of its component molecules or distortion of its initial morphology in response to an applied force. The nature of a specimen's response to applied stress can be correlated with its morphological and molecular characteristics; it is these relationships that are emphasized in this work. The mechanical properties of a specimen are controlled by its processing history within the limits imposed by its molecular characteristics. The typical mode of polyethylene

deformation is one of yielding and necking followed by strain hardening. Localized yielding is especially noticeable in samples with higher degrees of crystallinity.

The mechanical properties of polyethylene may be divided into two broad categories :(1) low strain properties such as yield stress and initial modulus and (2) high strain properties, typified by ultimate tensile strength and strain at break. To a first approximation, the low strain properties are controlled by sample's morphological features and the high strain properties by its molecular characteristics.

1.5.1 Tensile Properties

Tensile properties of polymers are measured on instruments that record the force required to elongate a sample as a function of applied elongation. It is common to plot the load as "engineering stress", that is, the force per unit area based upon the original cross-section of the specimen as a function versus the engineering strain calculated as the elongation divided by original gauge length. The polymer chain length and its distribution are important molecular parameters in controlling the physical, mechanical and processing characteristics of polymers. Tensile testing of the specimen is carried out following the ASTM D 638 standard. Stress and strain are sample dependent. The stress on any element of the sample is equal to the force experienced by the element divided by its effective cross-sectional area. If the cross-sectional area of the specimen varies along its length, the stress will vary accordingly, i.e., stress is not necessarily uniform along the length or across the width of the specimen.

The strain and percent strain for any portion of a specimen are defined as

$$\text{Strain} = \frac{\text{current sample dimension - original dimension}}{\text{original dimension}} \tag{1.6}$$

$$\text{Percent strain} = \frac{\text{current sample dimension - original dimension}}{\text{original dimension}} \times 100 \tag{1.7}$$

Most tensile samples start off as a "dogbone" (or dumbbell), the enlarged regions of which are gripped by the jaws of the tensile tester. Initially the gauge region elongates homogenously until it reaches a point at which one cross-sectional slice yields independently of the rest of the specimen. The onset of heterogeneous elongation corresponds to the yield point. As elongation continues, the incipient neck becomes better established until it forms a sharply defined region. Upon further elongation the neck propagates, growing to encompass the entire gauge length. The force required for neck propagation is essentially invariant, resulting in a "plateau" in the force versus elongation curve. Subsequent deformation, termed "strain hardening", is homogenous, with the necked region elongating uniformly until the sample breaks.

Depending on molecular weight (Mw) and its distribution (MWD), polyethylene can exist under a variety of formulations, each one with tailored properties for specific applications. The influence of Mw on mechanical properties is clearly depicted in the Figure 1.9 [3]. It is also important to note that some polymers may have different failure modes for different modes of deformation. In general all polymers at temperatures significantly below their glass transition temperatures (T_g –T >100°C) undergo brittle fracture. In the region above the brittle fracture regime, but below T_g polymers usually yield and undergo plastic deformation as the modulus decreases. This is illustrated in the bump that occurs in the stress-strain curves as shown in the Figure 1.10 [2].

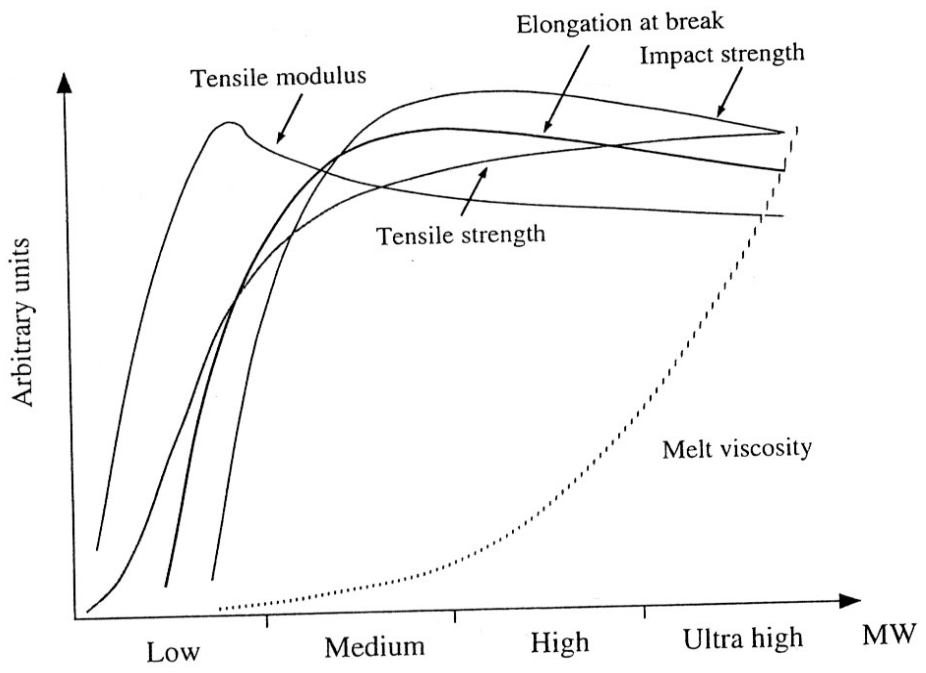

Figure 1.9: Effect of molecular weight on the mechanical properties of polymers [3]

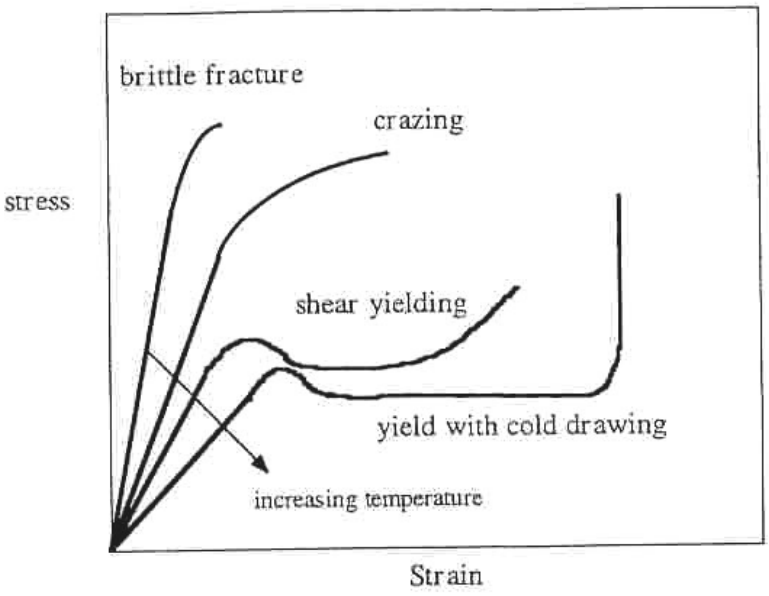

Figure 1.10: Schematic of some failure modes of glassy polymers [2]

1.5.2 Elastic Modulus

When a polyethylene sample is subjected to external stress there is an initial deformation prior to yield that is homogenous and is largely recoverable when the stress is removed. The value of elastic modulus is normally derived from the initial slope of the stress versus strain plot. The elastic modulus of a sample is a measure of its rigidity; the higher the modulus, the stiffer the sample. The two most commonly used units are pounds per square inch (psi) and megapascals (MPa). For the majority of isotropic samples, the increase of elastic modulus is approximately linear with the degree of crystallinity.

1.5.3 Yield Phenomena

Yielding occurs in a polyethylene specimen when it ceases to deform homogenously and starts to deform heterogeneously. Up to the yield point, deformation is principally elastic, whereas afterwards the sample takes on a permanent set. The nature of yield point varies greatly with the type of polyethylene examined and the conditions under which it was crystallized. In linear low density and low-density polyethylene samples, two distinct maxima may occur in close succession. In other cases an inflection may be followed by a diffuse maximum. The mechanisms associated with multiple yield peaks are the subject of speculation but may correspond to the yielding of bimodal distributions of lamellar populations.

The sharpness of the yield peak exhibited during stress versus strain measurements reflects the distinctness of the neck observed visually. Samples with very low levels of crystallinity exhibit neither localized necking nor a distinct yield peak. For isotropic samples the yield stress at room temperature is closely correlated with the degree of crystallinity and thus with the sample density. The yield stress of a specimen is of great interest from a practical point of view. In many cases it represents the maximum permissible load that a sample can withstand while still performing its assigned role. Once a sample has yielded, its dimensions are irrevocably changed, and it may no longer meet the requirements for continued service. In cases, where there is a distinct yield maximum in the stress versus strain curve, the force required to propagate a neck along the length of a sample is lower than the yield stress. Once such a sample has yielded, it will continue to elongate unless the applied load is removed.

1.5.4 Ultimate Tensile Stress

The ultimate tensile stress also known as the “tensile strength” of a sample is the force required to break it divided by its original cross-sectional area. The values of ultimate strength of low-density polyethylene samples are generally lower than that of linear low-density polyethylene samples largely because of the higher percent elongation values obtained for the linear low-density polyethylene samples. Actually, this is the property that gives LLDPE an advantage over LDPE in blown film packaging application.

1.5.5 Strain at break

This term refers to the strain of the sample at the point of tensile failure. The strain at break of the polyethylene sample is a function of its molecular nature and its initial orientation. The molecular characteristics that facilitate drawing are similar to those that promote the development of high degrees of crystallinity. Features that hinder the slippage of chains past one another during crystallization also inhibit the drawing process. The two principal inhibitors to chain movement are entanglements and branch points. Thus high molecular weight linear polyethylene resins and branched samples have lower strain at break values than low molecular weight unbranched samples. For ductile samples at a given molecular weight, the strains at break values fall as their comonomer content increases. Similarly, for a given comonomer content, the strain at break of ductile samples falls as the molecular weight increases. The molecular weight corresponding to the transition between brittle and ductile behavior increases as the comonomer content increases.

1.6 MICROHARDNESS

Hardness is defined as the resistance of a material against local surface deformation and it is usually computed as the ratio of indentation load to the projected area of contact between the indenter and the material in the plane of the deforming surface. The deformation caused by the indenter involves rearrangement of the initial morphology and hence depends on structural parameters similar to those involved in the short-range tensile deformation of polyethylene. The microhardness of a sample is thus strongly

correlated with its tensile yield stress and elastic modulus and hence its degree of crystallinity.

1.6.1 Correlation between microhardness and other physical and mechanical properties

As in the case of metals, it has been shown that for polymers the microhardness (H) is linearly related to the plastic stress (σ_o) with the ratio of H/σ_o approaching 3 for crystalline polymers. Figure 1.11 shows data for the microhardness as a function of the yield stress of polyethylene. The plot inset shows the variation of the ratio H/σ_o with the degree of crystallinity. The non-crystalline part in the polymer plays a major role in providing the elastic response of the material. A power law relation of the form given below can relate the elastic modulus of polymers to the microhardness.

$$H = a\, E^b \tag{1.8}$$

Where 'a' and 'b' are constants and 'E' is the elastic modulus.

The microhardness of the polymers has also been related to the microstructural parameters. The main factor that determines the hardness of polymers is the distribution and the amount of crystalline and amorphous phases present in the polymer. The rule of mixtures may be used to describe the microhardness of polymer with crystalline and amorphous phases present. According to this rule,

$$H = H_c \beta + H_a (1 - \beta) \tag{1.9}$$

Where H_c and H_a are the hardnesses of the crystalline and the amorphous phases respectively and β is the volume fraction of the crystalline phase.

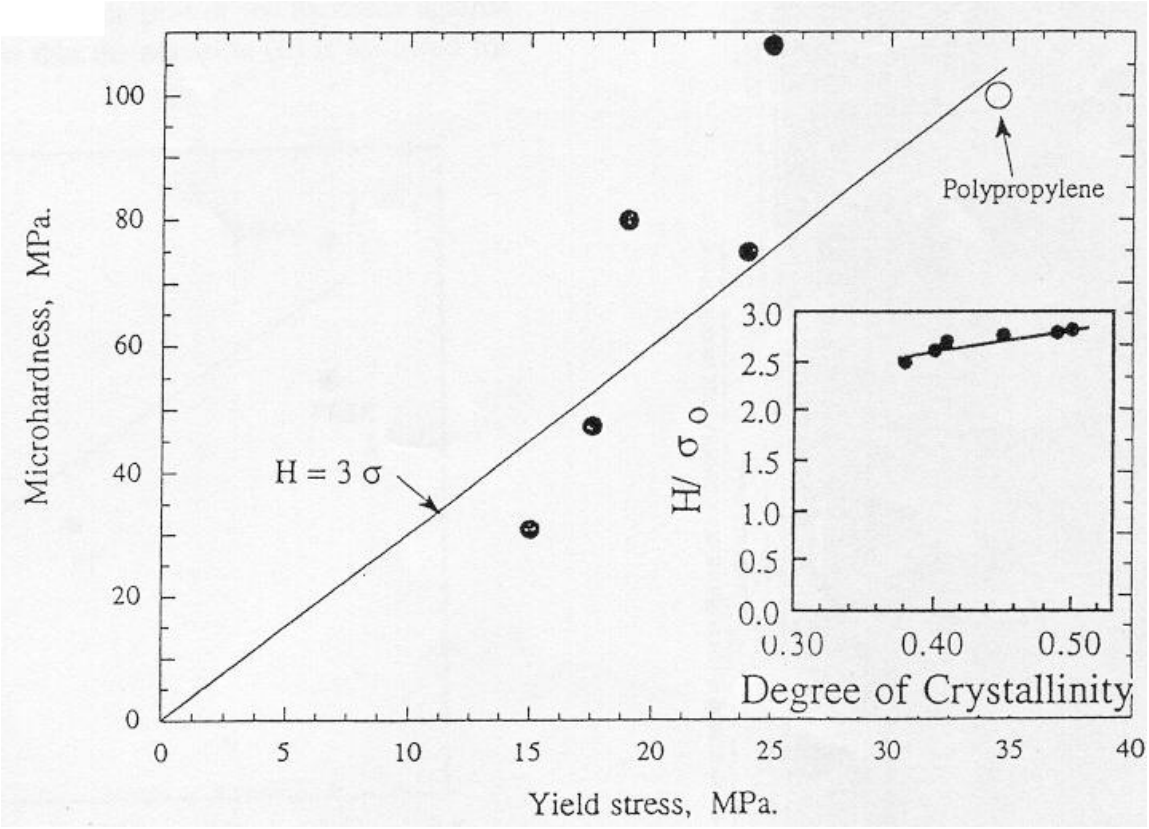

Figure 1.11: Microhardness as a function of yield stress for PE (●) [2]

CHAPTER 2

LITERATURE REVIEW

This chapter covers the essentials of work done by different researchers on the tensile and microhardness properties of metallocene polyethylenes and their blends. First, the literature survey on metallocene polyethylene is presented in section 2.1. Then the mechanical and thermal analysis of PE blends is discussed in section 2.2 and their structure-property relationships in section 2.3. Finally the survey on the characterization of PE blends is presented in section 2.4. The summary regarding the survey and the importance of the present study is given at the end of the chapter.

2.1 METALLOCENE POLYETHYLENES

A new family of metallocene polyethylene has an outstanding combination of processability, toughness and stiffness. These provided an opportunity to downguage and improved extrusion output in applications where blends of conventional Ziegler- Natta catalyzed linear low-density polyethylene (ZN-LLDPE) and high-pressure low density polyethylene (HP-LDPE) were used. The processability of metallocene polyethylene with their Ziegler- Natta counter parts was compared by Lue and Ching-Tai [8].

Chen et al [9] prepared the blends of very low-density polyethylenes (VLDPEs) with short branches using metallocene or Ziegler-Natta catalysts with low-density polyethylenes (LDPEs) or VLDPES with long branches and studied their crystallization and melting behavior using differential scanning calorimetry (DSC). It was concluded that the molar masses or melt flow indices were not significant in controlling the morphology; only the distributions of the branches along the chains was important.

Junting Xu et al [10] evaluated the short chain branching distribution (SCBD) of six metallocene- based ethylene copolymers by preparative temperature rising eluting fractionation of the samples at different temperatures. It was found that the SCBD of ethylene copolymers varies with the density of the copolymers and the type of comonomer. Both samples with narrow SCBD and samples with broad SCBD can be prepared using the same metallocene catalyst. The lamellar thickness distributions of the samples were also obtained by fitting the DSC melting traces. The reasons that lead to broad SCBD of metallocene-based LLDPE were also discussed.

Hussein et al [11] prepared new ultrahigh modulus tapes from metallocene-based linear polyethylene (LPE) using tensile drawing. Samples were prepared with a draw ratio in excess of 50 and a room temperature Young's modulus of 103GPa. Wide-angle X-ray scattering (WAXS) measurements suggest that the crystal size in the chain direction was as high as 460 Å, while small angle X-ray scattering (SAXS) measurements indicate a long period of 200 Å. This apparent contradiction was resolved by the inter-crystalline bridge model that correlated the modulus with the degree of crystal continuity determined from the longitudinal crystal thickness and the long period. The increase in

modulus attributed to an increase in crystallinity and crystal continuity along the draw direction without any extended chain crystallization.

Beagan and Malleja [12] have investigated the processability and mechanical performance of metallocene catalyzed polyethylene resins for packaging applications. Blends and co-extruded structures with metallocene catalyzed polyethylene resins and a conventional low-density polyethylene were produced. The effect of processing parameters, resin density, melt flow index, molecular weight, molecular weight distribution and co-monomer type on the viscosity characteristics and mechanical properties were investigated. The glass transition temperatures (T_g) of the films were measured using dynamic mechanical thermal analysis techniques and these T_g's were found to be much lower than the conventional linear low-density polyethylenes. The structural compatibility of the blends was determined using differential scanning calorimetry and dynamic thermal analysis. All blends were found to be compatible in the amorphous phase.

Sierra et al [13] studied the effect of metallocene polyethylene on heat-sealing properties of low-density polyethylene blends. According to various experimental studies of seal strength, hot tack and DSC, it was concluded that percentages around 15% of metallocene PE allowed the obtainment of the optimal balance for heat-sealing properties and cost.

2.2 MECHANICAL AND THERMAL ANALYSIS OF PE BLENDS

Martinez-Salazar and Balta-Calleja [14] have shown microhardness to be a promising technique for the microstructural investigation of polyblends of known

composition and it can provide information on the level of structural investigation. Solution crystallized mixed polyblends of high density (HD) and low-density (LD) PE with M_w of $50*10^3$ g/mol have been prepared in various composition ranges. The samples were crystallized in two modes: a) slow cooling at a rate of 0.2ºC/min; b) quenching to room temperature. Leitz tester measured the microhardness (MH). Figure 2.1 shows, for the materials slowly crystallized from the melt (curve A), the linear decrease of hardness of the linear polymer with increasing concentration of the branched material from $80MNm^{-2}$ down to $30MNm^{-2}$ for 100% low-density component. The hardness of the blends measured at higher temperatures showed substantially lower values. The hardness of the studies PE blends can be explained in terms of a parallel simple additive system of two independent components H_1 and H_2 (hardness values of the two independent components). The hardness of the amorphous turned out to be of the order of $0.5MNm^{-2}$ yielding a ratio H_c/H_a of 200(approx.) for melt crystallized linear PE.

Flores et al [15] have explored the correlation between microhardness, MH, tensile yield stress, Y_t, and Young's modulus, E, on various chain extended polyethylene (PE) samples and compared to chain folded PE. The tensile yield stress, Y_t, was shown to correlate with hardness following $H \cong 3Y_t$ while $H \cong E_t/10$ (E_t is Young's modulus derived from tensile experiments).

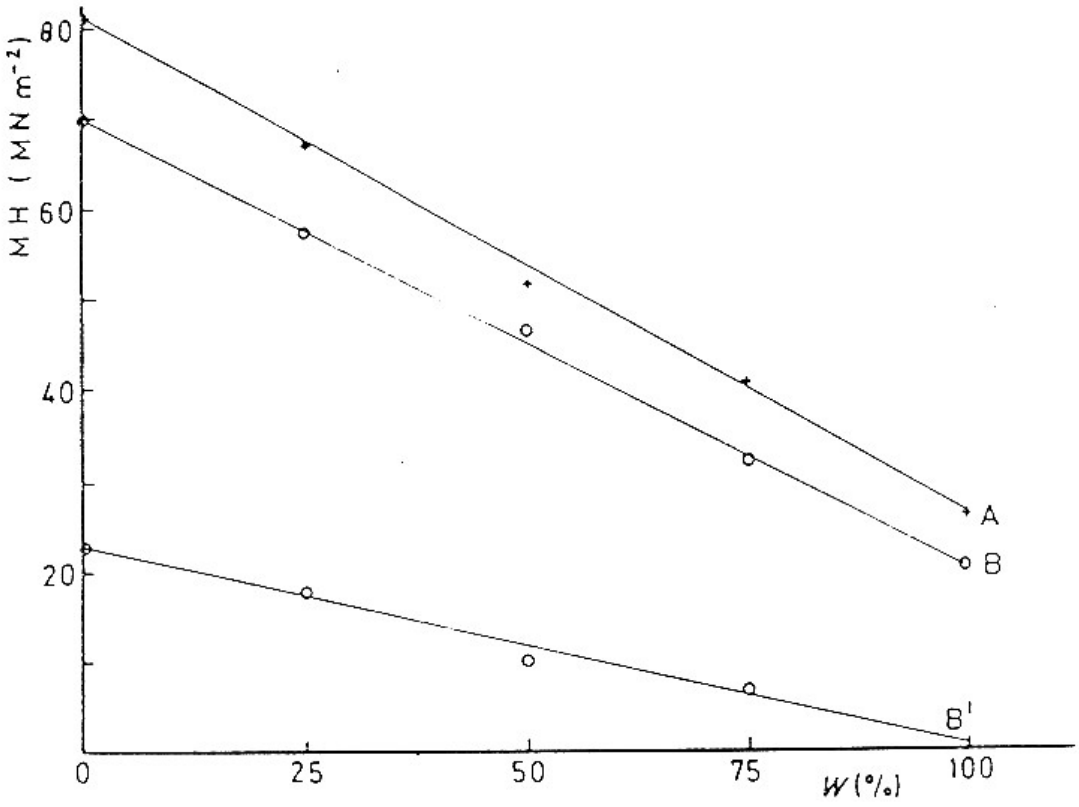

Figure 2.1**:** Microhardness of melt crystallized blends of HD and LDPE as a function of increasing weight concentration of LDPE. Curve A, slowly cooled samples; curve B material measured at room temp. and B' material measured at 110°C [14]

Rueda and Calleja [16] reported the data covering the physical properties of molten and solid samples of two binary blends of recycled polyethylene wastes. While some properties (density, fusion enthalpy) showed a linear behavior with composition. Other properties (microhardness, yield stress) showed a deviation from linearity. Deviation of microhardness additivity of the single components has been interpreted, after analysis of DSC thermograms, as being due to segregation and recombination of molecular species from both components during crystallization.

Zamfirova and Dimitrova [17] discussed some additional possibilities for microhardness investigations of polymer materials using a standard Vickers microhardness device. Two new investigation methods were suggested: determining the impression size under load; obtaining penetration curves. The role of entanglements on the microhardness of a series of melt-crystallized samples of linear polyethylene was investigated by Calleja FJ et al [18]. They concluded that the chain defects are responsible for the shearing mechanisms. A comprehensive review was presented of microhardness tests applicable to plastics were presented by John Lopez [19]. The methods were outlined and the effects of test variables were considered.

Fakirov et al [20] carried out microhardness model studies on branched polyethylene. Model samples of polyethylene with different degrees of branching (up to seven side groups, mostly of butyl type, at 100°C) are melt crystallized at two undercoolings, 10°C and 68°C, in order to obtain samples with various crystalline structures. The samples are characterized with respect to their density and microhardness (H).

It was emphasized that crystal size reflects rather the effect of crystal perfection. Via the extrapolation of H the equilibrium microhardness of PE crystals H_c = 160 MPa was determined. It was demonstrated that the application of the additivity law to multicomponent and/or multiphase systems was justified only in the case when all components (phases) have a melting or glass transition temperature above the temperature at which the H-measurements are carried out. In the case where the system contains a liquid like component, its contribution to the overall H is by changing the deformation mechanism and in order to apply the additivity law, H must be expressed as [20]:

$$H = 1.97T_g - 571 \tag{2.1}$$

The effect of temperature on yield energy of polyethylene was studied by conducting uniaxial tension tests by Bruce Hartman et al [21]. Yield energy was found to be a linear function of temperature extrapolating to zero at the melting point (140ºC). The ratio of yield stress to Young's modulus is 0.021 at room temperature and increases to 0.059 at 117ºC.

Shishesaz and Donatelli [22] studied the tensile properties of binary and ternary blends of low, medium and high-density polyethylene. The tensile properties of these materials indicated that the blends formed either compatible or semicompatible mixtures.

Seguela and Reitsch [23] reported the occurrence of double yield in polyethylene. According to these authors deformation takes place in two stages (i) Slip of crystal blocks past each other and (ii) Homogenous shear of crystal blocks.

Balsamo and Muller [24] studied the rate dependence of double yielding in LDPE, LLDPE (octane based, melt flow index of 1.0g $(10min)^{-1}$, $M_n=2.0*10^4$ g/mol and $M_w=1.33*10^5$ g/mol [26]) and their blends. The homopolymers and their blends were compression molded at 190ºC into 0.5mm thick sheets, which were either rapidly or slowly cooled. Figure 2.2 shows the typical stress-strain curves obtained at a strain rate of 50 mm min^{-1} for the blends. The arrows in this Figure show the first and second yield points. The blends were found to be compatible in all of the composition range. Infact the tensile moduli, yield stresses, yield strains, drawing stress and stress at break followed a simple rule of mixtures or positive deviations from it.

Yamada et al [25] presented a superstructural description of deformation process in uniaxial extension of pre-oriented isotactic polypropylene. The strains were separated over the whole range of deformation into three categories: crystallite boundary slip, uniform shear deformation of crystallites and restoration of molecular orientation from the shear-deformed state. Double yields during the tensile deformation of the polyethylenes and polytetramethylene terephthalate have been studied in a systematic manner [26-29].

Krishnaswamy and Lamborn [30] have prepared various LLDPE resins that encompassed those polymerized using Ziegler-Natta, metallocene and chromium oxide based catalysts. These resins were blown into film at similar process conditions, and the tensile properties of the resulting films were investigated in relation to the orientation characteristics.

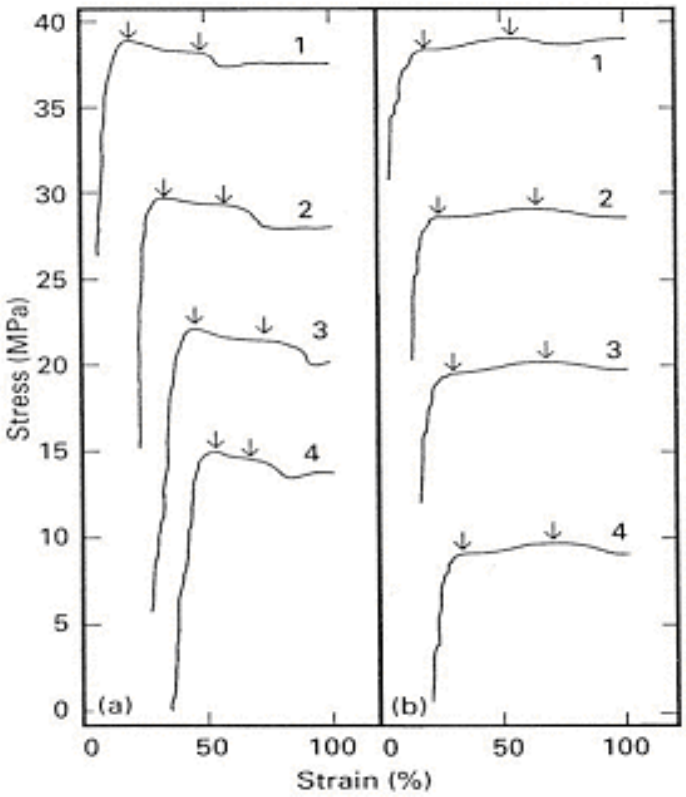

Figure 2.2: Typical stress- strain curves obtained at a strain rate of 50mm min^{-1} for the LDPE/LLDPE blends [24]; (a) slowly cooled and (b) rapidly cooled.(1) 100/0, (2) 65/35 (3) 35/65 and (4) 0/100

The tensile properties were observed to be significantly different from those of isotropic/un-oriented polyethylene specimens of similar density. These were explained in terms of lamellar organization and orientation characteristics of LLDPE blown films. Investigation of the temperature dependence (between –50ºC to +50ºC) of these tensile properties indicated an increase in modulus, yield stress and break stress with decreasing temperature pointing to the possible role played by the decreased mobility of the non-crystalline phase at lower temperatures.

Jafari et al [31] have prepared morphologically distinct binary polymer blends by melt mixing of HDPE and various LLDPEs for the entire range of blend composition under identical processing conditions. The morphology of the tensile fracture surfaces of blend, the parent polymers and their blends are quite interesting and show good correlation with thermal and mechanical properties. The HDPE forms linear and interpenetrating fibrils with a large number of interfibrillar separation, whereas, octane containing LLDPE (OLLDPE) with almost equal number of branching to that of HDPE shows nicely formed twisted fibrils. On the other hand, pentene containing LLDPE (PLLDPE) manifests a straight fibrillar with well-defined boundary comprising many thin fibrils with alternative thick and thin regimes and perfection, whilst butene containing LLDPE (BLLDPE) showed thick comparatively smooth and well-defined imperfect boundary of the tensile fracture.

Cho et al [32] investigated the melt rheology and mechanical properties of LLDPE/LDPE, LLDPE/HDPE and HDPE/LDPE blends. All three blends were miscible in the melt, but LLDPE/LDPE and HDPE/LDPE blends exhibited two crystallization and melting temperatures, indicating that those blends phase separated upon cooling from the

melt. The melt strength of the blends increased with increasing molecular weight of LDPE that was used. The mechanical properties of the LLDPE/LDPE blend were higher than calculated from a simple rule of mixtures, while those of LLDPE/HDPE blend conformed to the rule of mixtures, but the properties of HDPE/LDPE were less than that predicted by the rule of mixtures

Muller et al [33] studied the miscibility of two types of LDPE/LLDPE by DSC. DSC results suggested that the blends were partially miscible and phase separate in the melt depending on temperature and blend composition. The blends that contained 25% LLDPE (rapidly from the melt) were found to be mechanically compatible, with tensile properties that conform to a simple rule of mixtures or in some cases to positive deviations from it, inspite of their two-phase structure.

A study on the mechanical properties of low density and linear low-density polyethylene blends was carried out by La Mantia and D. Acierno [34]. They have reported that semicompatible mixtures resulted in the solid state for different investigated compositions. The mechanical properties of these blends were strongly influenced by LLDPE > 25 %.

La Mantia et al [35] studied the influence of structure of linear low-density polyethylene on the rheological and mechanical properties of blends with low-density polyethylene. They reported that the influence of comonomer was negligible, while the molecular weight exerted an important effect on properties.Datta and Birley [56] developed a thermal analysis method for the assessment of LD and HD polyethylene blends and LLD and HD polyethylene blends. LLDPE/HDPE blends were found to be

compatible where as LDPE/HDPE blends were found to be incompatible. These findings have been supported by X-ray diffraction and mechanical property measurements.

Structure and mechanical properties for the binary blends of a linear low-density polyethylene (LLDPE) (ethylene-1-hexene copolymer) were studied by Yamaguchi and Shigehiko [36]. The crystallization temperature of LDPE was higher than that of the LLDPE and was found to act as a nucleating agent for the crystallization of LLDPE. Consequently, the melting temperature, degree of crystallinity and hardness of the blend increased rapidly with increase in LDPE content in the blend.

Liu and Truss [37] studied the thin sheets of isotactic polypropylene and LLDPE blends by tensile testing, optical microscopy and DSC. Eyrings two-process yielding was used to analyze the data of yield stress as a function of strain rate and temperature and satisfactory curve fitting results were obtained.

Wilkes et al [38] studied the influence of molecular weight and thermal history on the thermal, rheological and mechanical properties of metallocene catalyzed linear polyethylenes. Several linear polyethylene homopolymers of varied molecular weight ($13 \leq M_w \leq 839$ kg/mol) were synthesized with a metallocene catalyst and characterized. The synthetic approach resulted in relatively narrow molecular weight distributions ($2.3 \leq M_w/M_n \leq 3.6$)) as measured by size exclusion chromatography. The small strain tensile deformation properties, Young's modulus, yield stress, and yield strain were directly related to percent crystallinity, independent of molecular weight. The large strain deformation properties, toughness and strain at break were influenced by the competing effects of percent crystallinity and molecular weight.

A study on thermal characterization of blends of single site linear and branched polyethylene was carried out by Tanem B.S. and A Stori [39]. They have reported that for a low content of the linear blend component, even 1.8-mol% comonomer content in the branched blend component was sufficient to create tow crystal populations during crystallization. For higher amounts of the linear blend component 2.5-mol% comonomer resulted in two crystal populations.

Lee et al [40] studied the crystallization behavior and mechanical properties of low-density polyethylene and metallocene linear low-density polyethylene blends with short branching content. Smaller 1-octene monomer content in m-LLDPE resulted in higher crystallization temperature and higher crystallinity of blends. The elastic modulus exhibited increasing behavior proportional to crystallinity, and the elongation at break of the blends increased with increasing m-LLDPE composition.

2.3 STRUCTURE-PROPERTY RELATIONSHIP IN PE BLENDS

The influence of structural and morphological factors on the mechanical properties of the polyethylenes was studied by Popli and Mandelkern [41]. They assessed the force-length relations at ambient temperature for a set of polyethylenes. They have reported that partial melting and recrystallisation process played an important role in the different aspects of deformation process. The influence of molecular weight manifested itself in the structure of interlamellar zone, which had major influence on the initial modulus and the ultimate properties. Copolymers and branched polymers displayed quite different behavior. The most striking difference was the invariance of the ultimate properties with molecular weight, branching and level of crystallinity. They have reported the occurrence

of double yield points at room temperatures for branched and linear low-density polyethylenes. These authors suggested that the phenomenon arose from a characteristic feature of the above materials, namely the very broad distribution of crystalline lamellae thicknesses.

La Mantia et al [35] studied the influence of structure of linear low-density polyethylene on the rheological and mechanical properties of blends with low-density polyethylene. They reported that the influence of comonomer was negligible, while the molecular weight exerted an important effect on properties.

Structure and mechanical properties for the binary blends of a linear low-density polyethylene (LLDPE) (ethylene-1-hexene copolymer) were studied by Yamaguchi and Shigehiko [36]. The crystallization temperature of LDPE was higher than that of the LLDPE and was found to act as a nucleating agent for the crystallization of LLDPE. Consequently, the melting temperature, degree of crystallinity and hardness of the blend increased rapidly with increase in LDPE content in the blend.

The force-length relations for a set of linear polyethylene fractions and polymers having most probable molecular weight distributions, encompassing a wide molecular weight range, have been investigated by Kennedy et al [42]. The polymers were crystallized in such a manner as to develop as wide a range as possible in the values of the independent structural variable that describes the crystalline state. The sharpness of the transition from a brittle to ductile type deformation was established, as was its dependence on molecular weight and certain key structural parameters. The ultimate properties were found to depend only on the weight average molecular weight that

indicated the importance of noncrystalline regions. They have reported that different portions of the stress-strain curves were governed by different structural and molecular features, indicating the complexity of the process.

Martinez-Salazar et al [43] carried out a combined WAXD and DSC study on blends on a series of commercial high density and low-density polyethylene samples that were rapidly crystallized from the melt. The melting curves of the materials are extensively analyzed and compared to those exhibited by individual components. The results, besides being indicative of a full compatibility of the two components, allow one to distinguish between a blend and LDPE having both the same average value of branching.

A study of the phase behavior of polyethylene blends using micro-Raman imaging was carried out by Hill et al [44]. Blends were crystallized to produce samples with large domains that is rich in linear material surrounding by a matrix that are rich in branched polymer. The micro-Raman imaging showed that the samples remixed to a homogenous distribution by branch content within the expected time scale, as estimated from the diffusion constants. However micro-Raman imaging can also be used to detect crystallinity variations and it reveals a biphasic structure in blends that display a morphological phase structure when examined in the transmission electron microscope.

Kristiansen et al [45] carried out isothermal crystallization of polyethylene monitored by insitu NMR and analyzed within the Avrami' model network. The crystallization rate as a function of crystallization temperature was derived and the results discussed within a thermodynamic framework. A slight increase in the molecular

correlation times with crystallization time was revealed for both the crystalline and intermediate phases. In particular, the molecular mobility within the intermediate phase was found to be approximately four times faster than in crystalline phase.

Hill et al [46] have studied the effect of cooling rate on two homogenously mixed blends. The crystalline textures of a blend of linear PE with LDPE and blend of deuterated linear PE with LDPE have been investigated as function of cooling rate from the melt. DSC, FTIR and transmission electron microscopy have been used to study co-crystallization and phase segregation. The degree of segregation was found to increase with decreasing cooling rate. The results support the argument that those rapidly samples, which contain two crystal types, do so because of phase separation in the melt and not because of phase separation on crystallization. The composition dependence of β-transition in ethylene copolymers has been reexamined by Popli and Mandelkern [47]. They showed that this transition was found in homopolymer linear polyethylene, and that it was a reflection of segmental motions that take place within the interfacial region.

The effect of composition distribution on miscibility and co-crystallization phenomena in the blends of LDPE with conventional and metallocene based ethylene-butene copolymers was studied by Junting, Xu et al [48]. Three ethylene butene copolymers and having different composition distributions were blended with LDPE in a wide composition range. The blends were rapidly from the melts and co-crystallization phenomena were investigated by DSC. The obtained results showed that composition distribution has greater influence on co-crystallization.

Weignall et al [49] carried out the investigations of solid-state morphology of blends of HDPE/LDPE by DSC, SANS (small angle neutron scattering) and SAXS (small angle X-ray scattering). These tests showed that the blends were homogenous, but may phase segregate on slow cooling due to structural and melting point differences between HDPE and LDPE. For high concentrations of HDPE, high rates of crystallization of the linear component led to the formations of separate stacks of HDPE and LDPE lamellae. The blend morphology is a strong function of the cooling rate of the samples.

Drummond et al [50] examined the crystallization of series of LDPE and LLDPE rich blends using DSC. DSC analysis after continuous slow cooling showed a broadening peak with increasing concentration of LDPE. Melt endotherms following stepwise crystallization detailed the effect of the addition of LDPE to LLDPE, showing a non-linear broadening in the melting distribution of lamellae, across the temperature range 80-140ºC, with increasing concentration of LDPE.

Gupta et al [51] conducted a study on crystallization behavior of HDPE/LLDPE blend using DSC and X-ray diffraction methods. These blends were prepared by melt mixing in an extruder in the entire range of blending ratio. Co-crystallization was evident in the entire range of blend composition, from the single peak character in DSC crystallization exotherms and melting endotherms and X-ray diffraction peaks. A detailed analysis of DSC crystallization exotherms revealed a systematic effect of the addition of LLDPE on nucleation rate and the subsequently developed crystalline morphology.

2.4 CHARACTERIZATION OF PE BLENDS

Utracki et al [52] carried out a study on compatibilisation of polymer blends. Most blends are immiscible and need to be compatibilised. The compatibilisation must (1) ascertain the optimum degree of dispersion (2) stabilize the morphology against the possible damage during the subsequent processing stage and (3) secure good interfacial interactions between phases in the solid state.

Stein et al [53] studied the characterization and properties of PE blends. Melting and crystallization phenomena in blends of LLDPE (ethylene butene-1 copolymer) with a conventional low-density branched polyethylene (LDPE) were explored with emphasis on composition by DSC and light scattering (LS). Two endotherms were evident from DSC studies for these blends suggesting the formation of separate crystals. Light scattering studies indicate that the blend system is predominantly volume filled by the LLDPE component whereby the LDPE component crystallized as a secondary process within the domain of LLDPE spherulites.

Prasad A [54] has developed an accurate and rapid test scheme to identify the type and composition of alpha-olefin in LDPE/LLDPE. This technique utilizes DSC and FTIR techniques. Separate calibrations for butene-1, hexane-1 and octane-1 LLDPEs had been developed to quantify the blend composition from DSC thermograms where the alpha-olefin type was successfully identified by FTIR over the entire blend composition range.

Datta and Birley [55] developed a thermal analysis method for the assessment of LD and HD polyethylene blends and LLD and HD polyethylene blends. LLDPE/HDPE blends were found to be compatible where as LDPE/HDPE blends were found to be

incompatible. These findings have been supported by X-ray diffraction and mechanical property measurements.

Lee and Denn M [56] employed rheological measurements of PE blends in the melt and solid state, together with thermal analysis, to infer phase behavior. Partial-miscibility in the melt was characterized by use of double-reptation model to define the complex modulus of the continuous phase for input into the emulsion model for the blend; this approach introduced a new fitting parameter, the fraction of the minor component contained in the continuous phase. The results on binary systems suggested that the use of HDPE as a compatibilizer for LLDPE/LDPE blends, apparently creating a fully miscible ternary system.

Krishnaswamy et al [30] have explored the effects of blending metallocene catalyzed LLDPE of reasonably differing molecular weights on the performance and orientation characteristics of blown films. The presence of relatively longer molecules in a metallocene catalyzed LLDPE resulted in blown films with relatively lower machine direction (MD) tear resistance, lower impact strength and higher transverse direction (TD) tear resistance. Morphological investigations of the blend films indicated the potential significance of microstructural anisotropy on blown film impact performance.

From the literature survey it can be concluded that limited work has been reported on either tensile or microhardness properties of m-LLDPE/LDPE blends; however, work related to mechanical properties of pure polyethylene has been studied extensively. Mechanical properties (tensile and microhardness) of PE blends have not been studied comprehensively. The influence of branch type and branching distribution of m-LLDPE

on the tensile properties of m-LLDPE/LDPE blends have not been reported in literature. The concept of double yield phenomena in polyethylene has not been comprehensively studied. The work in this regard is of really great importance in understanding the deformation characteristics of the tensile samples of m-LLDPE/LDPE blends. Several important generalizations can be made from this study.

On the basis of literature survey conducted, it can be concluded that a study of tensile and microhardness properties of m-LLDPE/LDPE blends is an open area of research and the results of the study will be a useful addition to the existing literature and will be much beneficial from the practical applications point of view.

CHAPTER 3

EXPERIMENTAL PROCEDURE

3.1 MATERIALS CHARACTERISTICS

Exxon Mobil Inc., and Nova Chemical Company supplied all the studied resins in the form of extruded pellets. The resins were selected with similar molecular weight (M_w), molecular weight distribution (MWD) and melt flow index (MFI) in order to study the effect of branch type on the thermal and mechanical properties. GPC and NMR and thermal analyses of the samples were done to determine the molecular constitution such as M_w, MWD and branch content. The physical properties of the selected polymers are listed in Table 3.1.

3.1.1 Preparation of blend samples

In this work, the eight polymers listed in Table 3.1 were studied for preliminary results. The chosen m-LLDPE polymers differ in branch type with similar branch content, which facilitated the study of the influence of branch type of m-LLDPE on the thermal and mechanical properties of m-LLDPE/LDPE blends.

Table 3.1 Properties of Resins

Type	M_n	M_w	M_z	MWD= M_w/M_n	MI	Density	CH3/1000C*
LDPE	24.22	100.38	243.10	4.14	1.20	0.923	11.0**
LDPE	17.96	116.81	325.57	6.50	0.75	0.919	N/A
B-LLDPE	33.58	110.66	273.03	3.30	1.00	0.918	N/A
B-LLDPE	55.38	107.95	178.55	1.95	1.20	0.910	14.5
H-LLDPE	57.25	107.78	174.31	1.83	1.20	0.900	18.02
H-LLDPE	47.88	102.38	192.37	2.14	1.20	0.912	14.4
O-LLDPE	47.62	94.67	167.45	1.99	1.10	0.882	32.67
O-LLDPE	44.36	90.44	159.08	2.04	1.10	0.902	16.32

* ^{13}C NMR, ** Total number of short and long branches

All the blend samples were prepared by melt-mixing the homopolymers in Haake Polydrive melt blender as shown in Figure 3.1. The mixing conditions were 190°C, 50 rev/min and 10 min. The blends and as well as 'pure' polymers were conditioned in the presence of adequate amounts of extra antioxidant (AO). 1000 ppm of Antioxidant (50/50 mixture of Irganox 1010 and Irgafos 168) was added to ensure that there is no thermal degradation in the blends The pure polymers were also subjected to the same procedure. The investigated compositions, are 0/100, 10/90, 30/70, 50/50, 70/30, 90/10 and 100/0 wt % of m-LLDPE/LDPE.

3.1.2 Preparation of discs

The specimens differing in thermal history were prepared to study its influence on mechanical properties. The polymers for this study were one sample of low-density polyethylene (LDPE) and three samples of metallocene catalyzed linear low-density polyethylene differing in the branch type (Table 3.1). For each composition, a 9 cm diameter disc was prepared in a special mold cell mounted on Carver Laboratory Press as shown in Figure 3.1. After melting the polymer inside the mold, a pressure of 1.5 MPa in a Carver press was applied. The set of samples were prepared by holding at the pressure of 1.5 MPa in a Carver press for about 15 min and then down to the room temperature by water at a cooling rate of about 50°C/min. Then the specimen discs are taken out for punching.

Figure 3.1: Haake Polydrive Melt blender

Figure 3.2: Compression mold is being mounted on a hydraulic Carver press

3.1.3 Tensile Specimens

Dumb-bell specimens (Figure 3.3) as per ASTM Standard D638 (Type-V) were cut from these discs prepared for tensile testing. Six samples were punched out from the prepared disc. All the tensile testing of the prepared samples were carried out according to ASTM D 638 [61] procedure.

3.2 MECHANICAL TESTING

3.2.1 Tensile Testing Equipment

Stress-strain tests were carried out using an Instron Tensile testing machine model 5567. The controlling limits can be viewed on the digital control panel at any time during the test along with other test variables (e.g. start and stop of the test, gauge length adjustment etc.). The photograph of the testing equipment is shown in Figure 3.4. The machine is equipped with manual gripping system. Any preloading induced during clamping was adjusted to zero prior to testing by the recalibration of the load cell after clamping. The Instron Series IX data acquisition, control and analysis software for material testing was used. A PC, interfaced with the testing frame is required for using this software.

This software provides position and corresponding load of the test with a constant position increment till fracture at the ultimate tensile strength, which is logged along the final position before fracture. The speed of testing for the samples was 125 mm/min according to ASTM D638 [61]. The gauge length was 2.54 cm.

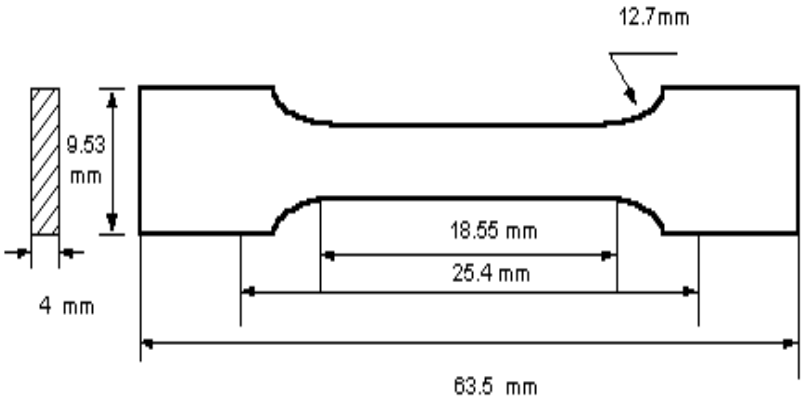

Figure 3.3: Tensile specimen as per ASTM D 638[61]

Figure 3.4: Instron 5567 equipped with Merlin Series IX for tensile testing

3.2.2 Microhardness Testing

Microhardness measurements were carried out using Vickers's Hardness tester (Figure 3.5) equipped with diamond indentor and a load of 10 gf was applied to obtain the deformation pattern. All the measurements are averages of at least 5 measurements.

3.3 THERMAL TESTING

3.3.1 DSC Testing Equipment

Mettler DSC822^{e} (Figure 3.6) was used in this work for the thermal analysis of the prepared samples. Temperature calibration was made with indium. DSC samples were prepared by cutting small samples from the prepared discs. They were sealed in an aluminium pan and an empty aluminium pan was used as a reference. The crystalline melting thermograms were obtained by heating the samples from 20°C to 140°C at a programmed heating rate of 10°C/min. Crystallization thermograms were obtained by heating the samples to a temperature of 180˚C and holding there for 10 minutes to eliminate the thermal history in the prepared samples and then cooling down to the room temperature at a cooling rate of 10˚C /min under nitrogen atmosphere.

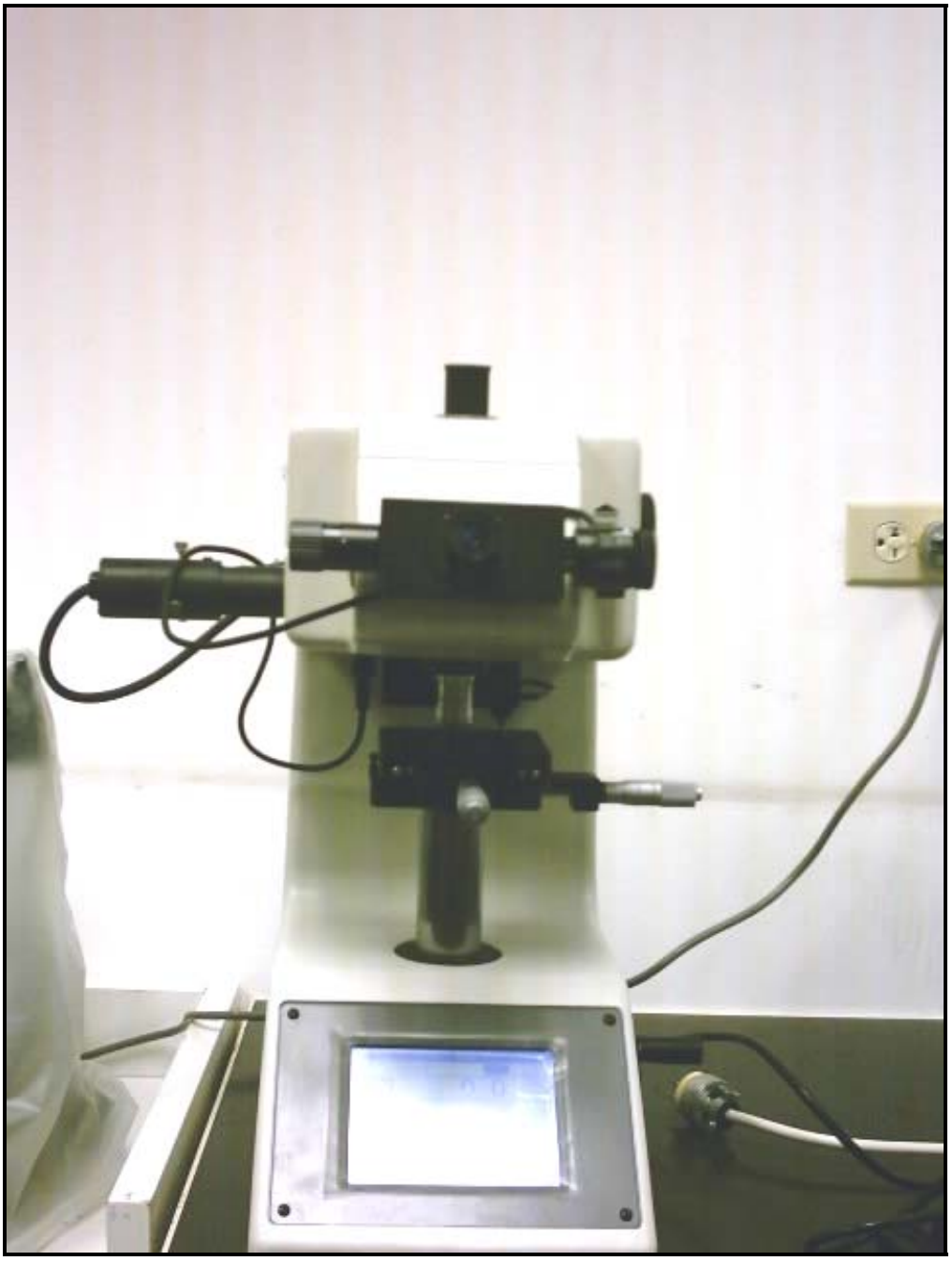

Figure 3.5: Vickers Hardness Tester

Figure 3.6: Mettler DSC 822e Equipment

CHAPTER 4

EXPERIMENTAL RESULTS

4.1 INTRODUCTION

4.2 THERMAL ANALYSIS

The thermal analyses of all samples were conducted using the Mettler DSC822^e. The DSC instrument was calibrated with indium. The temperature and the heat of fusion calibration have been checked at each start up of the instrument to ensure the accuracy of the results. The crystalline melting thermograms were obtained by heating the samples from 20°C to 140°C at a heating rate of 10°C/min.

4.2.1 DSC Scans of Pure Samples

DSC melting thermograms for all four polymers are shown in Figure 4.1. The results of average DSC scans are summarized in Table 4.1. It is clear that the melting peaks of all the m-LLDPE samples are lower than that of the LDPE. DSC scans of LDPE and B-LLDPE reveal narrow melting behavior with peaks at 111°C and 107°C, respectively; whereas, H-LLDPE and O-LLDPE show a relatively broader melting behavior with peaks at 108°C and 98°C, respectively.

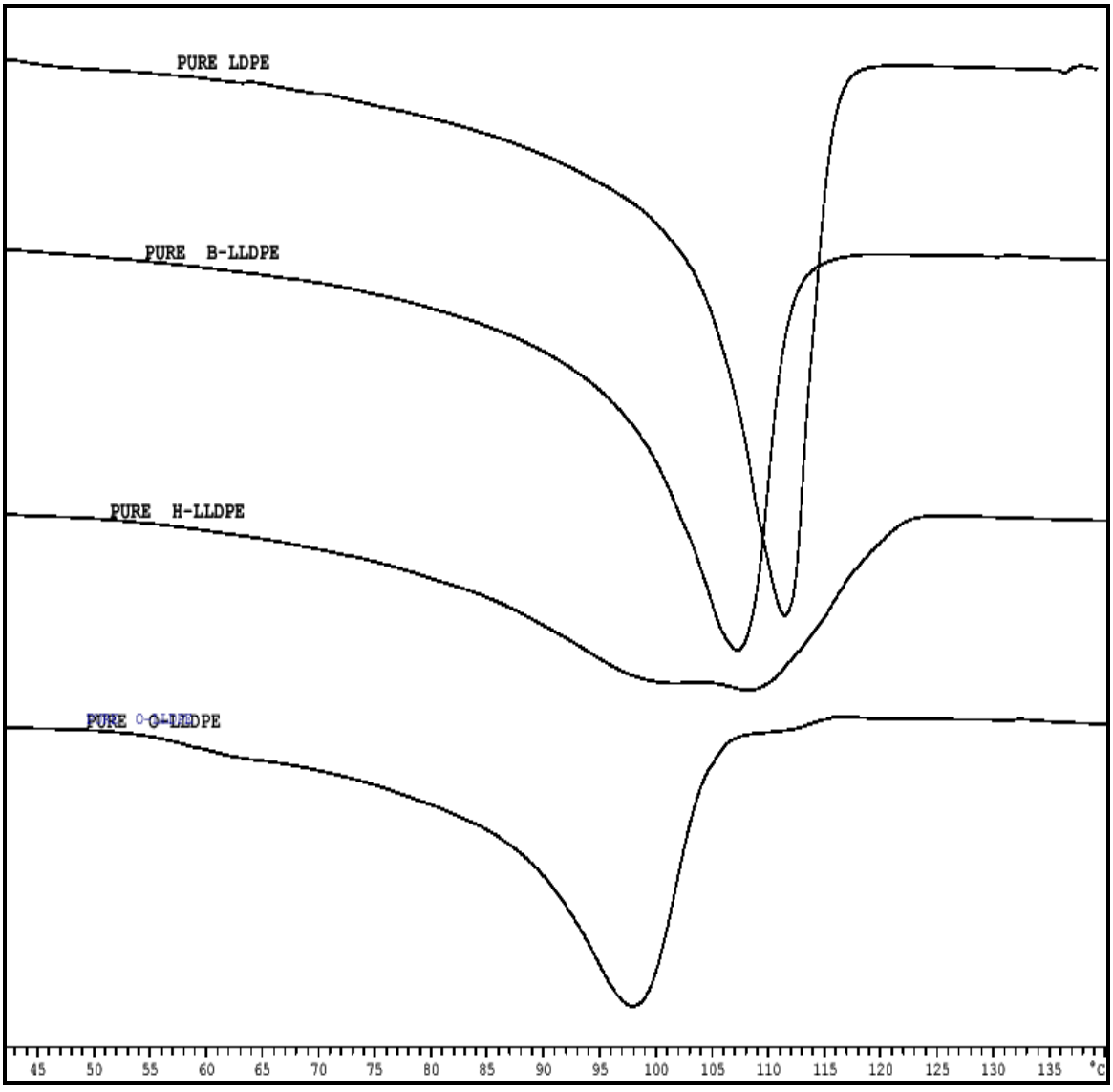

Temperature (°C)

Figure 4.1: DSC scans of pure polymers showing the nature of the melting peaks

Table 4.1 Thermal characterization data of pure polymers

POLYMER	PEAK MELTING TEMP, °C	ENDSET MELTING TEMP, °C	PERCENT CRYSTALLINITY
LDPE	111	118	37
B-LLDPE	108	115	30
H-LLDPE	109	123	29
O-LLDPE	98	108	27

In addition, the DSC scan of H-LLDPE shows the existence of two broad melting peaks at 99°C and 108°C. For the B-LLDPE, it is obvious that only a single melting peak is observed. Figure 4.1 shows DSC melting thermogram for O-LLDPE. A similar behavior in the melting peaks as that of the B-LLDPE is observed. When comparing the crystallinity values of pure B-LLDPE to that of O-LLDPE, it is evident that the latter has lower amount of crystallinity. It is also observed that the pure H-LLDPE shows a melting behavior intermediate between pure B-LLDPE and O-LLDPE.

4.2.2 DSC scans of B-type blends

DSC melting thermograms for all the B-type blend systems are shown in Figure 4.2. It is clear that the melting peak of the B-LLDPE sample is lower than that of the LDPE. It is obvious that only a single melting peak is observed in each blend; irrespective of blend composition. The thermal characterization data for all the blend ratios is reported in Table 4.2. It can be seen that there is a slight increase in the percent crystallinity values of the blend samples with the increase of LDPE content. There is an improvement in the melting peaks with the addition of LDPE for the blends.

4.2.3 DSC Scans of O-type blends

Figure 4.3 shows DSC melting thermograms for O-type blends. A similar behavior in the melting peaks to that of the B-type is observed. The thermal characterization data for all the blend ratios is reported in Table 4.3.

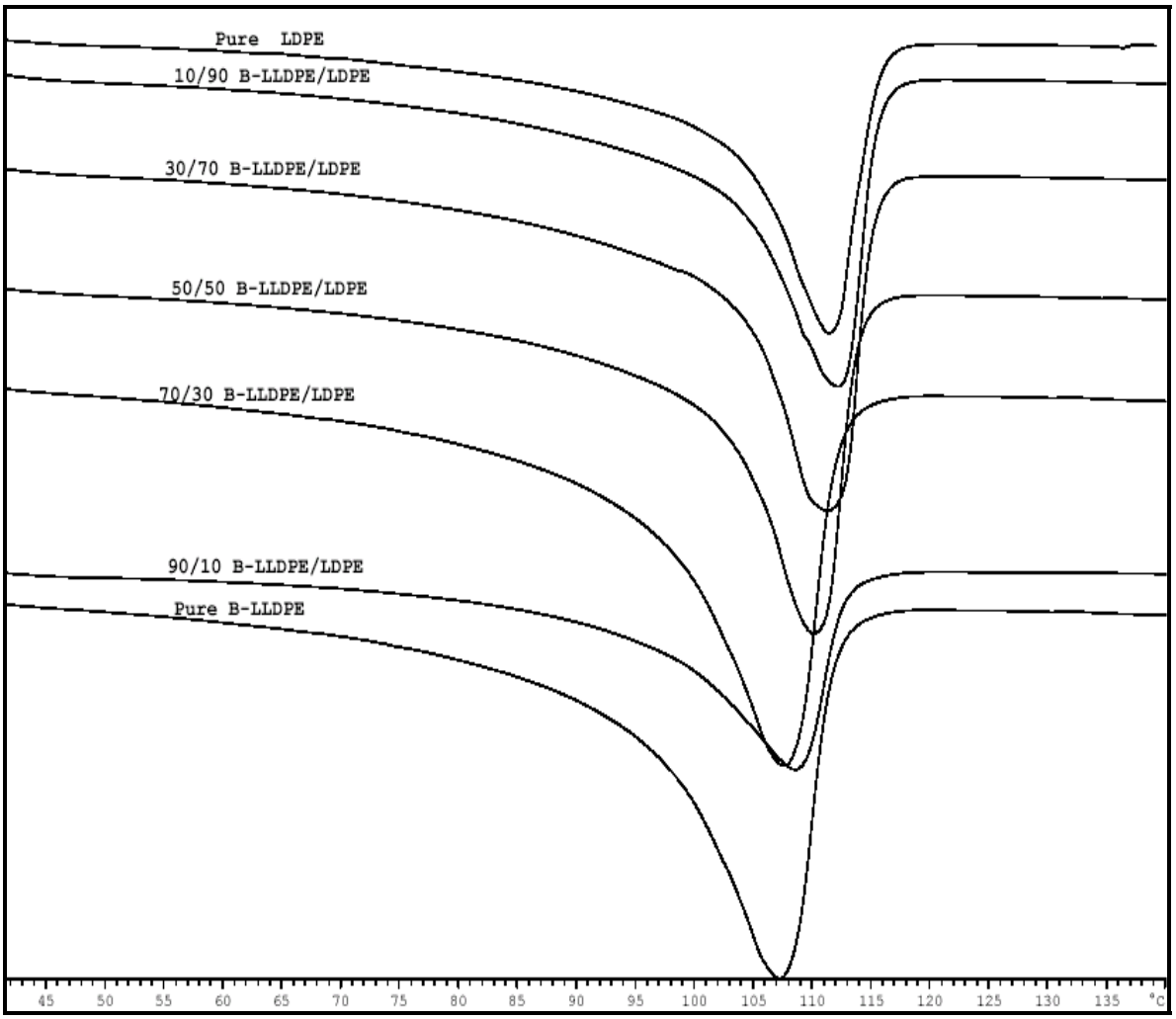

Figure 4.2**:** DSC scans of B-type blends showing the nature of melting peaks at different blend ratios

Table 4.2 Thermal characterization data of B-type blends

TYPE	LLDPE/LDPE	CRYSTALLINITY (DSC)	MELTING TEMP, °C	ENDSET, °C
S15 (B-LLDPE)	100/0	29.93	107.07	115.53
	90/10	30.84	108.18	117.2
	70/30	32.2	108.79	117.2
	50/50	31.63	109.65	117.33
	30/70	33.12	110.82	118.41
	10/90	35.04	111.5	118.35
S5 (LDPE)	0/100	37.29	110.94	118.47

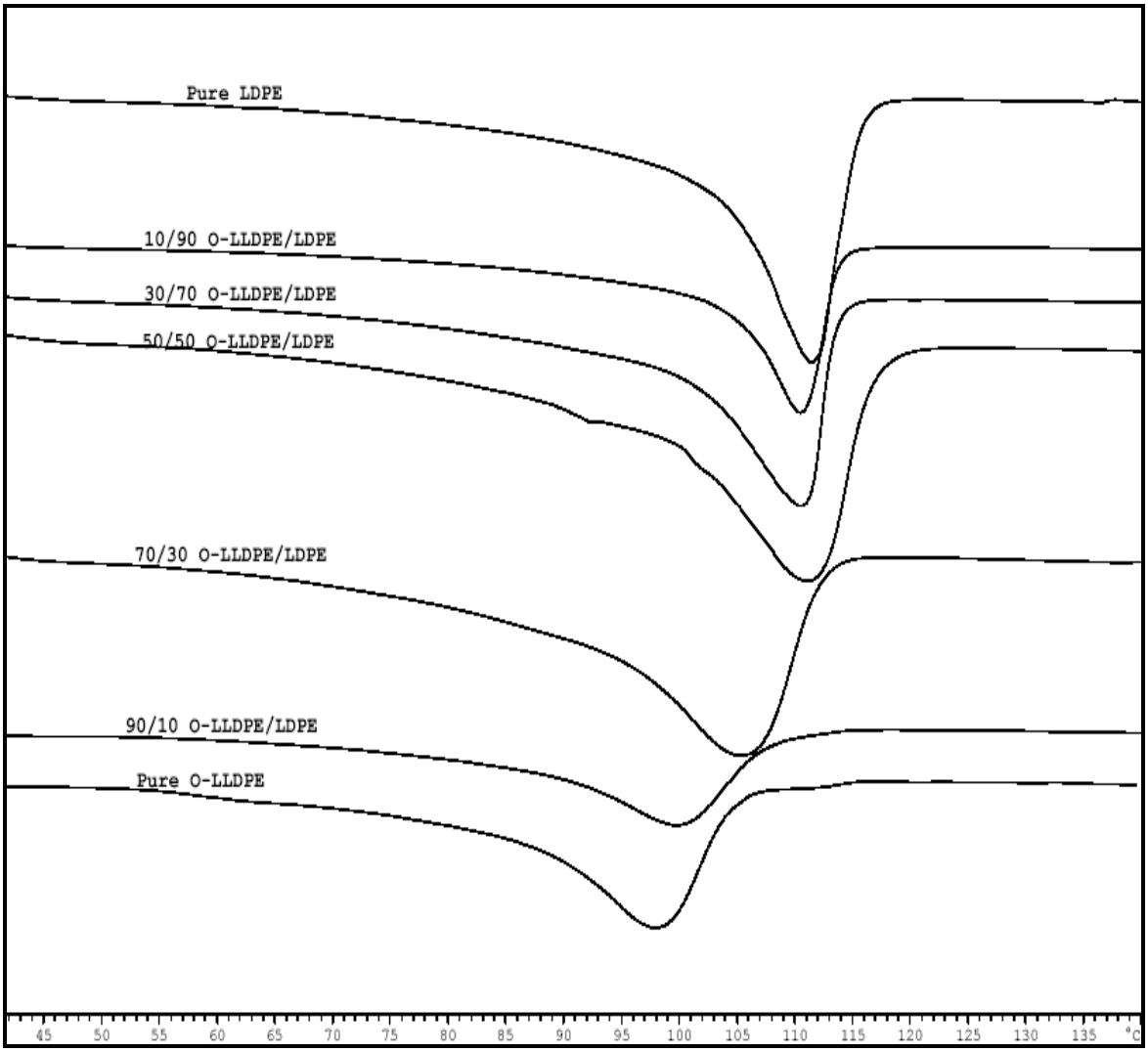

Figure 4.3: DSC scans of O-type blends showing the nature of melting peaks

Table 4.3 Thermal characterization data of O-type blends

TYPE	LLDPE/LDPE	CRYSTALLINITY (DSC)	MELTING TEMP, °C	ENDSET, °C
S26 (O-LLDPE)	100/0	26.67	97.76	108.12
	90/10	22.62	99.65	113.68
	70/30	26.94	104.93	114.9
	50/50	27.11	110.54	116.12
	30/70	29.03	110.14	114.54
	33147	31.99	110.24	115.04
S5 (LDPE)	0/100	37.29	110.94	122.28

4.2.4 DSC Scans of H-type Blends

DSC scans of H-type blends are presented in Figure 4.4. According to this figure, pure H-LLDPE shows broad melting behavior with two shallow peaks at 99°C and 108°C. The DSC scans also reveal that the two peaks merge into a single higher value melting peak when LDPE content is greater than 10% in the blend. With the increase in LDPE composition of the blend, it is found that the broad shallow peaks in H-LLDPE tend to become quite narrow in nature and the peak is shifted towards the higher value. The thermal characterization data for all the blend ratios is reported in Table 4.4.

4.3 TENSILE RESULTS

All the mechanical property measurements were carried out ASTM D638 [61] procedure. The yield point is defined as the point where, for a slight increase in strain there is no change in the value of stress or the highest point on the stress-strain curve before necking. The value of stress corresponding to the yield point is taken as the yield stress of the polymer sample. The initial modulus of the sample is calculated from the slope of the linear portion of the stress-strain curve. To ensure the accuracy of this measurement, a trend line is drawn using the linear regression fit. The slope of this line is taken as the initial modulus of the polymer sample. The speed of testing for all the samples was 125 mm/min. The gauge length was 25.4 mm and all the results averages of at least 4 measurements.

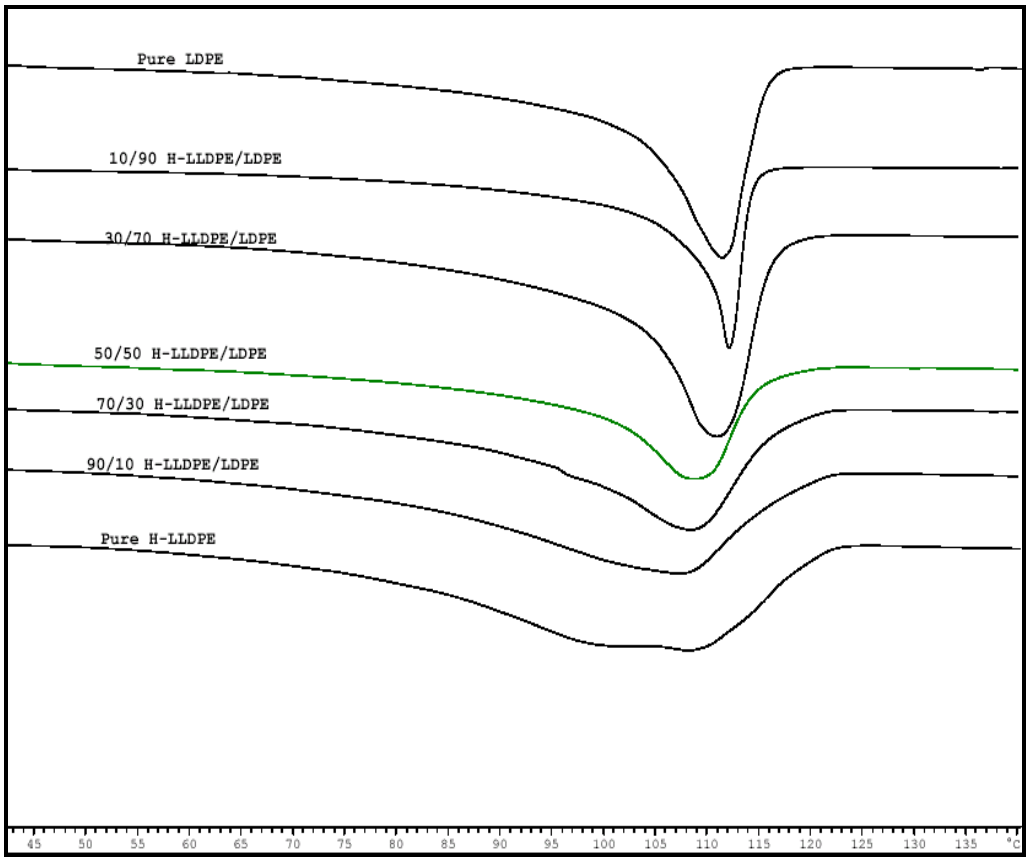

Temperature (°C)

Figure 4.4: DSC scans of H-type blends showing the nature of melting peaks

Table 4.4 Thermal characterization data of H-type blends

TYPE	LLDPE/LDPE	CRYSTALLINITY (DSC)	MELTING TEMP, °C	ENDSET, °C
S18 (H-LLDPE)	100/0	28.54	108.46	122.85
	90/10	28.92	107.99	122.44
	70/30	27.26	108.33	122.46
	50/50	29.7	108.55	121.36
	30/70	32.15	110.51	120.67
	10/90	31.31	116.83	119.21
S5 (LDPE)	0/100	37.29	110.94	118.47

4.3.1 Pure Samples

We use engineering stress, σ and engineering strain, ε. Yield stress, σy, is defined as the value obtained at the point where a distinct yield onset is observed. Stress-strain curves for all the samples are reported in Figures 4.5-4.8. The characterization data for the samples is reported in Table 4.5.

All the studied polymers display ductile behavior. The discussion regarding the occurrence of double yield points and the explanation concerning it is dealt in the next chapter. The summary of tensile results for all the samples is reported in Table 4.6.

4.4 EFFECT OF THE BRANCH TYPE OF M-LLDPE

It is important to investigate the influence of branch type of LLDPE on the thermal and mechanical properties of m-LLDPE/LDPE blends. The selected polymers for this study are: 1) low-density polyethylene (LDPE); 2) metallocene linear low-density polyethylene (m-LLDPE) containing butene branches; 3) m-LLDPE containing hexene; and 4) m-LLDPE containing octene branches. Hereby we designate the three blend systems as B-type (B-LLDPE/LDPE), H-Type (H-LLDPE/LDPE) and O-type (O-LLDPE/LDPE).

4.4.1 B Type Blend System (B-LLDPE/LDPE)

Stress-strain curves for all the pure cooled samples are reported in Figures 4.9-4.13

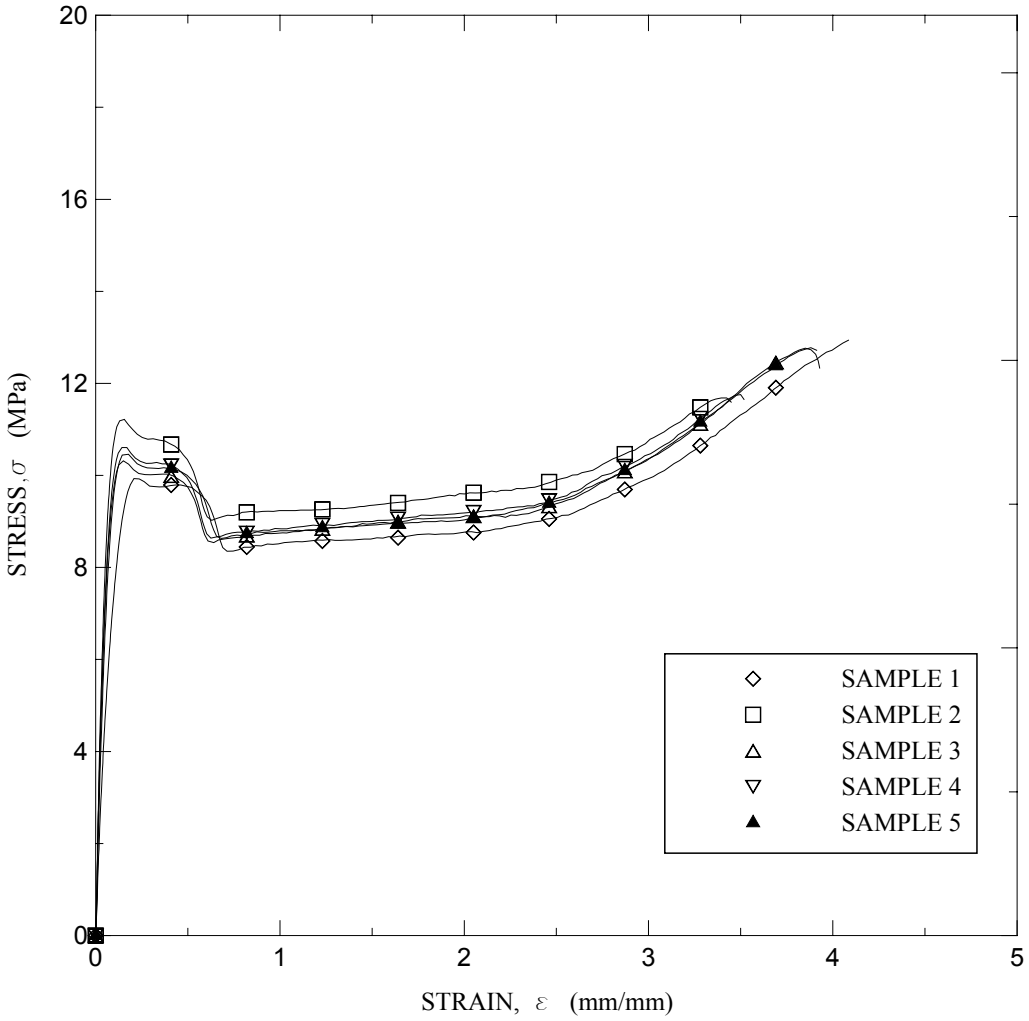

Figure 4.5: Stress-strain curves for the pure LDPE samples

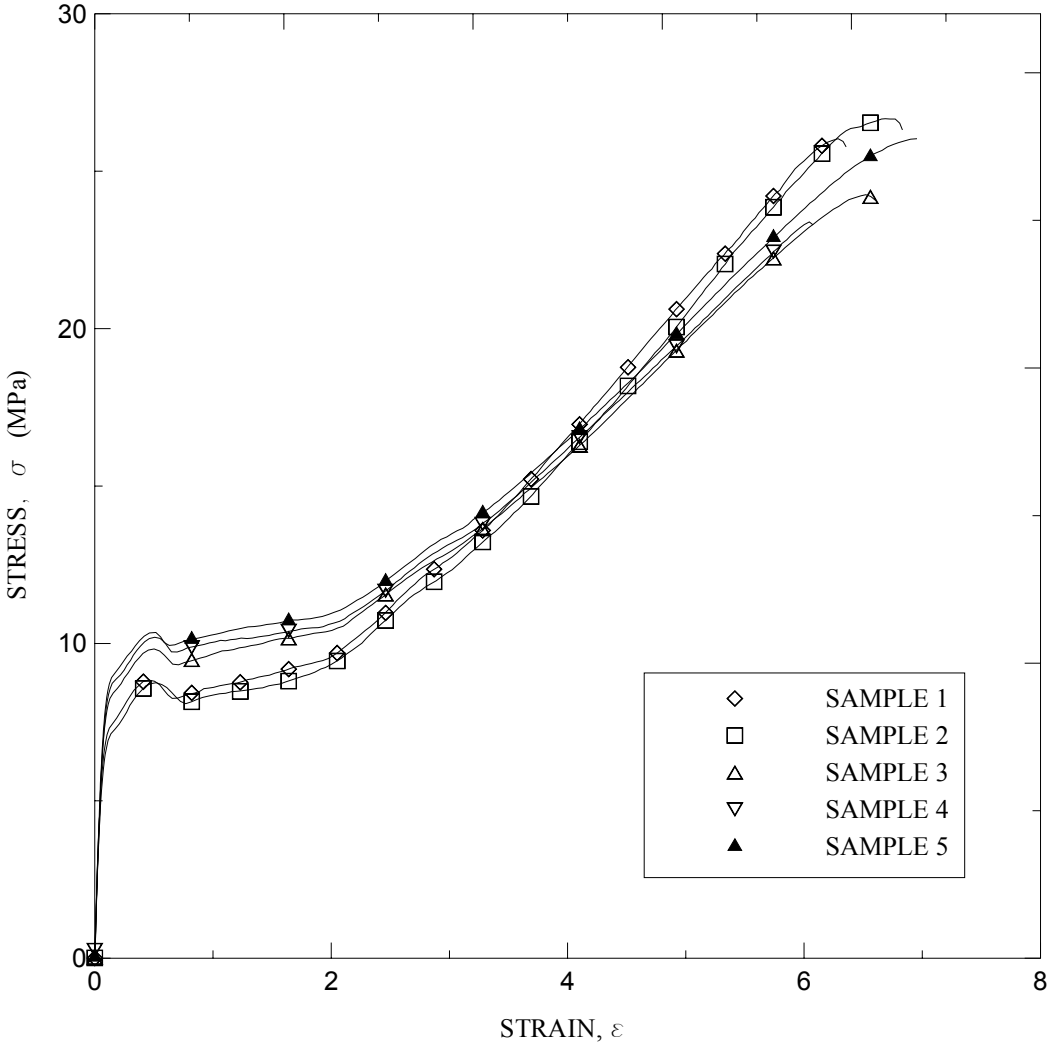

Figure 4.6: Stress-strain curves for the pure B-LLDPE samples

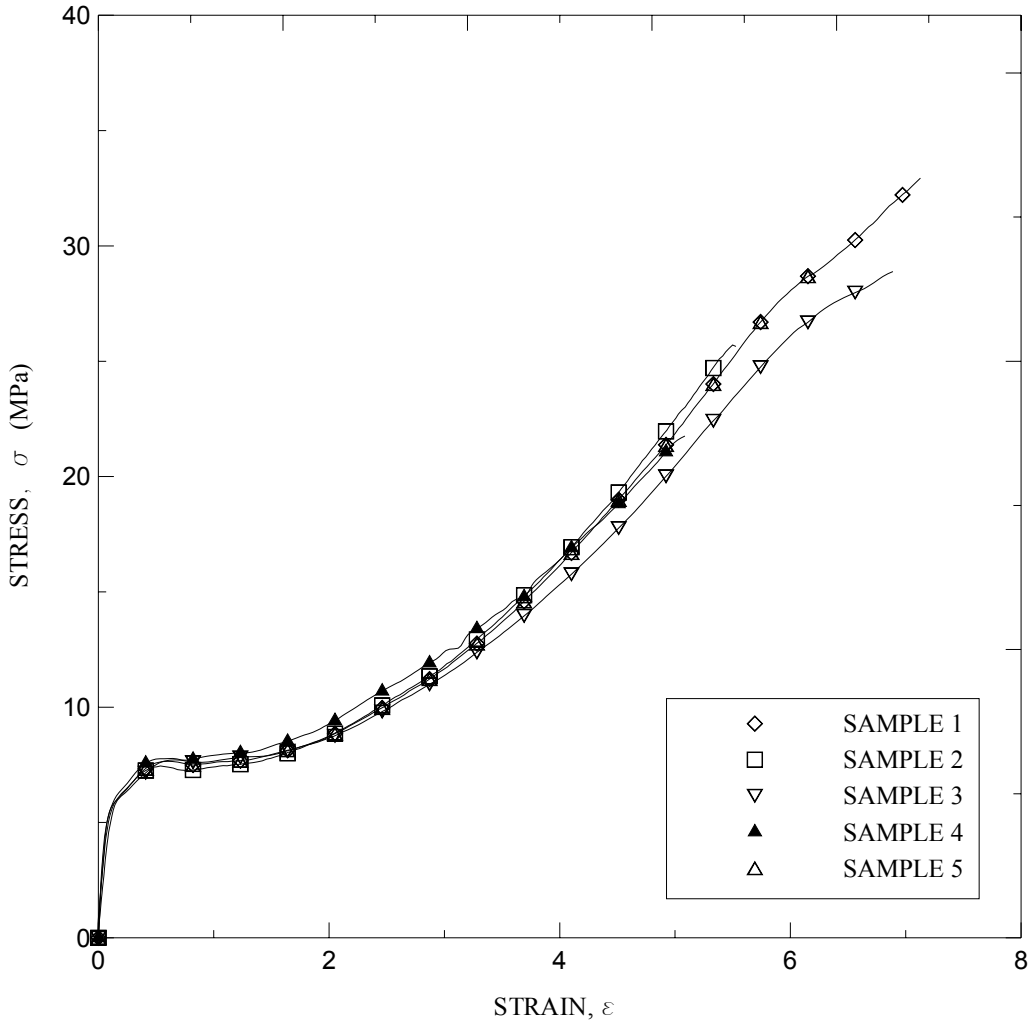

Figure 4.7: Stress-strain curves for the pure H-LLDPE samples

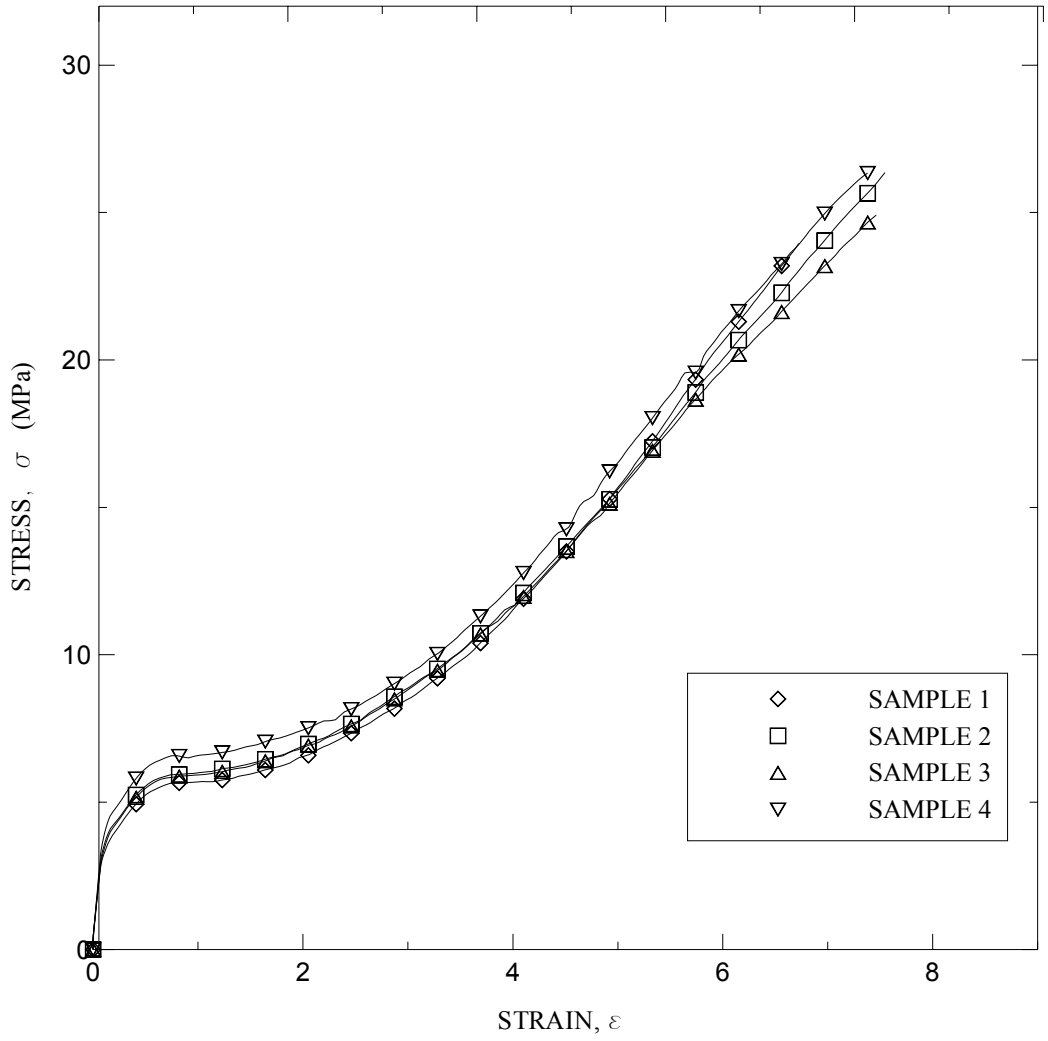

Figure 4.8: Stress-strain curves for the pure O-LLDPE samples

Table 4.5 Mechanical properties of samples

S5

SAMPLE	YIELD (MPa)	MODULUS (MPa)	TENSILE STRENGTH (MPa)	STRAIN AT BREAK (mm/mm)
Sample 1	9.8	203.8	12.76	4.41
Sample 2	11.66	208.5	11.98	3.14
Sample 3	10.24	194.5	12.66	3.39
Sample 4	10.36	211.4	12.32	3.14
Sample 5	10.3	200.1	12.88	3.11
Average	10.47	203.66	12.52	3.44
Stdev	0.70	6.71	0.37	0.56

S15

SAMPLE	YIELD (MPa)	MODULUS (MPa)	TENSILE STRENGTH (MPa)	STRAIN AT BREAK (mm/mm)
Sample 1	8.22	133.25	25.36	6.78
Sample 2	8.14	125.36	27.24	6.98
Sample 3	9.1	132.45	26.36	6.63
Sample 4	10.08	133.45	24.25	6.88
Sample 5	10.11	126.35	27.12	7.03
Average	9.13	130.17	26.07	6.86
Stdev	0.96	3.97	1.26	0.16

S18

SAMPLE	YIELD (MPa)	MODULUS (MPa)	TENSILE STRENGTH (MPa)	STRAIN AT BREAK (mm/mm)
Sample 1	7.55	116.23	32.24	6.71
Sample 2	7.64	115.96	26.65	6.702
Sample 3	8.01	118.95	30.24	6.81
Sample 4	8.06	117.45	30.33	6.69
Sample 5	8.1	114.32	31.01	6.678
Average	7.87	116.58	30.09	6.72
Stdev	0.26	1.73	2.08	0.05

S26

SAMPLE	YIELD (MPa)	MODULUS (MPa)	TENSILE STRENGTH (MPa)	STRAIN AT BREAK (mm/mm)
Sample 1	5.88	67.24	28.96	7.88
Sample 2	6.1	66.89	30.78	7.03
Sample 3	5.94	70.12	31.24	6.88
Sample 4	7.21	65.23	30.21	6.56
Average	6.28	67.37	30.30	7.09
Stdev	0.63	2.03	0.99	0.56

Table 4.6 Summary of the mechanical properties of the samples

POLYMER	INITIAL MODULUS (MPa)	YIELD STRESS (MPa)	TENSILE STRENGTH (MPa)	STRAIN AT BREAK (mm/mm)
LDPE	203	10.5	12.5	3.4
B-LLDPE	130	9.1	26.0	6.8
H-LLDPE	117	7.9	30.0	6.7
O-LLDPE	68	6.3	30.0	7.0

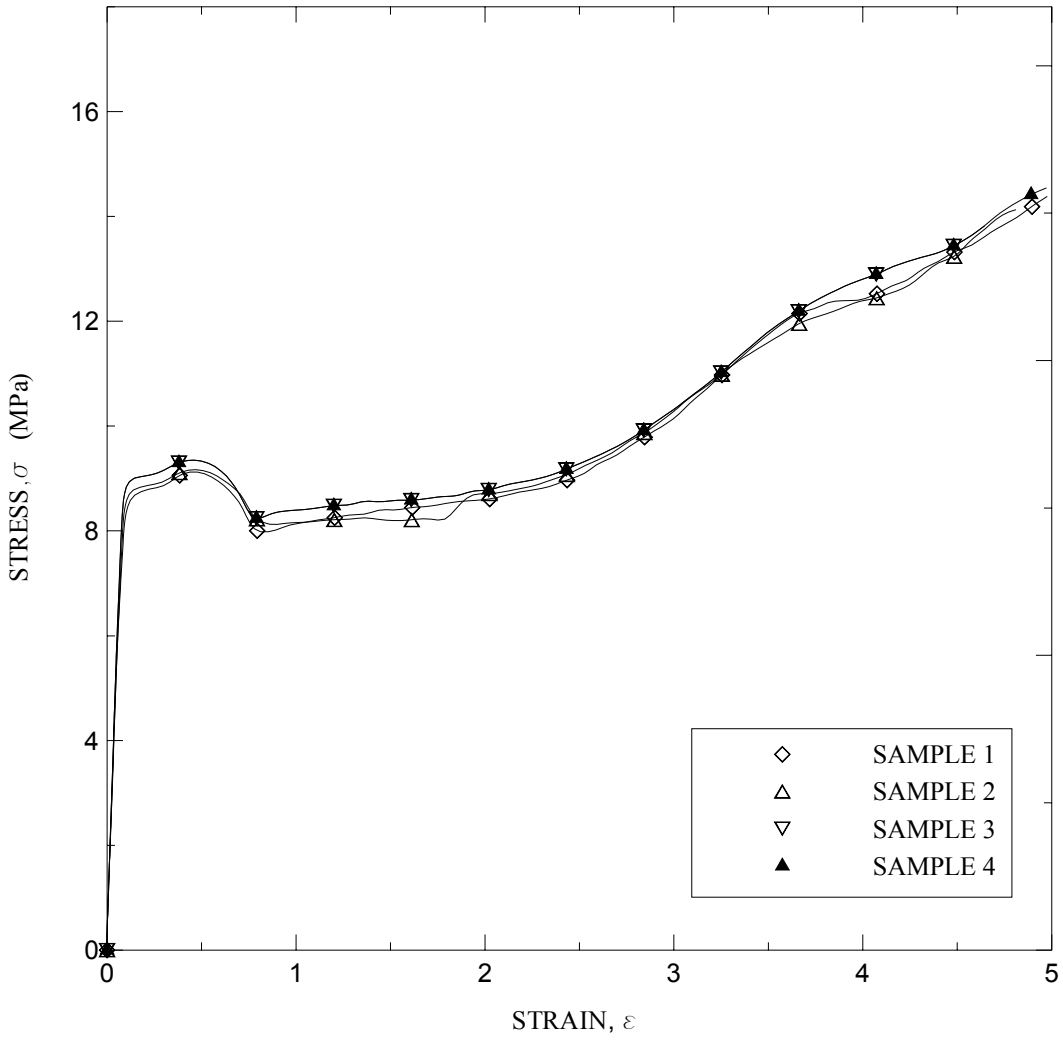

Figure 4.9: Stress-strain curves for 10/90 blends (B-LLDPE/LDPE)

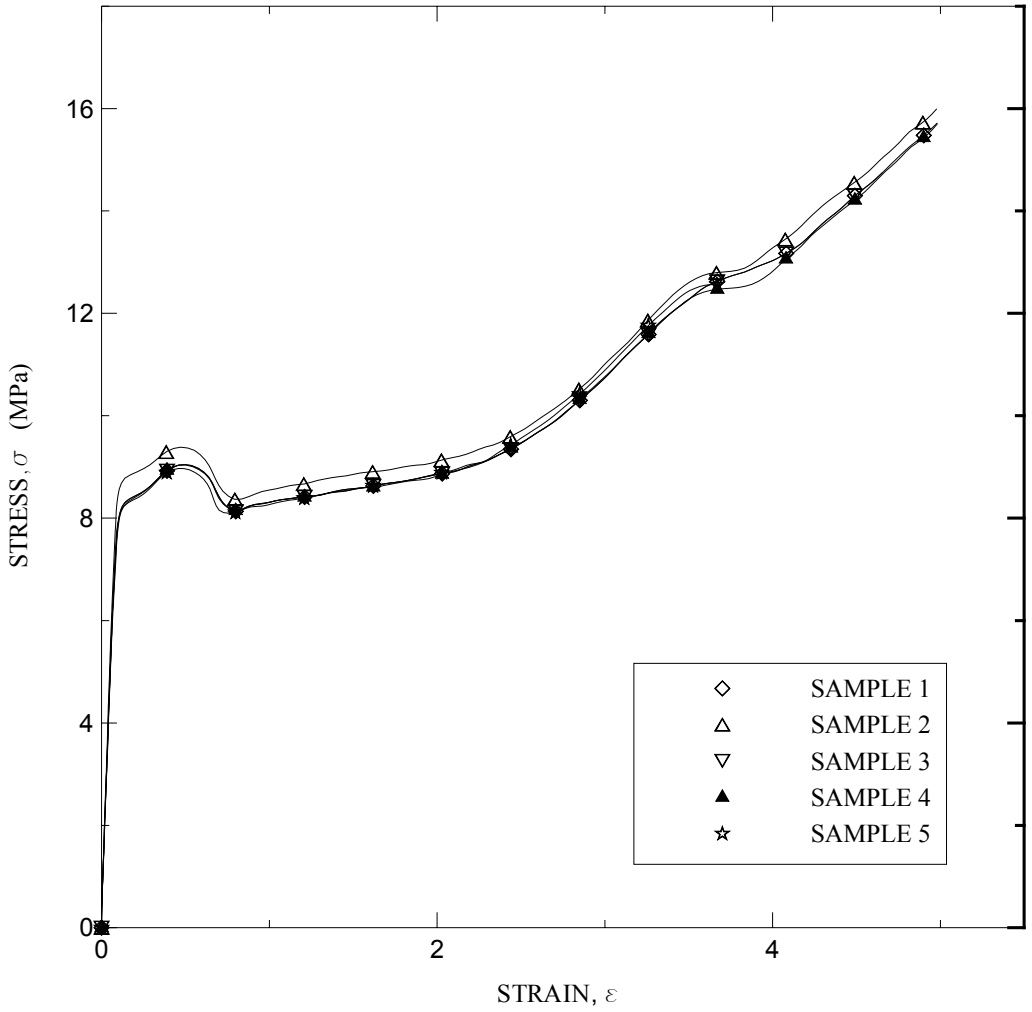

Figure 4.10: Stress-strain curves for 30/70 blends (B-LLDPE/LDPE)

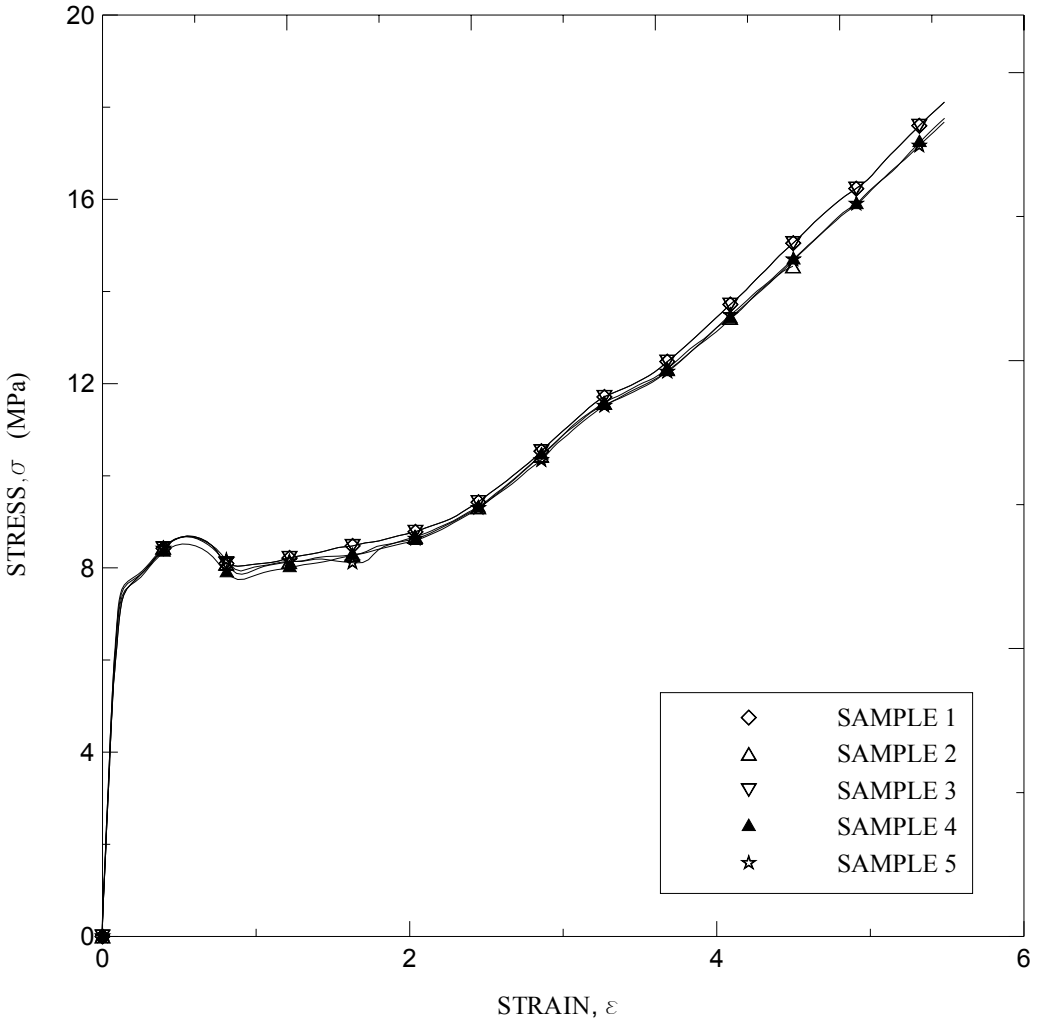

Figure 4.11: Stress-strain curves for 50/50 blends (B-LLDPE/LDPE)

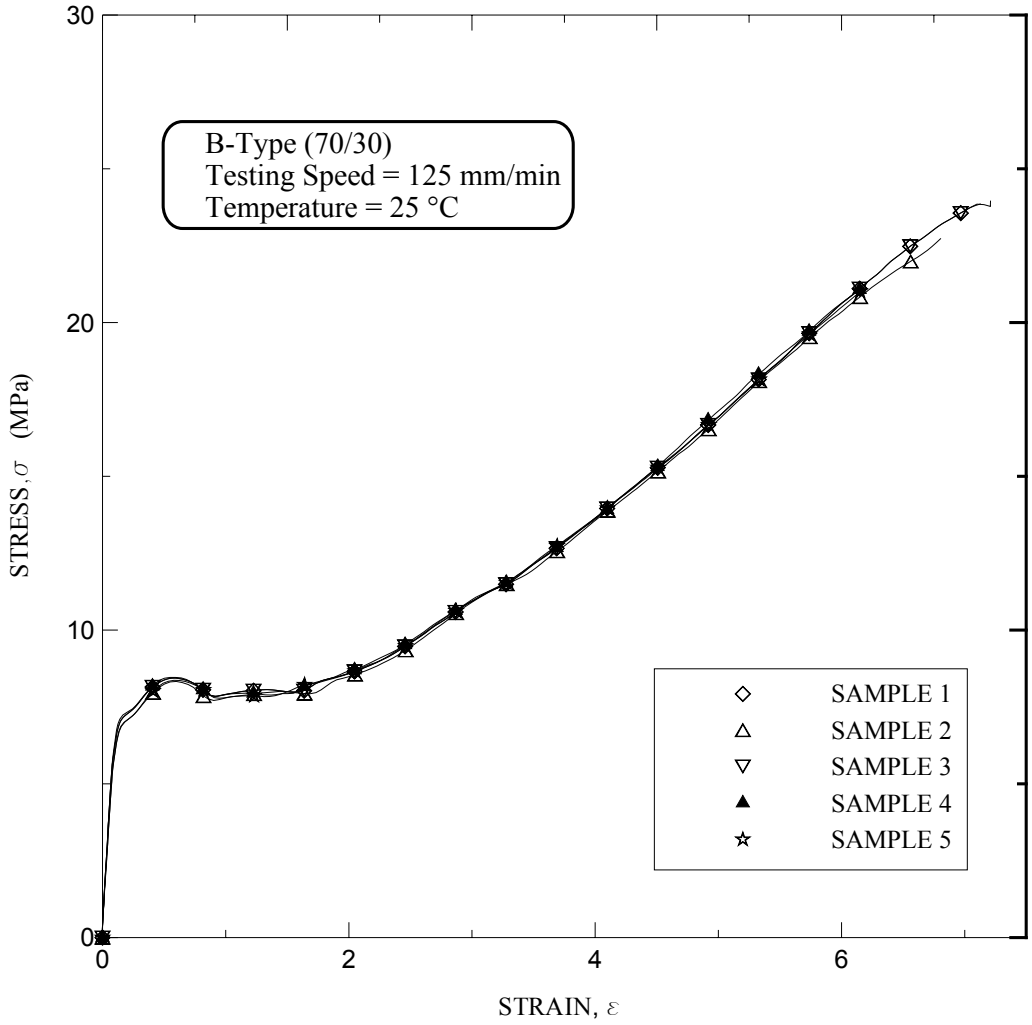

Figure 4.12: Stress-strain curves for 70/30 blends (B-LLDPE/LDPE)

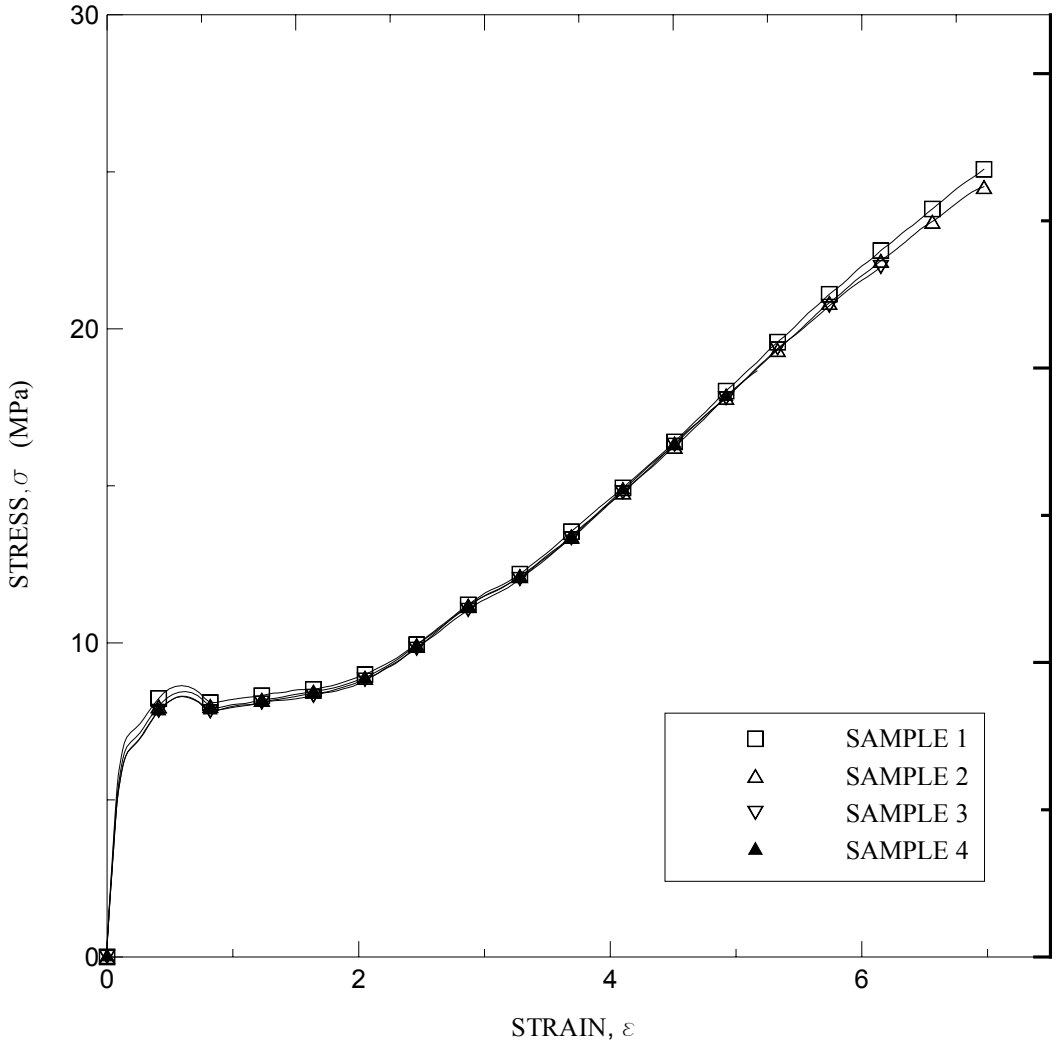

Figure 4.13: Stress-strain curves for 90/10 blends (B-LLDPE/LDPE)

Tensile results of the B-type samples are reported in Tables 4.7 and 4.8. The summary of the tensile results for B-type blends is reported in Table 4.9.

4.4.2 H-type Blend System (H-LLDPE/LDPE)

Stress-strain curves for all the H-type blend samples are reported in Figures 4.14-4.18. The tensile results for the H-type blend samples are reported in Tables 4.10 and 4.11. The large-scale deformation properties like ultimate stress and strain at break are higher for m-LLDPE compared to pure LDPE. The summary of the mechanical properties is reported in Table 4.12.

4.4.3 O-type Blend System (O-LLDPE/LDPE)

Stress-strain curves for all the O-type blend samples are reported in Figures 4.19-4.23. All the studied polymers display ductile behavior accompanied with the neck formation at the yield point. The tensile results of the blend samples are reported in Tables 4.13 and 4.14. The summary of the tensile results for the blends is reported in Table 4.15.

4.5 MICROHARDNESS RESULTS

Vicker's hardness tester is used for the microhardness measurement of the samples. The results are presented in terms of Vickers hardness number (VHN). A pyramidal diamond indenter with an included angle of 136° has been used.

Table 4.7 Mechanical properties of B-type blends

90/10 B-LLDPE/LDPE

SAMPLE	YIELD (MPa)	MODULUS (MPa)	TENSILE STRENGTH (MPa)	STRAIN AT BREAK (mm/mm)
Sample 1	8.24	132.04	24.65	6.88
Sample 2	8.12	129.568	25.13	6.91
Sample 3	8.11	127.568	25.62	6.85
Sample 4	8.1	132.45	24.31	6.78
Average	8.14	130.41	24.93	6.86
Stdev	0.07	2.28	0.57	0.06

70/30

SAMPLE	YIELD (MPa)	MODULUS (MPa)	TENSILE STRENGTH (MPa)	STRAIN AT BREAK (mm/mm)
Sample 1	8.41	150.26	23.4	6.31
Sample 2	8.32	162.34	24.13	6.24
Sample 3	8.38	150.12	23.14	6.28
Sample 4	8.36	148.9	20.36	6.55
Sample 5	8.3	146.31	21.44	6.18
Average	8.35	151.59	22.49	6.31
Stdev	0.04	6.22	1.55	0.14

50/50

SAMPLE	YIELD (MPa)	MODULUS (MPa)	TENSILE STRENGTH (MPa)	STRAIN AT BREAK (mm/mm)
Sample 1	8.61	145.12	18.1	5.51
Sample 2	8.54	140.2	17.8	5.56
Sample 3	8.48	142.65	17.4	5.44
Sample 4	8.46	141.66	17.56	5.41
Sample 5	8.41	143.12	16.63	5.39
Average	8.50	142.55	17.50	5.46
Stdev	0.08	1.82	0.55	0.07

Table 4.8 Mechanical properties of B-type blends

30/70 B-LLDPE/LDPE

SAMPLE	YIELD (MPa)	MODULUS (MPa)	TENSILE STRENGTH (MPa)	STRAIN AT BREAK
Sample 1	8.55	172.35	15.87	5.41
Sample 2	9.21	174.41	16.25	5.51
Sample 3	8.54	170.16	15.01	5.4
Sample 4	8.56	171.33	15.6	5.31
Sample 5	8.5	170.021	16.1	5.48
Average	8.67	171.65	15.77	5.42
Stdev	0.30	1.81	0.49	0.08

10/90 B-LLDPE/LDPE

SAMPLE	YIELD (MPa)	MODULUS (MPa)	TENSILE STRENGTH (MPa)	STRAIN AT BREAK
Sample 1	9.1	184.5	14	5.11
Sample 2	9.12	184.23	14.5	5.16
Sample 3	9.14	181.14	13.94	5.18
Sample 4	9.21	186.31	13.85	5.13
Average	9.14	184.05	14.07	5.15
Stdev	0.06	2.62	0.08	0.04

Table 4.9 Summary of the mechanical properties of B-type blends

POLYMER	INITIAL MODULUS, MPa	YIELD STRESS, MPa	TENSILE STRENGTH, MPa	STRAIN AT BREAK, mm/mm
B-LLDPE	130	9.13	26.0	6.8
10/90	131	8.14	24.9	6.8
30/70	152	8.35	22.5	6.3
50/50	143	8.50	17.5	5.4
70/30	172	8.67	15.7	5.42
90/10	184	9.14	14.07	5.14
LDPE	203	10.47	12.52	3.44

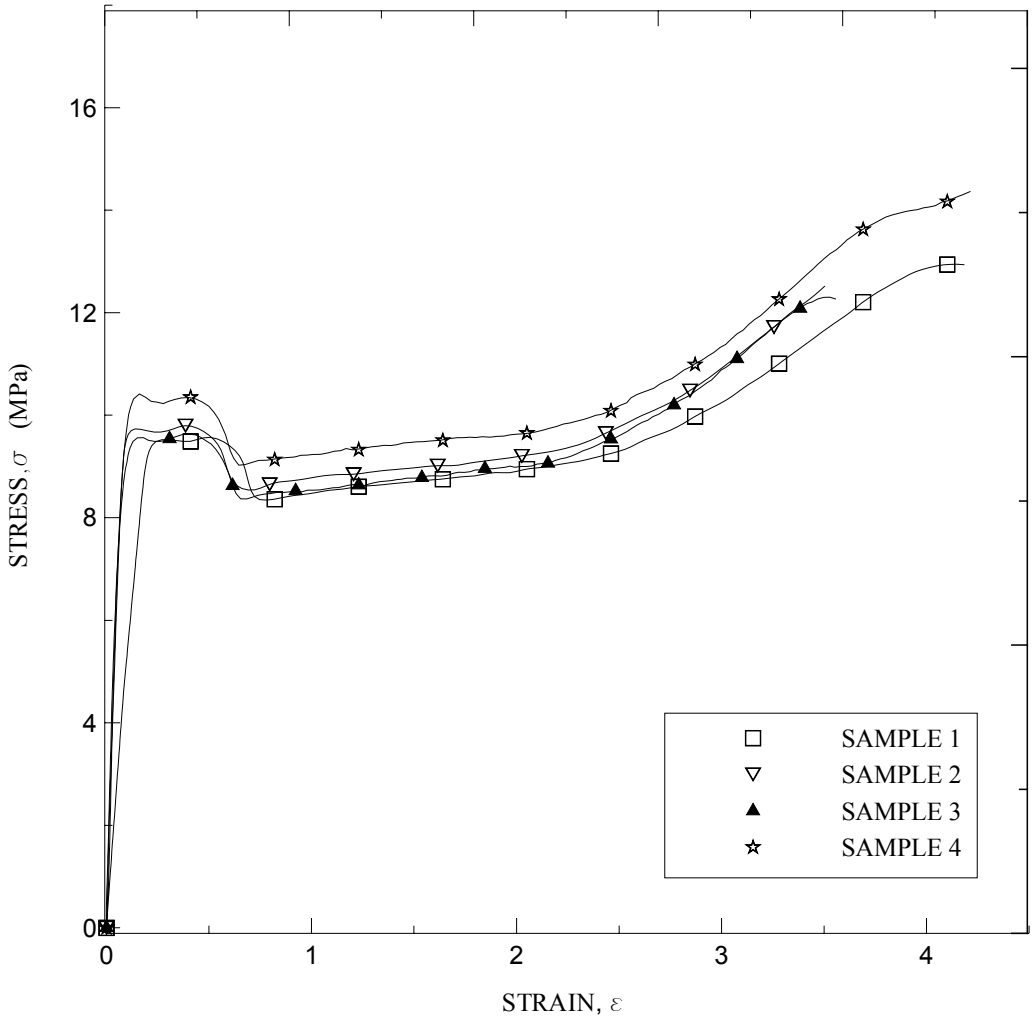

Figure 4.14: Stress-strain curves for 10/90 blends (H-LLDPE/LDPE)

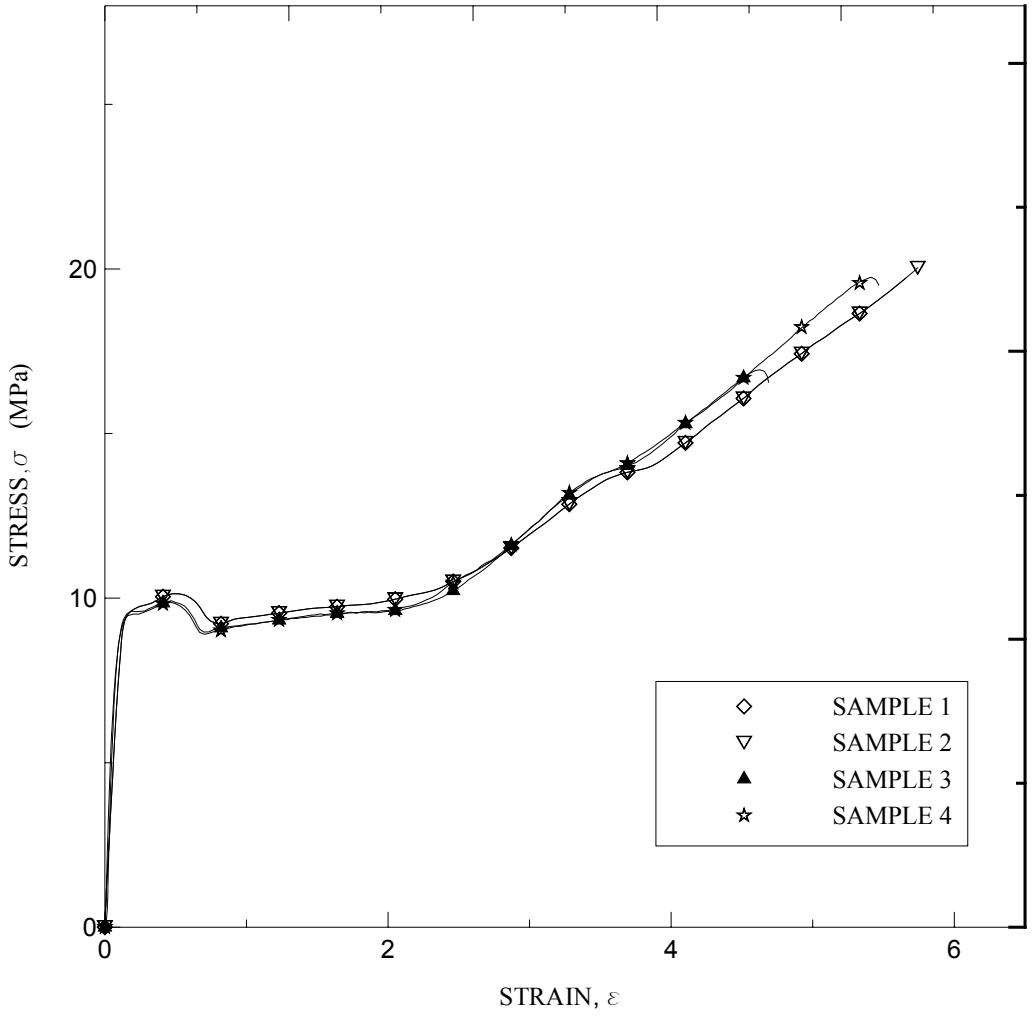

Figure 4.15: Stress-strain curves for 30/70 blends (H-LLDPE/LDPE)

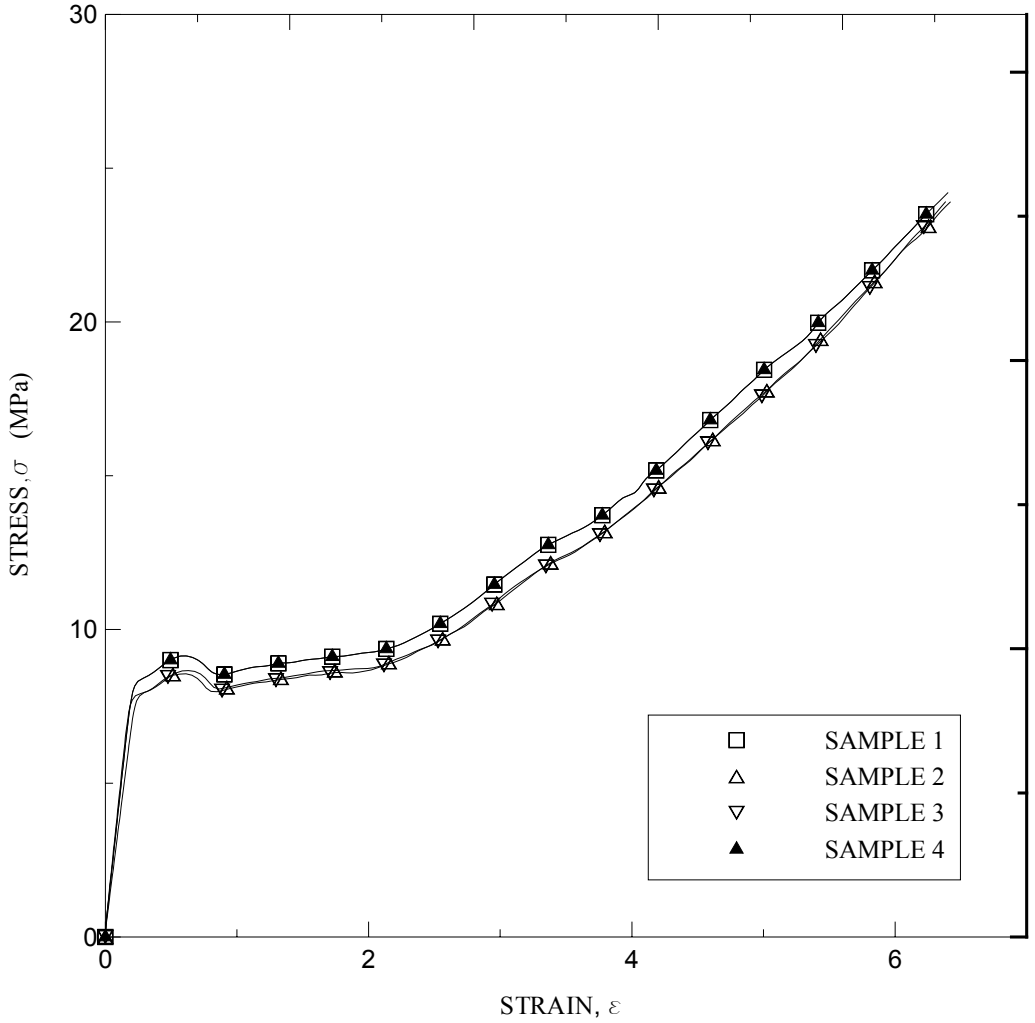

Figure 4.16: Stress-strain curves for 50/50 blends (H-LLDPE/LDPE)

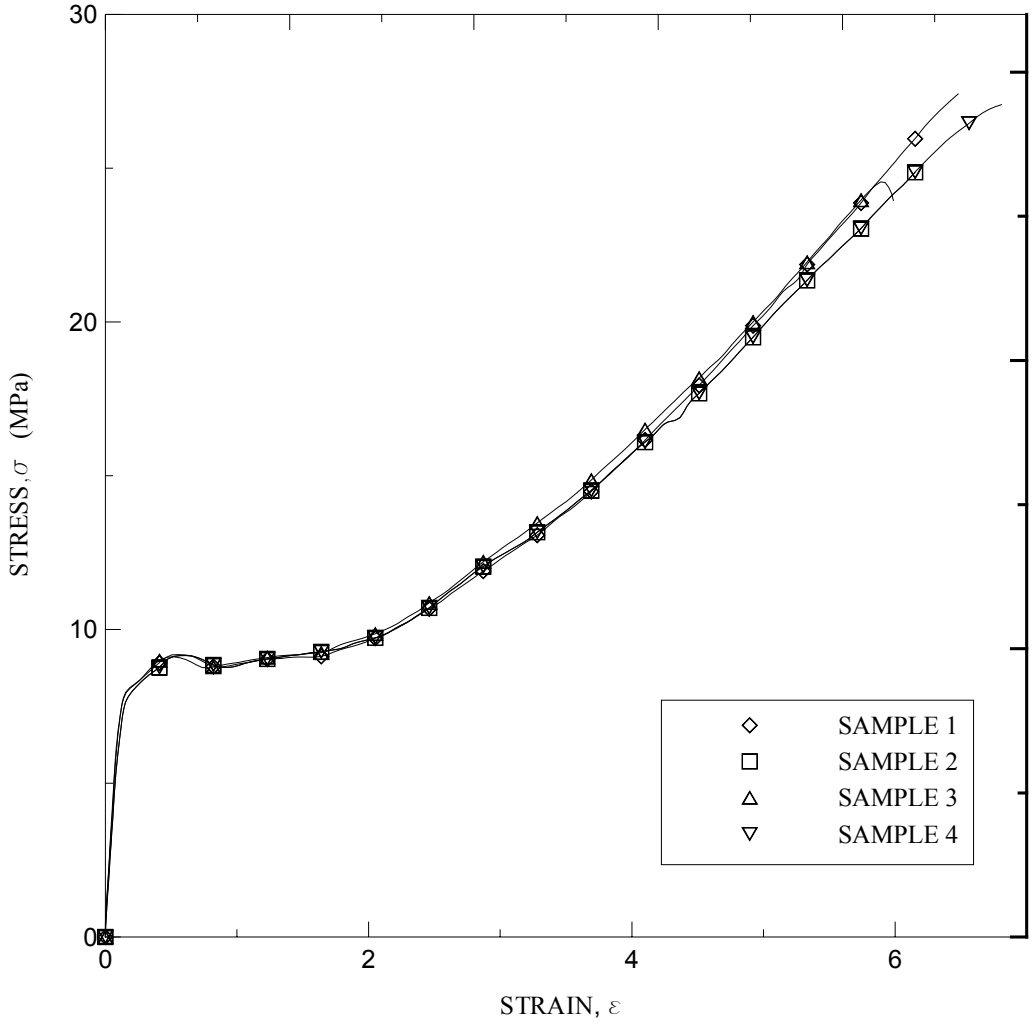

Figure 4.17: Stress-strain curves for 70/30 blends (H-LLDPE/LDPE)

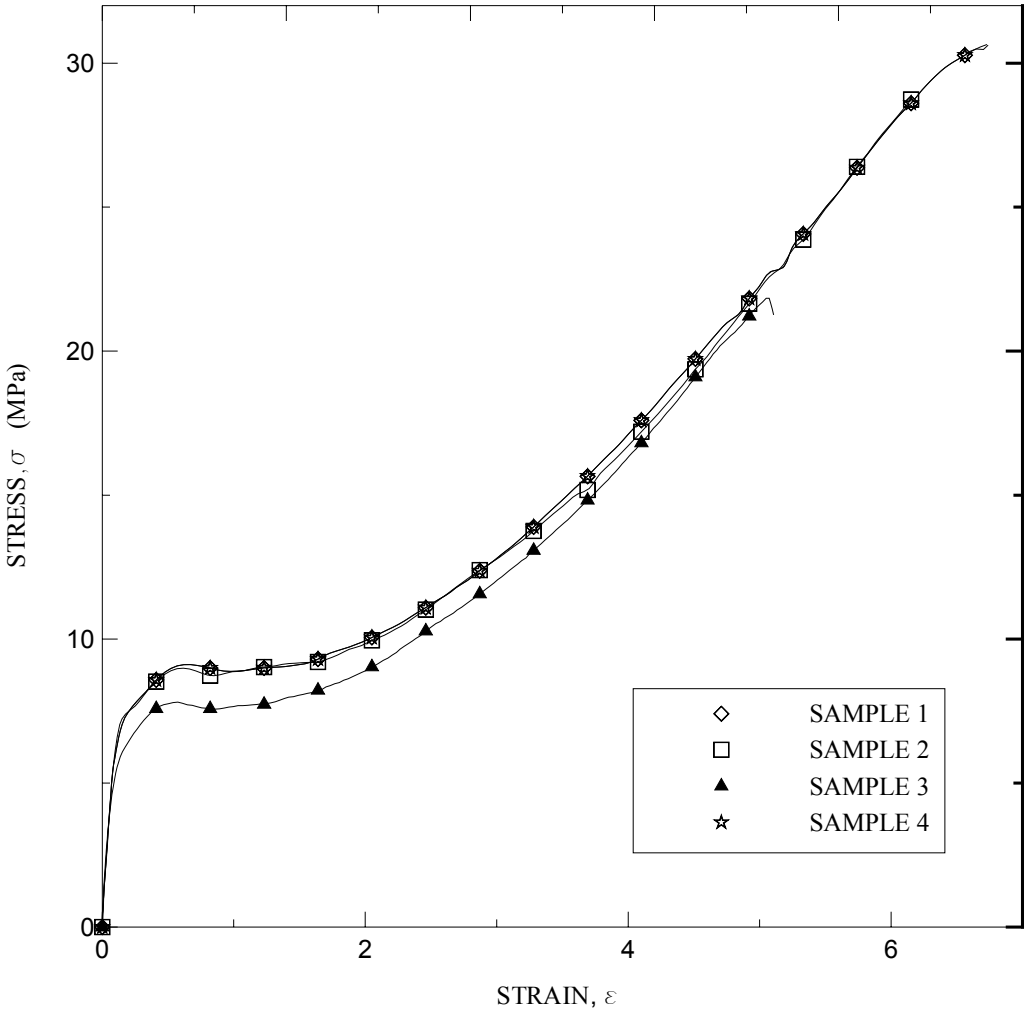

Figure 4.18: Stress-strain curves for 90/10 blends (H-LLDPE/LDPE)

Table 4.10 Mechanical properties of H-type blends

H-LLDPE/LDPE **90/10**

SAMPLE	YIELD (MPa)	MODULUS (MPa)	TENSILE STRENGTH (MPa)	STRAIN AT BREAK (mm/mm)
Sample 1	9.11	125.64	30.1	6.55
Sample 2	9	122.21	28.86	6.51
Sample 3	8.94	126.12	28.44	6.62
Sample 4	7.88	125	27.11	6.58
Average	8.73	124.74	28.63	6.57
Stdev	0.57	1.75	1.23	0.05

70/30

SAMPLE	YIELD (MPa)	MODULUS (MPa)	TENSILE STRENGTH (MPa)	STRAIN AT BREAK (mm/mm)
Sample 1	9.11	160.12	26.1	6.55
Sample 2	9.14	164.25	26.65	6.61
Sample 3	9.1	161.24	24.5	6.64
Sample 4	9.2	163.36	24.98	6.51
Average	9.14	162.24	25.56	6.58
Stdev	0.05	1.90	0.99	0.06

50/50

SAMPLE	YIELD (MPa)	MODULUS (MPa)	TENSILE STRENGTH (MPa)	STRAIN AT BREAK (mm/mm)
Sample 1	9.14	168.23	24.1	6.51
Sample 2	8.89	169.21	25.32	6.48
Sample 3	8.96	165.48	22.46	6.36
Sample 4	8.24	166.23	23.64	6.4
Average	8.81	167.29	23.88	6.44
Stdev	0.39	1.73	1.18	0.07

Table 4.11 Mechanical properties of H-type blends

30/70

SAMPLE	YIELD (MPa)	MODULUS (MPa)	TENSILE STRENGTH (MPa)	STRAIN AT BREAK (mm/mm)
Sample 1	10.08	162.5	22.31	6
Sample 2	9.88	164.32	20.34	6.1
Sample 3	9.94	166.31	21.34	5.89
Sample 4	9.82	167.81	21.14	5.94
Average	9.93	165.24	21.28	5.98
Stdev	0.11	2.32	0.81	0.09

10/90

SAMPLE	YIELD (MPa)	MODULUS (MPa)	TENSILE STRENGTH (MPa)	STRAIN AT BREAK (mm/mm)
Sample 1	10.24	166.45	14.5	4.41
Sample 2	9.98	168.27	12.99	4.11
Sample 3	9.68	167.31	12.54	4.31
Sample 4	9.78	169.01	13.1	4.38
Average	9.92	167.76	13.28	4.30
Stdev	0.15	0.85	0.30	0.14

Table 4.12 Summary of the mechanical properties of H-type blends

POLYMER	MODULUS, MPa	YIELD STRESS, MPa	TENSILE STRENGTH, MPa	STRAIN AT BREAK, mm/mm
H-LLDPE	117	7.87	30	6.7
10/90	125	8.73	28.62	6.565
30/70	162	9.14	25.46	6.56
50/50	167	8.81	23.7	6.43
70/30	165	9.93	21.2	5.96
90/10	168	9.92	13.28	4.3
LDPE	203	10.47	12.52	3.44

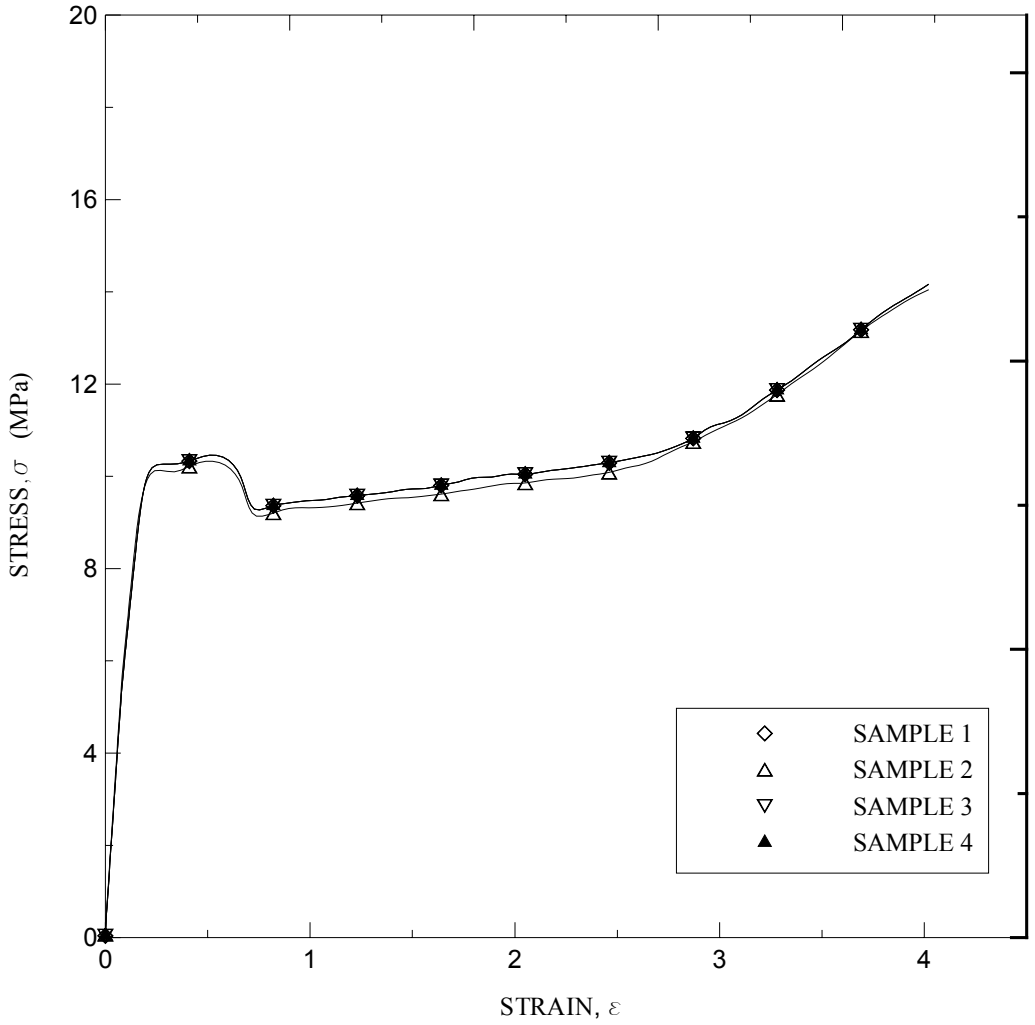

Figure 4.19: Stress-strain curves for 10/90 blends (O-LLDPE/LDPE)

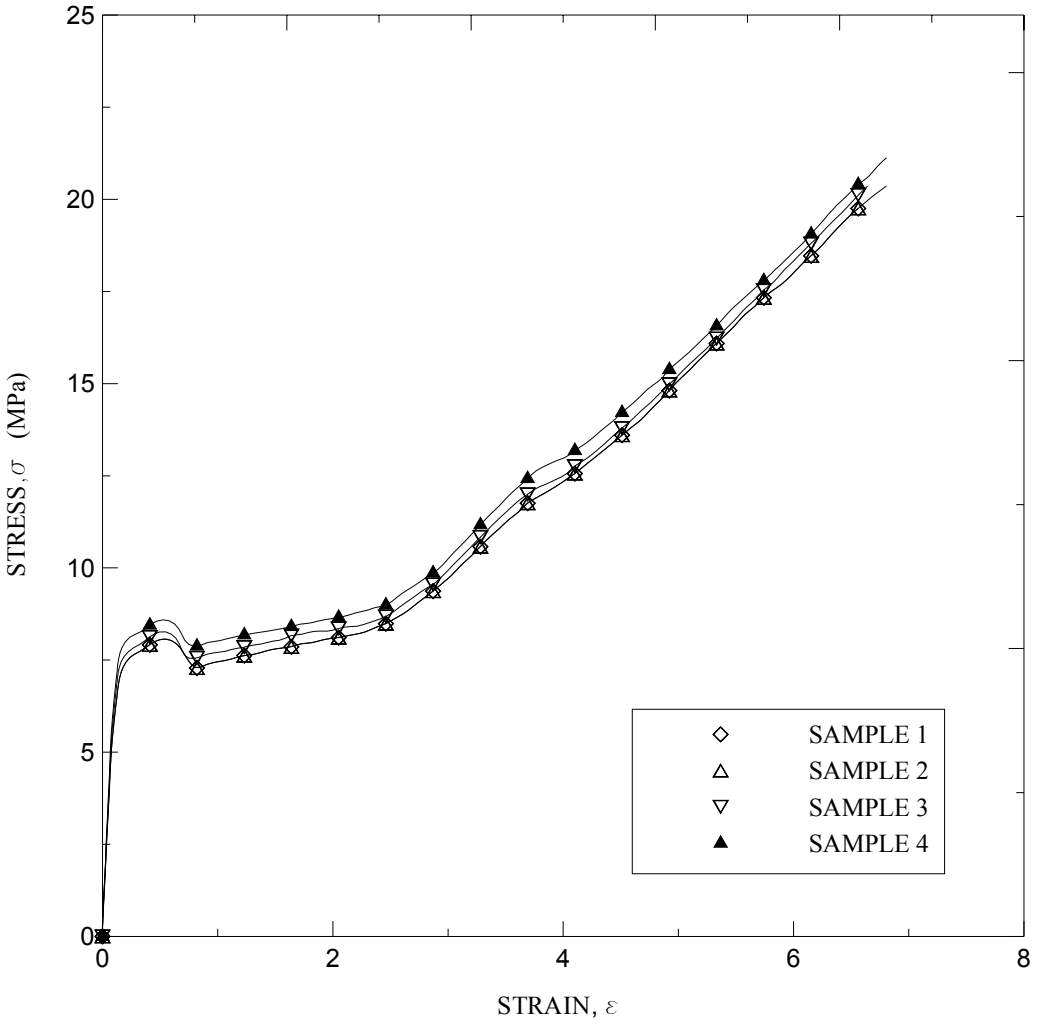

Figure 4.20: Stress-strain curves for 30/70 blends (O-LLDPE/LDPE)

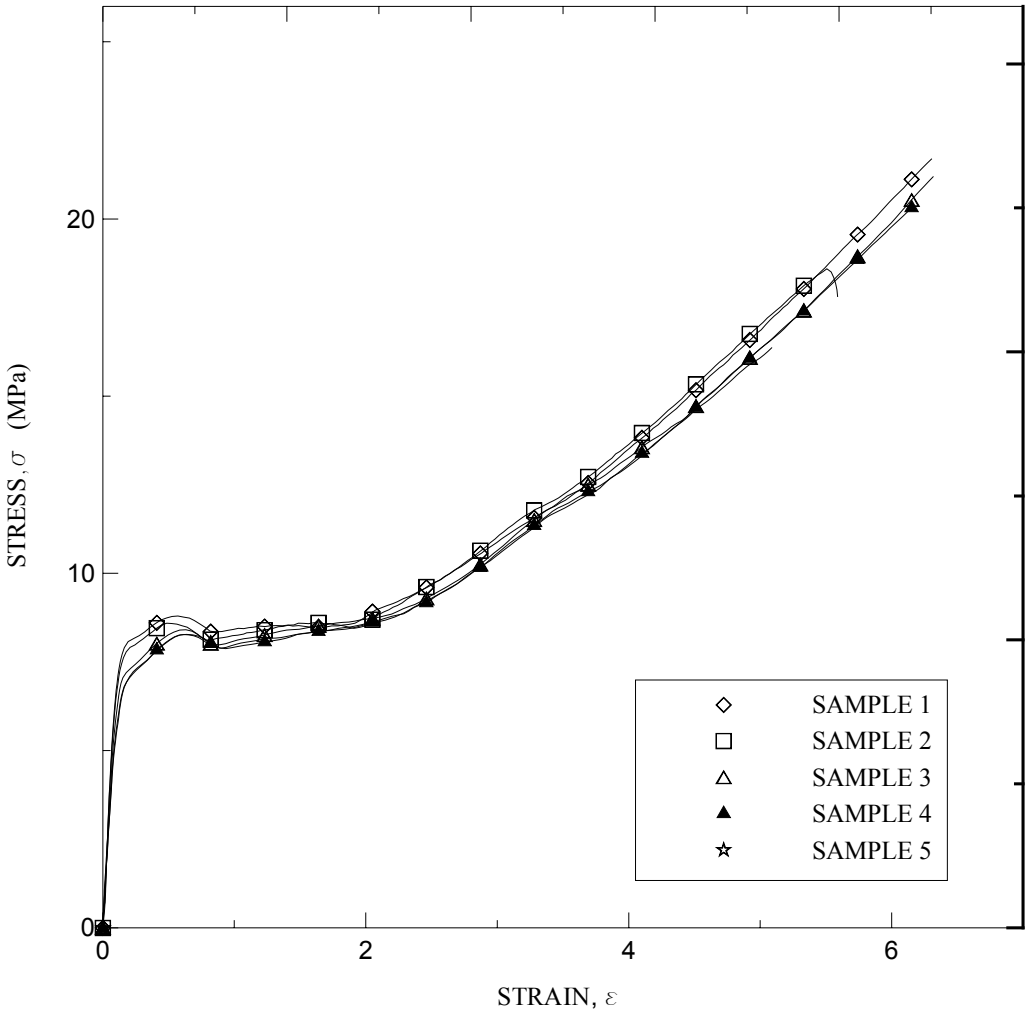

Figure 4.21: Stress-strain curves for 50/50 blends (O-LLDPE/LDPE)

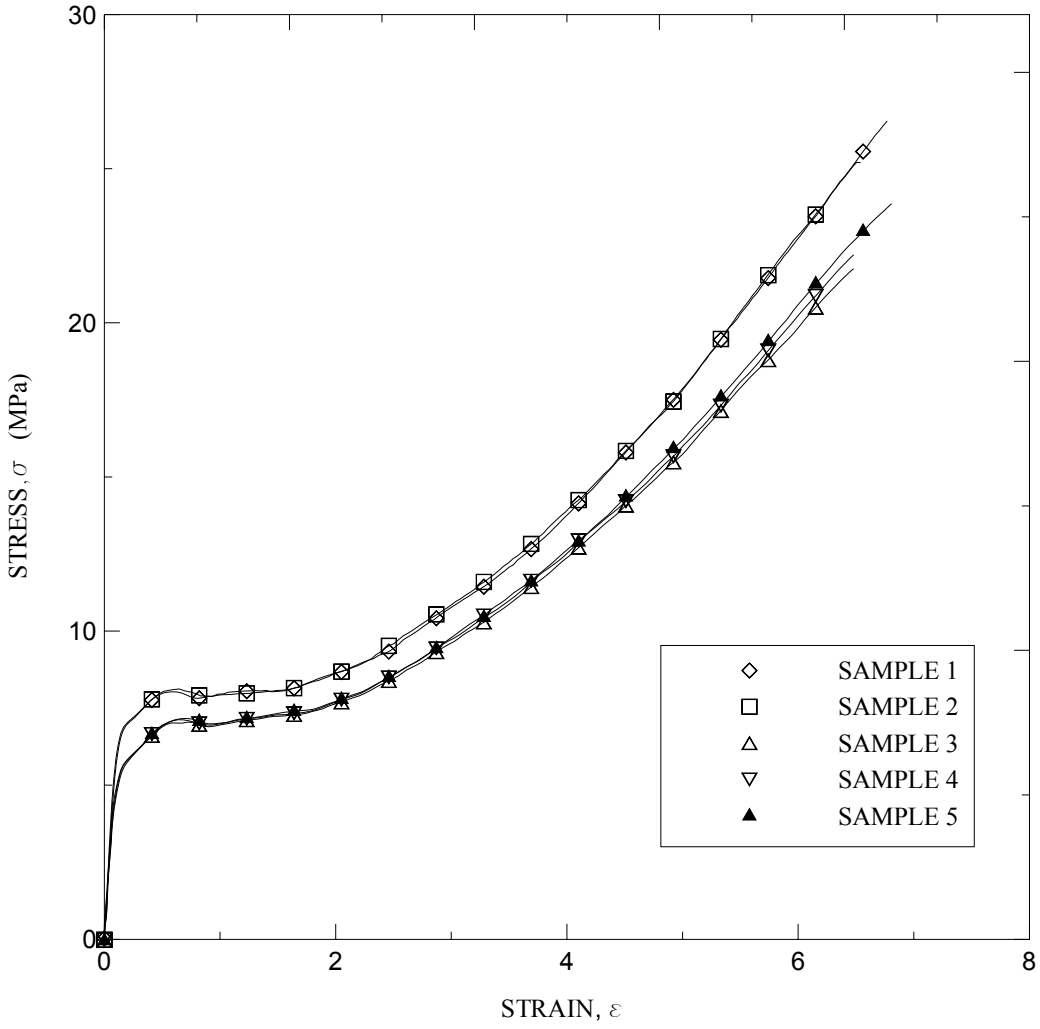

Figure 4.22: Stress-strain curves for 70/30 blends (O-LLDPE/LDPE)

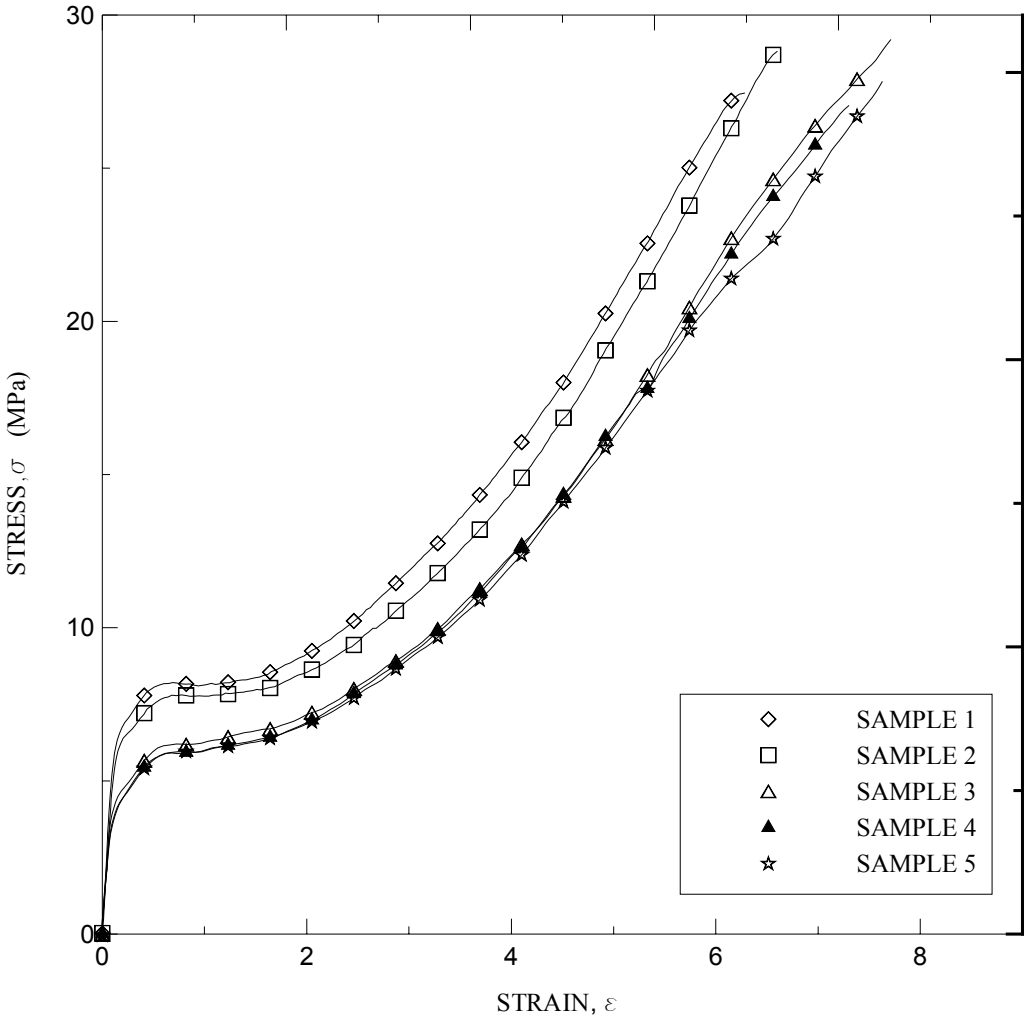

Figure 4.23: Stress-strain curves for 90/10 blends (O-LLDPE/LDPE)

Table 4.13 Mechanical properties of O-type blends

90/10 O-LLDPE/LDPE

SAMPLE	YIELD (MPa)	MODULUS (MPa)	TENSILE STRENGTH (MPa)	STRAIN AT BREAK (mm/mm)
Sample 1	7.81	60.89	28.15	7.01
Sample 2	7.41	62.14	29.14	5.98
Sample 3	6.14	62.24	29	6.64
Sample 4	6.18	63.1	28.55	6.12
Sample 5	6.21	60.99	28.41	6.24
Average	6.75	61.87	28.65	6.40
Stdev	0.80	0.93	0.41	0.42

70/30

SAMPLE	YIELD (MPa)	MODULUS (MPa)	TENSILE STRENGTH (MPa)	STRAIN AT BREAK (mm/mm)
Sample 1	7.74	77.21	26.07	6.54
Sample 2	7.92	76.15	25.1	6.68
Sample 3	6.89	75.68	24.68	6.63
Sample 4	6.68	77.1	23.64	6.62
Sample 5	6.68	76.66	25.64	6.65
Average	7.18	76.56	25.03	6.62
Stdev	0.60	0.65	0.94	0.05

50/50

SAMPLE	YIELD (MPa)	MODULUS (MPa)	TENSILE STRENGTH (MPa)	STRAIN AT BREAK (mm/mm)
Sample 1	8.21	92.1	22.1	6.14
Sample 2	8.04	93.4	21.56	5.21
Sample 3	8	85.46	20	5.64
Sample 4	8.08	84.21	20.46	6.22
Sample 5	8.21	83.5	20.16	6.31
Average	8.11	87.73	20.86	5.90
Stdev	0.10	4.66	0.92	0.47

Table 4.14 Mechanical properties of O-type blends

30/70

SAMPLE	YIELD (MPa)	MODULUS (MPa)	TENSILE STRENGTH (MPa)	STRAIN AT BREAK (mm/mm)
Sample 1	8.86	69.1	22.05	6.94
Sample 2	8.84	68.24	21.89	6.89
Sample 3	8.78	70.24	22.46	6.64
Sample 4	8.62	70.36	23	6.71
Average	8.78	69.49	22.35	6.80
Stdev	0.11	1.01	0.50	0.14

10/90

SAMPLE	YIELD (MPa)	MODULUS (MPa)	TENSILE STRENGTH (MPa)	STRAIN AT BREAK (mm/mm)
Sample 1	10.33	108.64	14.1	3.99
Sample 2	10.24	109.21	14	4.04
Sample 3	10	107.36	12.68	4.06
Sample 4	10.15	107.11	12.4	3.98
Average	10.18	108.08	13.30	4.02
Stdev	0.14	1.01	0.88	0.04

Table 4.15 Summary of the mechanical properties of O-type blends

POLYMER	MODULUS, MPa	YIELD STRESS, MPa	TENSILE STRENGTH, MPa	STRAIN AT BREAK, mm/mm
O-LLDPE	68	6.28	30	7.00
10/90	62	6.75	29	6.40
70/30	77	6.68	25	6.62
50/50	88	8.11	20.85	5.91
70/30	69	8.78	22.4	6.82
90/10	108	10.18	13.3	4.01
LDPE	203	10.47	12.52	3.44

All the results are averages of at least six measurements. The indentation time was 10 seconds and the applied load is 10gf for all the samples tested.

4.5.1 Blend Samples

Microhardness results of samples are reported in Table 4.16. Microhardness results of B-type, H-type and O-type blend samples are reported in Tables 4.17-4.19.

4.5.2 Effect of Indentation Time

To study the effect of indentation time on VHN, the tests are carried out different indentation times as reported in Tables 4.20 and 4.21. These tests were carried out for the samples of pure LDPE and pure B-LLDPE samples.

Figure 4.24 depicts the relationship between indentation times and VHN for the two polymers (LDPE and B-LLDPE).

Table 4.16 Microhardness results for pure samples

Polymer	Test 1	Test 2	Test 3	Test 4	Test 5	Test 6	Average	Stdev
LDPE	2.50	2.50	2.40	2.60	2.60	2.60	2.53	0.08
B-LLDPE	2.10	2.20	2.00	2.00	2.00	2.00	2.05	0.08
H-LLDPE	1.90	1.70	1.80	1.90	1.80	1.90	1.83	0.08
O-LLDPE	1.50	1.40	1.50	1.40	1.50	1.40	1.45	0.05

Table 4.17 Microhardness results for B-type blend samples

Polymer	Test 1	Test 2	Test 3	Test 4	Test 5	Test 6	Average	Stdev
B-LLDPE	2.1	2.2	2	2	2	2	2.06	0.08
90/10	1.9	1.9	1.9	2	2	1.9	1.94	0.05
70/30	1.9	2.1	2.2	2	2.3	2.2	2.10	0.15
50/50	2.1	2.2	2.3	2.3	2.2	2.1	2.22	0.09
30/70	2.2	2.2	2.3	2.4	2.4	2.5	2.30	0.12
10/90	2.5	2.4	2.6	2.7	3	3.1	2.64	0.28
LDPE	2.5	2.5	2.4	2.6	2.6	2.6	2.52	0.08

Table 4.18 Microhardness results for H-type blend samples

Polymer	Test 1	Test 2	Test 3	Test 4	Test 5	Test 6	Average	Stdev
H-LLDPE	1.9	1.7	1.8	1.9	1.8	1.9	1.83	0.08
90/10	1.6	2.2	1.8	1.9	1.8	1.7	1.83	0.21
70/30	1.8	1.8	1.8	1.9	1.9	1.8	1.83	0.05
50/50	2	2	2	2.1	1.9	2.1	2.02	0.08
30/70	2	2.1	2.2	2.1	2.2	2.2	2.13	0.08
10/90	2.2	2.2	2.4	2.4	2.4	2.4	2.33	0.10
LDPE	2.5	2.5	2.4	2.6	2.6	2.6	2.53	0.08

Table 4.19 Microhardness results for O-type blend samples

Polymer	Test 1	Test 2	Test 3	Test 4	Test 5	Test 6	Average	Stdev
O-LLDPE	1.5	1.4	1.5	1.4	1.5	1.4	1.45	0.05
90/10	1.3	1.3	1.3	1.5	1.5	1.5	1.40	0.11
70/30	1.4	1.6	1.6	1.6	1.7	1.6	1.58	0.10
50/50	1.6	1.7	1.8	2	1.9	1.9	1.82	0.15
30/70	1.8	2.1	2	2	2.1	2.1	2.02	0.12
10/90	2.5	2.2	2.2	2.3	2.4	2.4	2.33	0.12
LDPE	2.5	2.5	2.4	2.6	2.6	2.6	2.53	0.08

Table 4.20 VHN at different indentation times for pure LDPE sample

VHN	TIME (s)
2.52	10
2.5	15
2.4	20
2.4	30
2.4	40
2.4	50

Table 4.21 VHN at different indentation times for pure B-LLDPE sample

VHN	**TIME(s)**
2.06	10
2	15
2	20
1.8	30
1.9	40
1.9	60
1.7	80
1.7	90

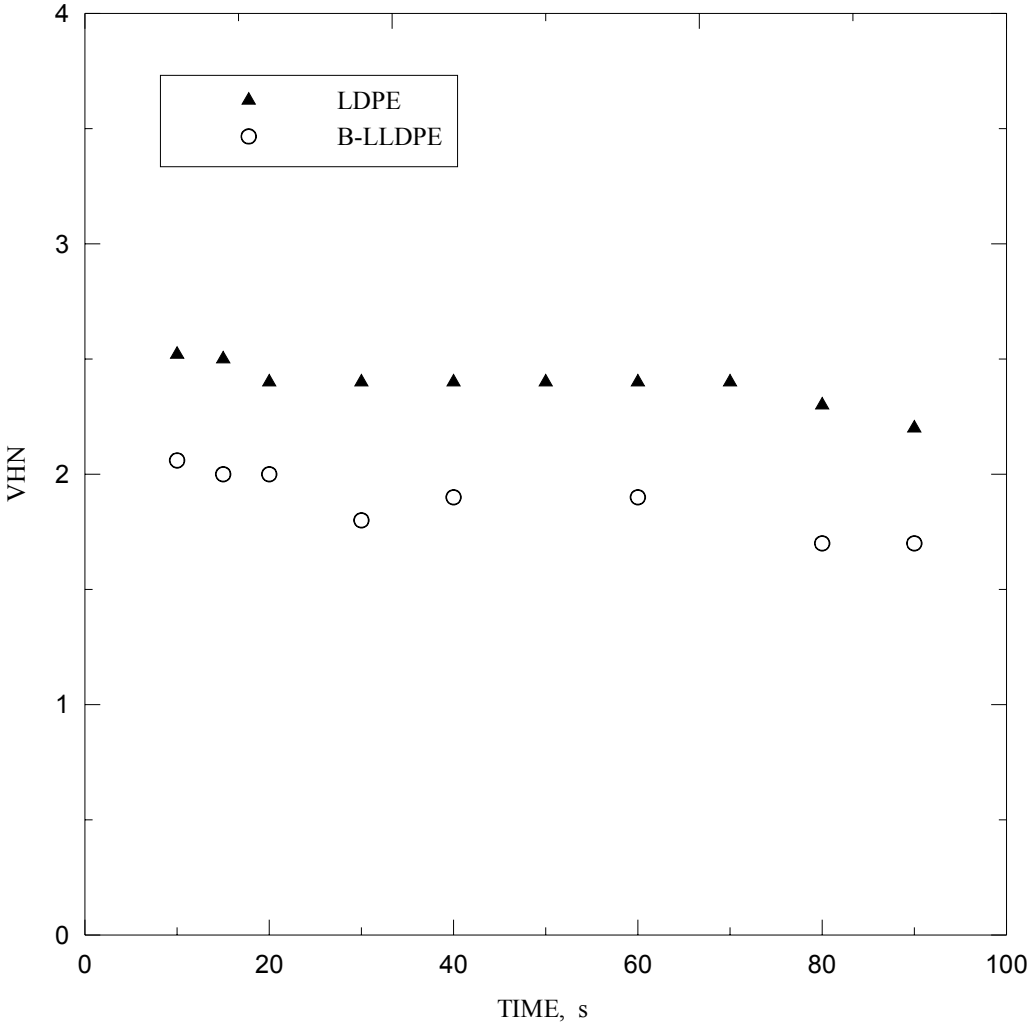

Figure 4.24: Effect of indentation time(s) on VHN

CHAPTER 5

DISCUSSION

5.1 INTRODUCTION

The blend samples shall be discussed in terms of compatibility. Compatible can be defined in terms of linear additive rule of mixtures, which can be given by

$$M = x_1 m_1 + x_2 m_2 \tag{5.1}$$

Where 'M' is any mechanical property (Initial Modulus, Yield stress, Tensile strength etc), 'x1' is the weight fraction of the component 1; 'm1' is the mechanical property of the component. Similarly 'x2' and 'm2' for the component 2. Semi-compatible, if the properties are intermediate to that of parent polymers but vary in non-linear fashion and incompatible if the properties of the blend ratios show negative deviations to the rule of mixtures.

5.2 THERMAL ANALYSIS

The thermal analyses of all the prepared samples were conducted using the Mettler DSC822^{e}. The crystalline melting thermograms were obtained by heating the samples from 40°C to 140°C at a heating rate of 10°C/min.

5.2.1 DSC Scans of Pure Samples

DSC melting thermograms for all four polymers are shown in Figure 4.1. The results of DSC scans are summarized in Table 4.1. Rana et al [58] investigated the thermal and mechanical properties of the blends of ethylene 1-octene copolymer synthesized by Ziegler-Natta and metallocene catalysts. Starck and Lofgren [59] investigated the thermal properties of ethylene/long chain α- olefin copolymers produced by metallocenes. Higher α- olefins were characterized by dynamic scanning caloriemeter (DSC) and dynamic mechanical analysis (DMA). The DMA measurements confirmed the decrease in crystallinity at increasing comonomer incorporation.

It is clear that the melting peaks of all the m-LLDPE samples are lower than that of the LDPE. According to results of Table 3.1, the branch content of LDPE is lower than that of m-LLDPE samples. As a result, thicker lamellae structure is more susceptible for developing during the solidification process of LDPE. From previous studies, it is well known fact that the melting behavior of polymers is proportional to the lamellae thickness [60].It is observed that the thicker the lamellae, the higher the melting peak. Consequently, high melting points are observed in the DSC scan of LDPE. DSC scans of

LDPE and B-LLDPE reveal narrow melting behavior with peaks at 111°C and 107°C, respectively; whereas, H-LLDPE and O-LLDPE show a relatively broader melting behavior with peaks at 108°C and 98°C, respectively. In addition, the DSC scan of H-LLDPE shows the existence of two broad melting peaks at 99°C and 108°C. It is well known that in polymers, there exists a distribution of molecular weights, chain lengths and lamellae thickness. This existence of the two peaks in the melting behavior of the pure H-LLDPE samples is most probably attributed to the bimodal (predominantly two types) distribution of the lamellae thickness.

5.2.2 DSC Scans of B-type Blends

For the B-type blend system (Figure 4.2), it can be seen that only a single melting peak is observed in each blend irrespective of blend composition. Figure 5.1 shows the compositional dependence of melting temperature (T_m), endset temperature and percent crystallinity for B-type blend system. The melting peaks and endset temperatures of the blends are intermediate between those of the individual pure polymers. The increase in melting temperature (Figure 5.1a) of the blend with the increase in LDPE can be attributed to the development of thicker lamellae microstructure. A nearly compatible behavior is resulted in this case. Figure 5.1(b) shows a little improvement in the endset temperatures of blends with the LDPE content. The endset temperatures remains constant after an initial improvement till 50% LDPE. At higher concentration of LDPE, the endset temperature values of all the blends are closer to that of pure LDPE.

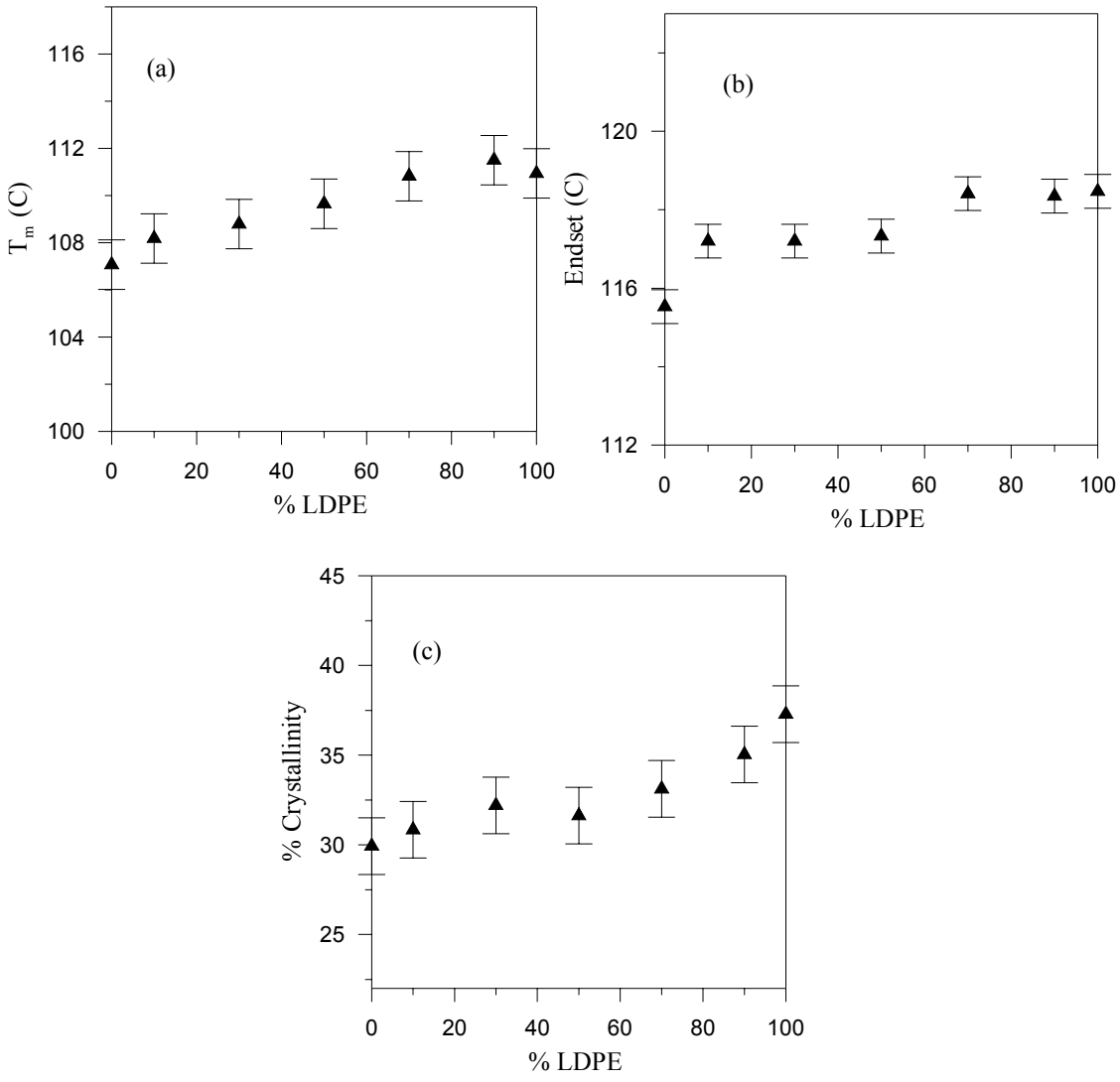

Figure 5.1: Thermal characterization of B-Type blends (a) Melting temperature versus %LDPE (b) Endset melting temperature versus % LDPE (c) Crystallinity versus % LDPE.

This indicates that thicker lamellae are growing in all the B-type blends. However, this improvement in lamellae thickness did not enhance the amount of crystallinity. According to Figure 5.1c, the percent crystallinity increased linearly with LDPE content up to 30% LDPE. However, at higher % LDPE, the crystallinity is lower than that expected from the rule of mixture. This fact is due to the branch content difference between the two polymers. According to Table 3.1, LDPE has lower branched content (11.0) compared to that of B-LLDPE (14.5). On one hand, at low concentration of LDPE, the crystallization is improved because LDPE molecules have larger linear segments, which are able to crystallize much easier. For example these segments can easily attach themselves to smaller lamellae crystals. On the other hand, at concentration higher than 50% of LDPE (for example 30/70), the B-LLDPE molecules with smaller linear segments will slow the nucleation as well as the crystal growth of LDPE molecules. This results in lower crystallinity. Since the sample preparation is being conducted at very fast cooling rate (200°C/min), there is not enough time for many LDPE crystals to grow. As a consequence, lower crystallinity value is obtained.

5.2.3 DSC Scans of O-type Blends

A similar behavior in the melting peaks to that of the B-type is observed (Figure 4.2). The thermal characterization data for all the blend ratios of O-type blends is reported in Table 4.3. It can be inferred from Figure 5.2a that the melting temperatures of the blends increase rapidly for LDPE <50%, and then stabilize at the melting temperature of pure LDPE

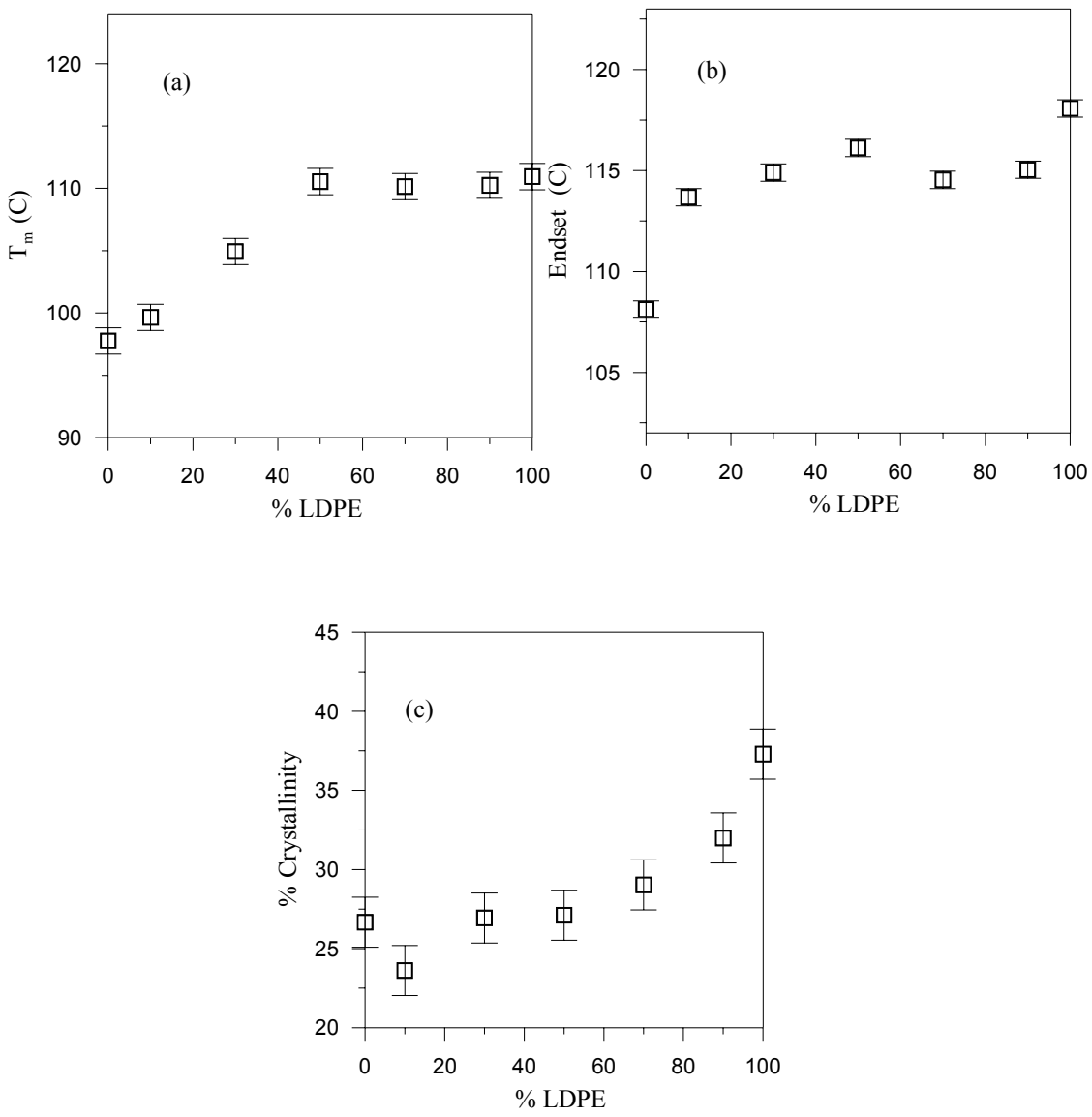

Figure 5.2: Thermal characterization of O-Type blends (a) Melting temperature versus %LDPE (b) Endset melting temperature versus % LDPE(c) Crystallinity versus % LDPE.

Figure 5.2b, which represents the endset melting temperature of O-type blends, indicates that thicker lamellae structure is developed for all the blend ratios. This indicates that LDPE is enhancing the development of large crystals. However, the amount of crystallinity is not improving with the addition of LDPE up to 50% mixture. According to Figure 5.2c, small addition of O-type LLDPE molecules to LDPE polymers results in large decrease in crystallinity. This phenomenon can be explained with the fact that O-type branch content is higher than that of LDPE, which results in smaller linear segments in O-LLDPE molecules. As a consequence, O-LLDPE molecules will slow down the nucleation and the crystal growth rates of LDPE molecules. This in turn will result in the lower crystallinity. When comparing the crystallinity values of pure B-LLDPE to that of O-LLDPE, it is clear that the latter has lower amount of crystallinity. This fact is due to the octene branches being larger than the butene branches and also higher branch content exists in O-LLDPE relative to the other m-LLDPE used in this study.

5.2.4 DSC Scans of H-type Blends

According to the Figure 4.4, pure H-LLDPE shows broad melting behavior with two shallow peaks at 99°C and 108°C. The broad melting behavior of H-LLDPE sample can be attributed to the existence of two types of lamellae thicknesses; one is thin, which is responsible for the low-temperature melting peak, and a thicker one responsible for the higher melting temperature. The existence of two different lamellar thicknesses in pure H-LLDPE sample can be attributed to the existence of broad branching distributions in the polymer molecules. Thinner lamellae may have been developed owing to the closer arrangement of branches, and thicker lamellae from the wider arrangement of branches

along the main backbone chain. This result can also be confirmed by the nature of high endset melting of H-LLDPE (Figure 4.5). It is found that, the endset melting temperature is not sharp but it is rather diffuse indicating the existence of broad distribution of lamellae thickness in the sample. The DSC scans also reveal that the two peaks merge into a single higher value melting peak when LDPE content is greater than 10% in the blend. With the increase in LDPE composition of the blend, it is found that the broad shallow peaks in H-LLDPE tend to become quite narrow in nature and the peak is shifted towards the higher value indicating the improvement of lamellae thickness. It is also observed that the pure H-LLDPE shows a melting behavior intermediate between pure B-LLDPE and O-LLDPE. This is probably due to the existence of mainly two types of arrangements of branches along the main backbone chain as explained earlier. The high-end melting temperature peak of the H-LLDPE blends is illustrated in Figure 5.3a.

According to this figure, the melting temperature remained almost constant at 108°C for blends up to 50% LDPE before it increases and stabilizes at 111°C for the remaining blends. According to Figure 5.3b, endset temperatures are found to decrease linearly with the addition of LDPE. Figure 5.3c shows a sharp decrease in crystallinity when H-LLDPE molecules are added to LDPE. This decrease can be attributed to the presence of O-LLDPE molecules with smaller linear segments that slow down the nucleation as well as the crystal growth of LDPE molecules, which results in lower crystallinity. This phenomenon has been observed with other types of m-LLDPE.

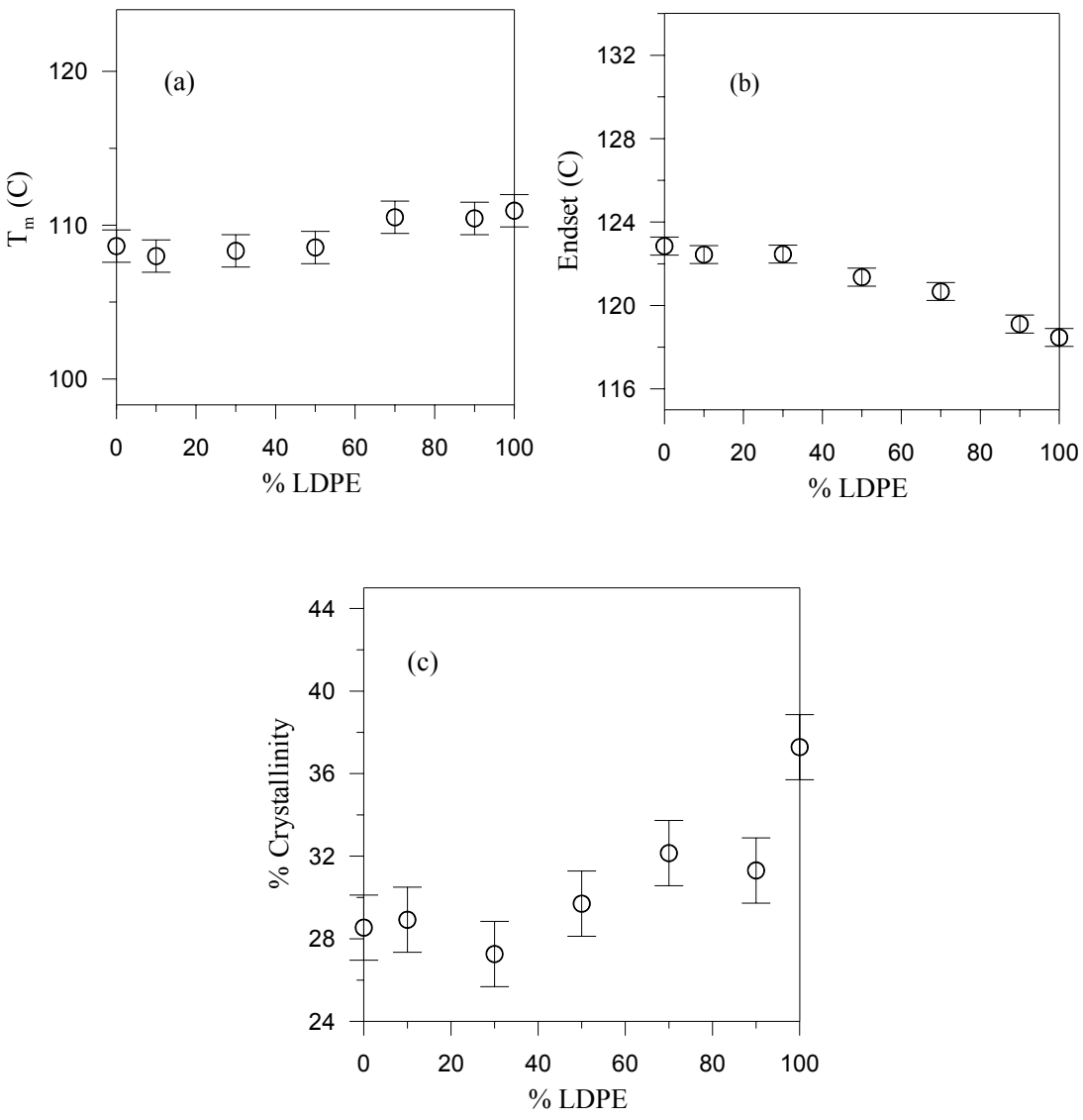

Figure 5.3: Thermal characterization of H-Type blends(a) Melting temperature versus %LDPE (b) Endset melting temperature versus % LDPE (c) Crystallinity versus % LDPE

It can be concluded from the above discussion that an addition of small amount of any branch type (B, H or O) of m-LLDPE to LDPE results in a sharp decrease of crystallinity. Furthermore, an addition of small amount of LDPE to any type of m-LLDPE does not improve the crystallinity of the blend.

5.3 TENSILE RESULTS

5.3.1 Pure Samples

One stress-strain curve of each polymer is plotted in the Figures 5.4a and 5.4b. All the studied polymers display ductile behavior accompanied with the neck formation at the yield point. The summary of tensile results for all the samples is reported in Table 4.5. It was earlier believed that most of the polymers show a single yield point in the stress-strain curve. But the double yielding phenomenon was found to exist in most of the polymers. Popli and Mandelkern [41] attributed the double yielding phenomenon to the broad distributions of relatively thin crystallites existing in the polyethylenes. According to Seguela and Reitsch [23], two processes governed the yielding: (i) the slip of crystal blocks; and (ii) the homogenous shear of the crystal blocks. Muller and Balsamo [24] found that the double-yielding phenomenon was quite sensitive to the crystallization conditions of the samples.

5.4 EFFECT OF THE BRANCH TYPE OF M -LLDPE ON THE MECHANICAL PROPERTIES

Stress-strain curves for the B-type blend system are shown in Figures 5.5a and 5.5b.

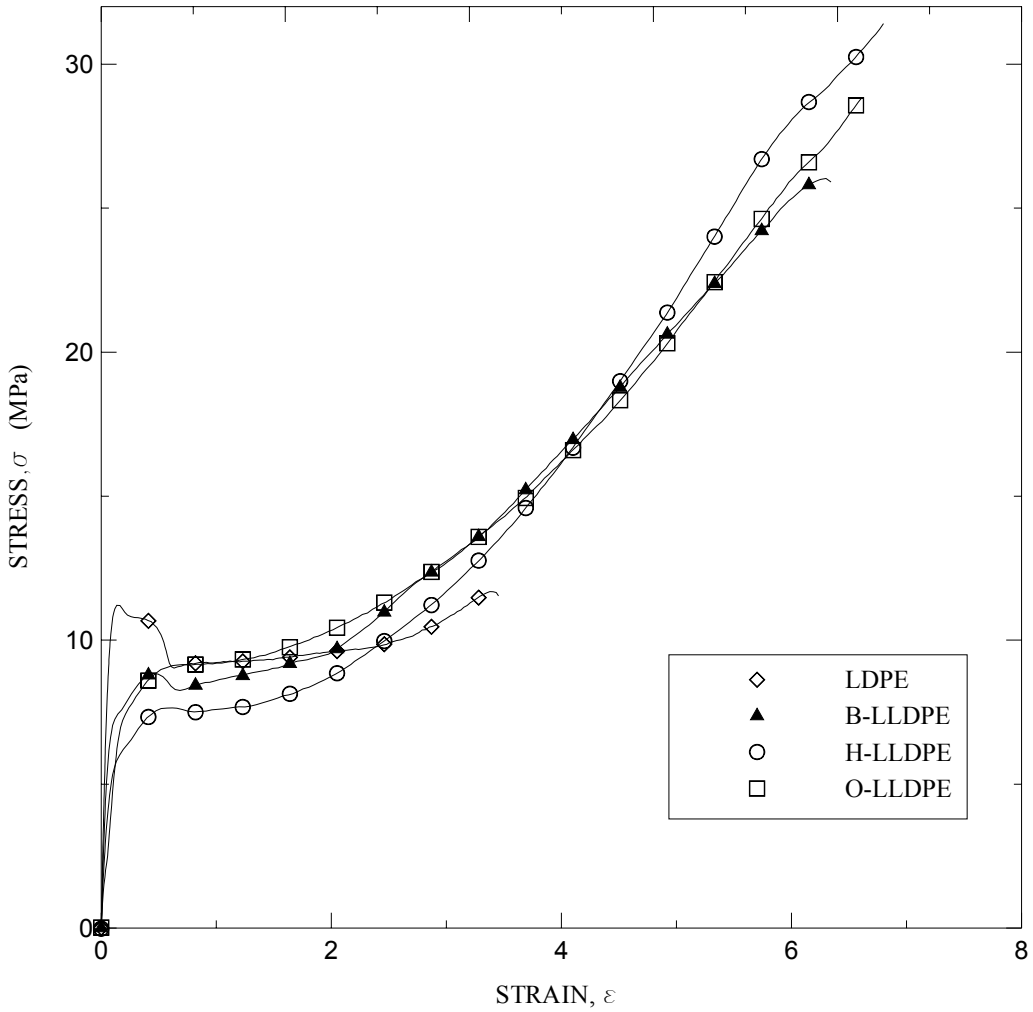

Figure 5.4a: Stress-strain curves for all the samples

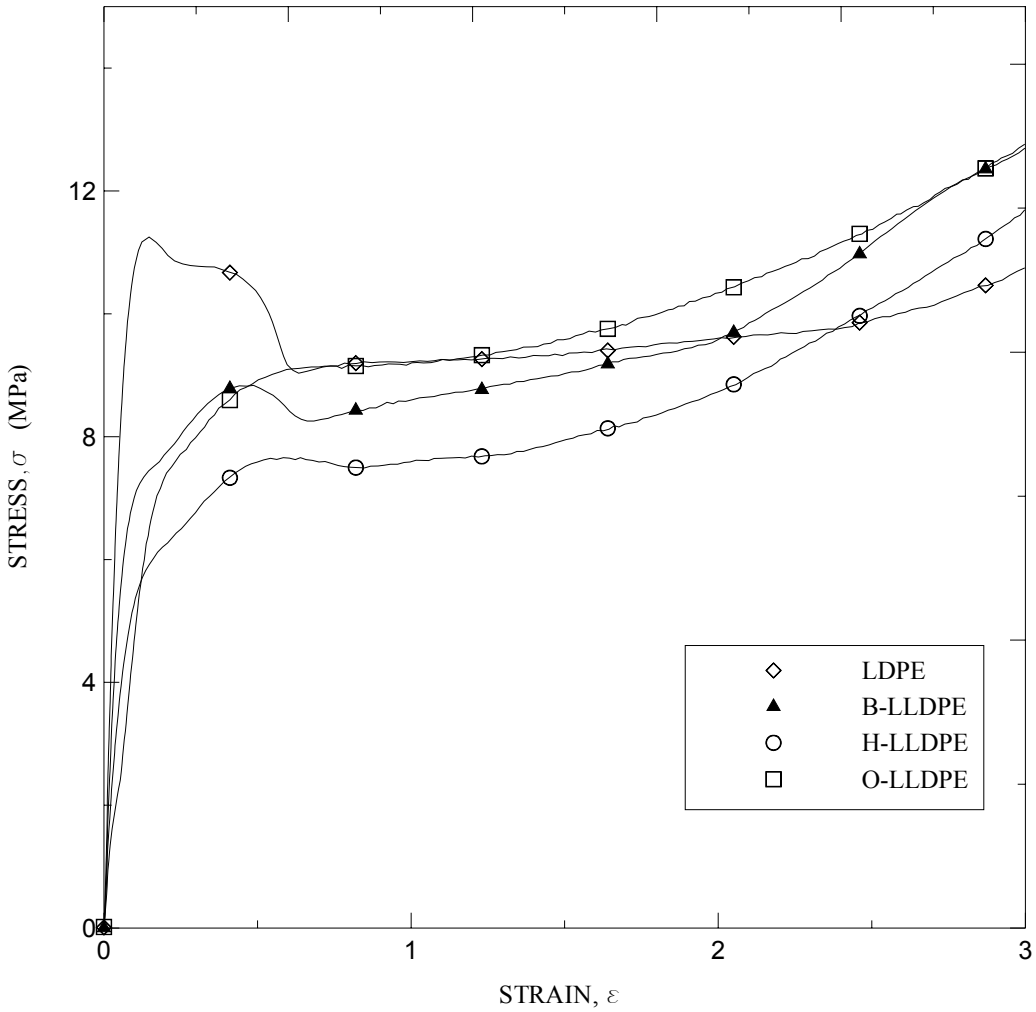

Figure 5.4b: Magnification in the vicinity of the yield

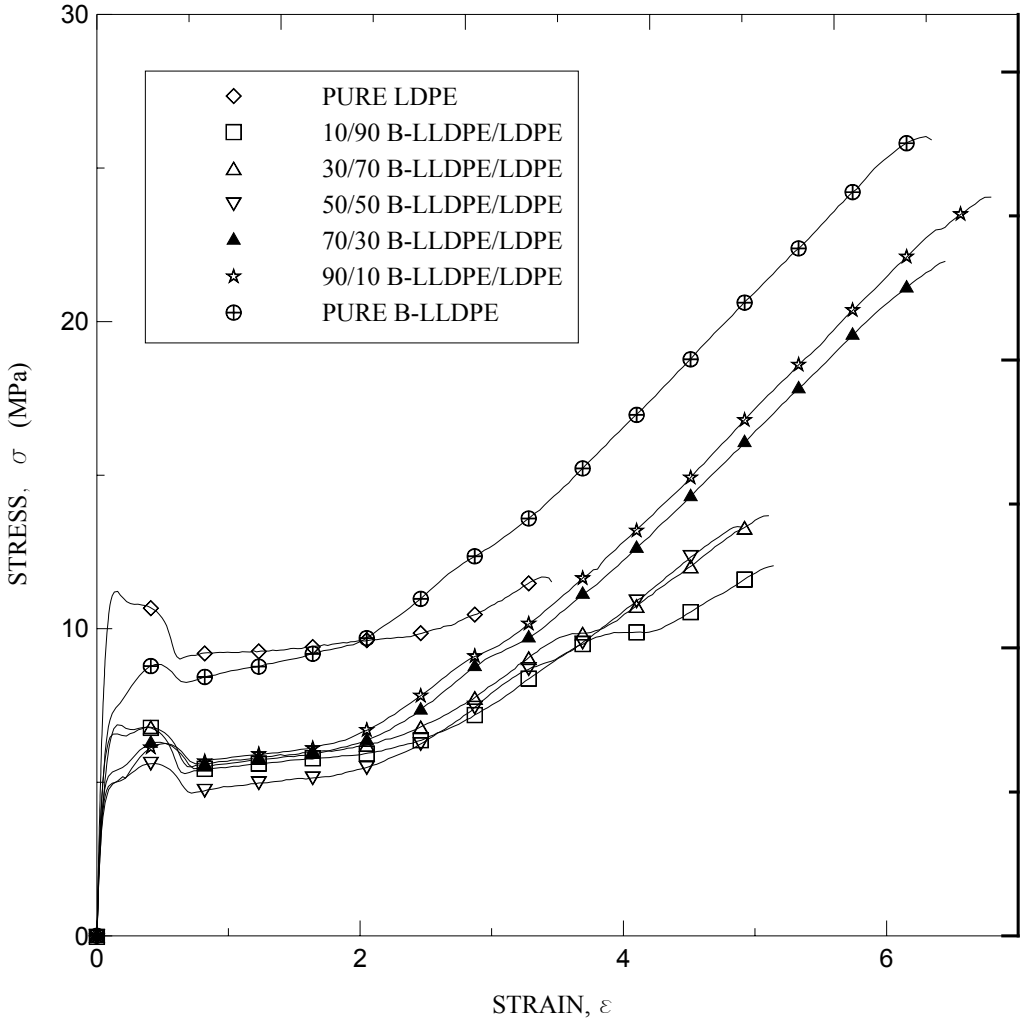

Figure 5.5a: Stress-strain curves for the B-Type Blend system (B-LLDPE/LDPE)

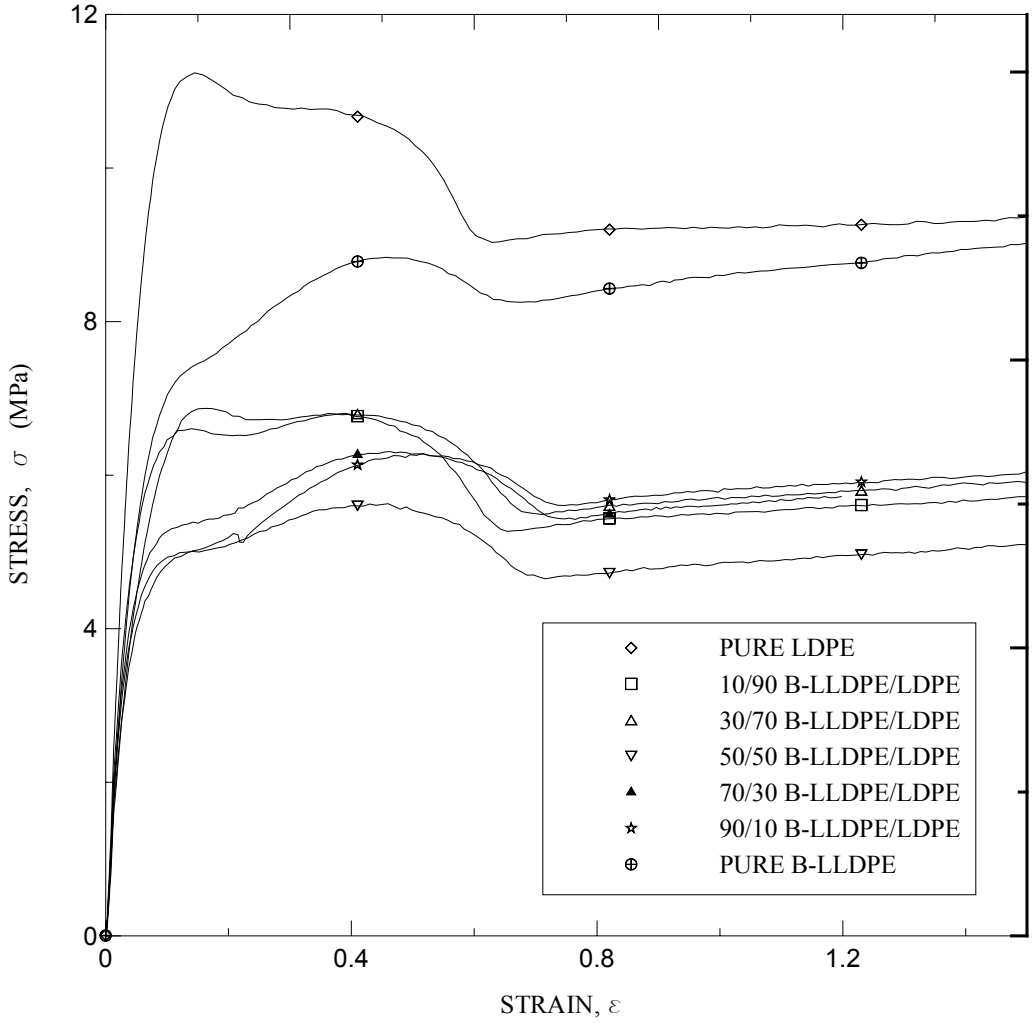

Figure 5.5b: Magnification in the vicinity of the yield for B-type Blend system

In general, first yield point is taken as the point where there existed a deviation from the linearity and the second yield point is considered as the highest stress point before the starting of the necking phenomenon. Rosario et al [57] studied the influence of chemical composition distribution and thermal history on the mechanical properties and viscoelastic relaxations of ethylene-1-butene copolymers. They found that the large strain mechanical properties and the strain hardening behavior were affected by the degree of homogeneity in the distribution of comonomer along the different chains. From Figure 5.5a, it is observed that the second yield point is lower than the first yield point. With the increase in B-LLDPE it was found that the second yield point was higher for the rapidly samples, which is in accordance with the findings of Muller and Balsamo [24].

Similar observations are concluded for H-LLDPE (Figure 5.6) and O-LLDPE (Figure 5.7). The tensile properties of all the three blend systems including the pure polymers as a function of LDPE content and percent crystallinity (DSC) are plotted in Figures 5.8-5.21 and discussed in terms of: (i) initial modulus; (ii) yield stress; (iii) tensile strength, and (iv) strain at break.

5.4.1 Variation of Initial Modulus

Figure 5.8 illustrates the variation of initial modulus versus the percent crystallinity values for pure polymers. The modulus of pure LDPE, B-LLDPE, H-LLDPE and O-LLDPE are 203 MPa, 128 MPa, 115 MPa, and 70 MPa, respectively. It is evident that the initial modulus of pure LDPE is higher than that of m-LLDPE used in this study.

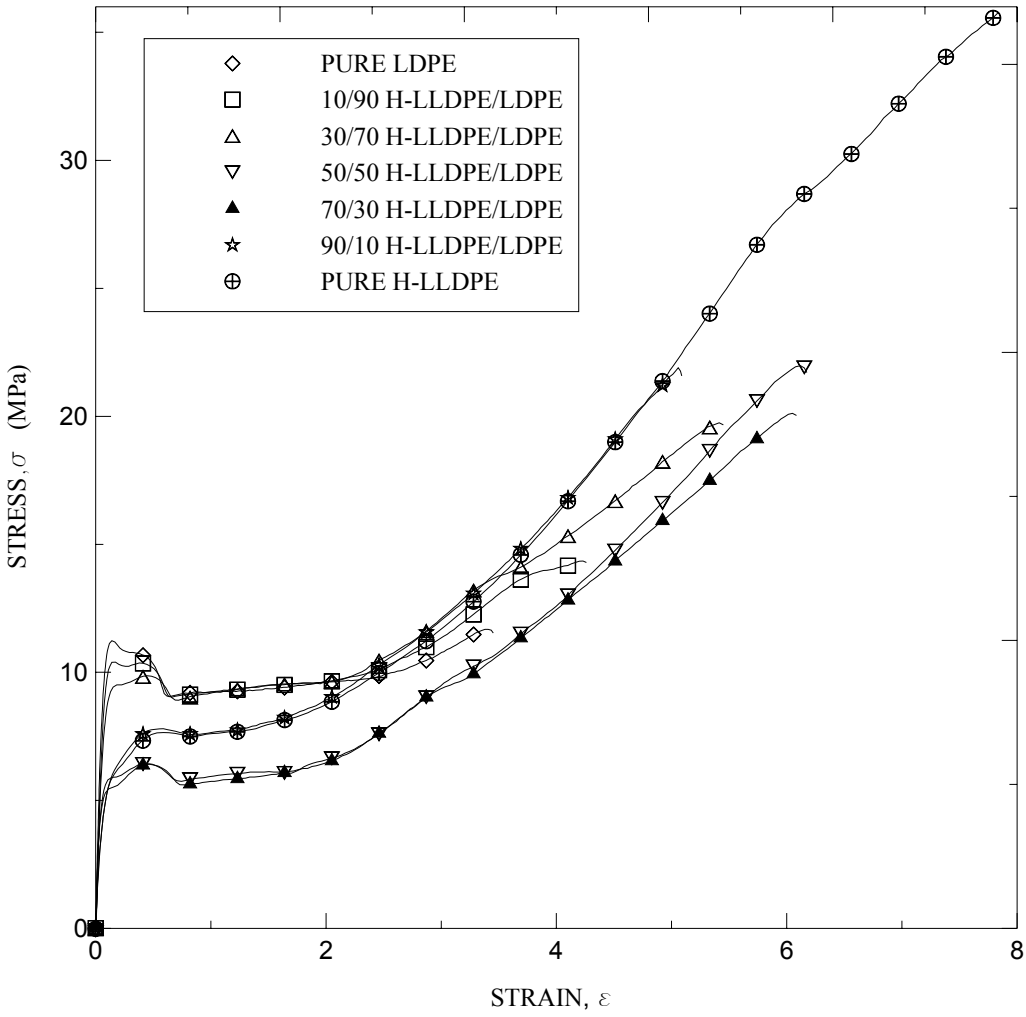

Figure 5.6a: Stress-strain curves for the H-Type blend system (H-LLDPE/LDPE)

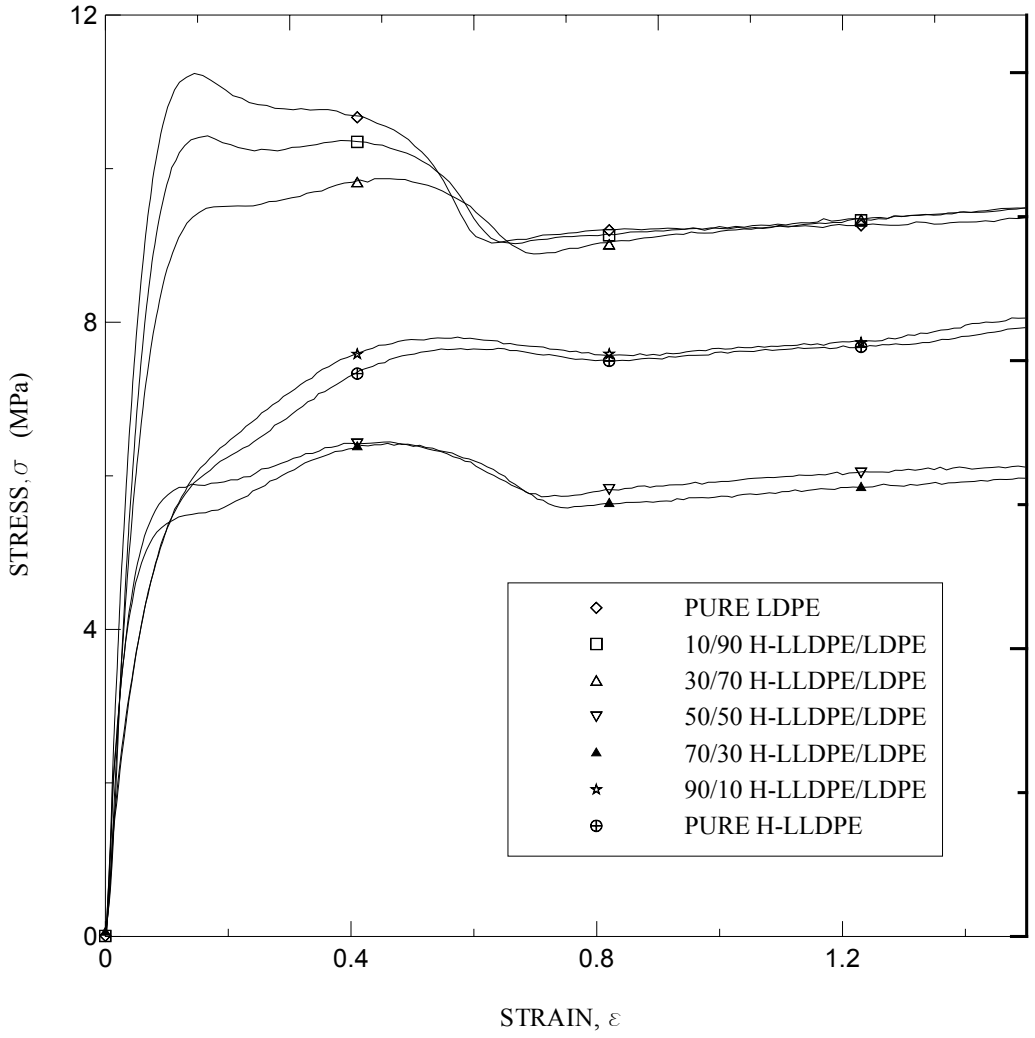

Figure 5.6b: Magnification in the vicinity of the yield for H-type blend system

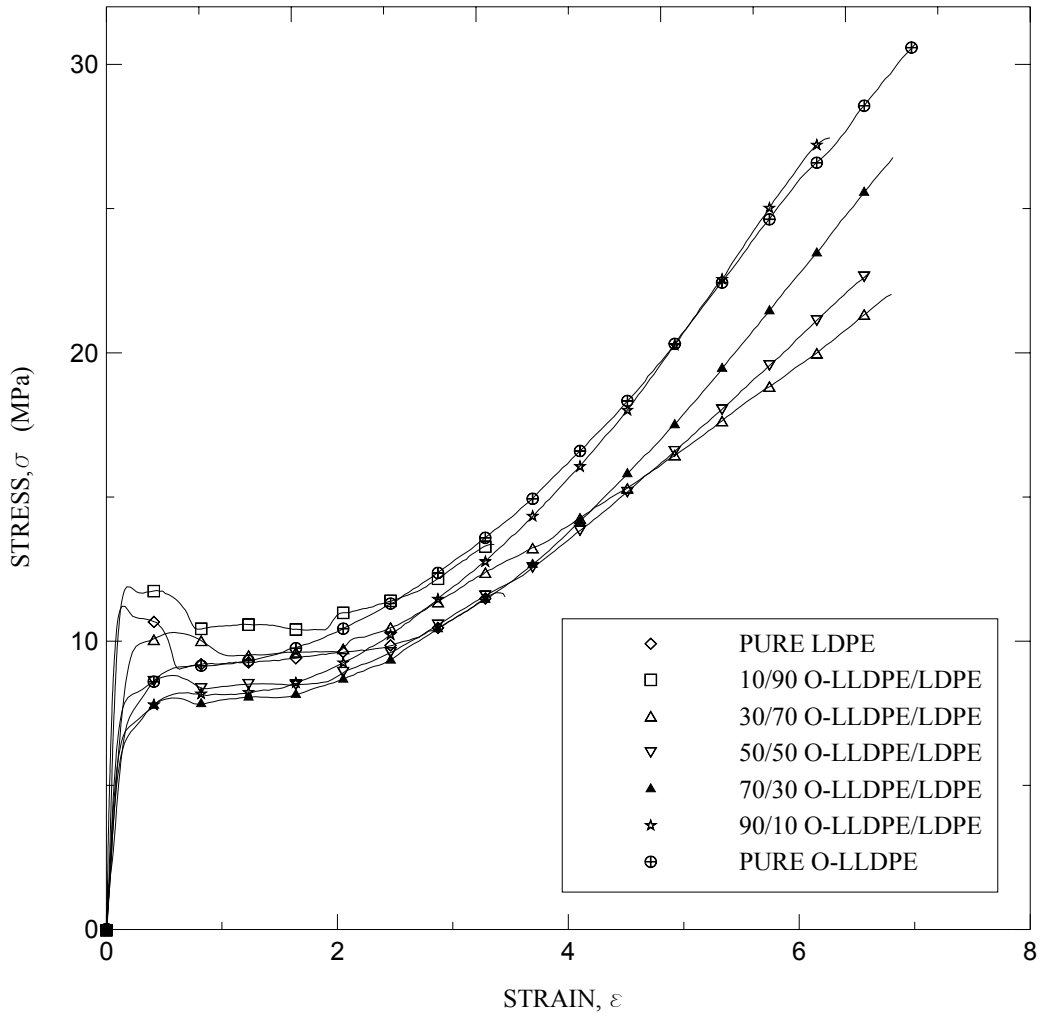

Figure 5.7a: Stress-strain curves for the O-Type blend system (O-LLDPE/LDPE)

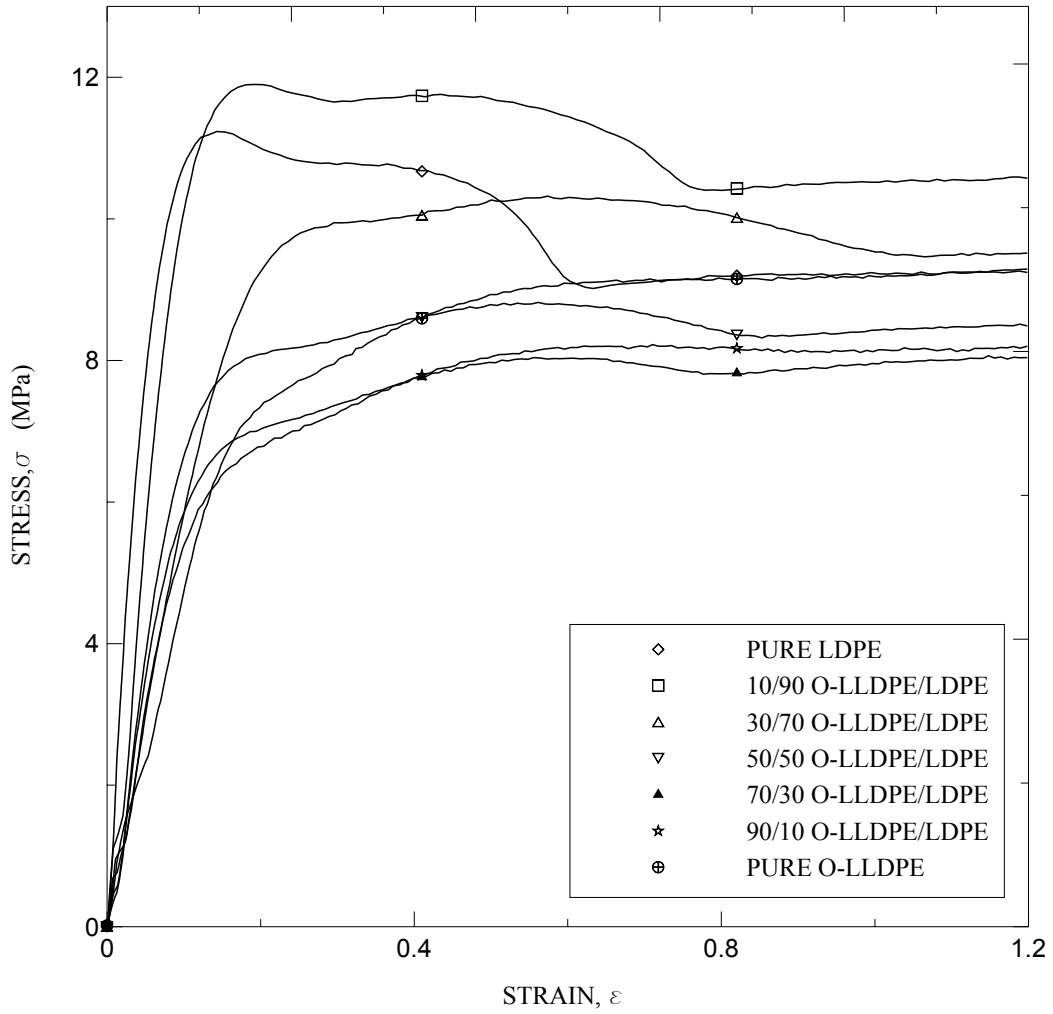

Figure 5.7b: Magnification in the vicinity of the yield for O-type blend system

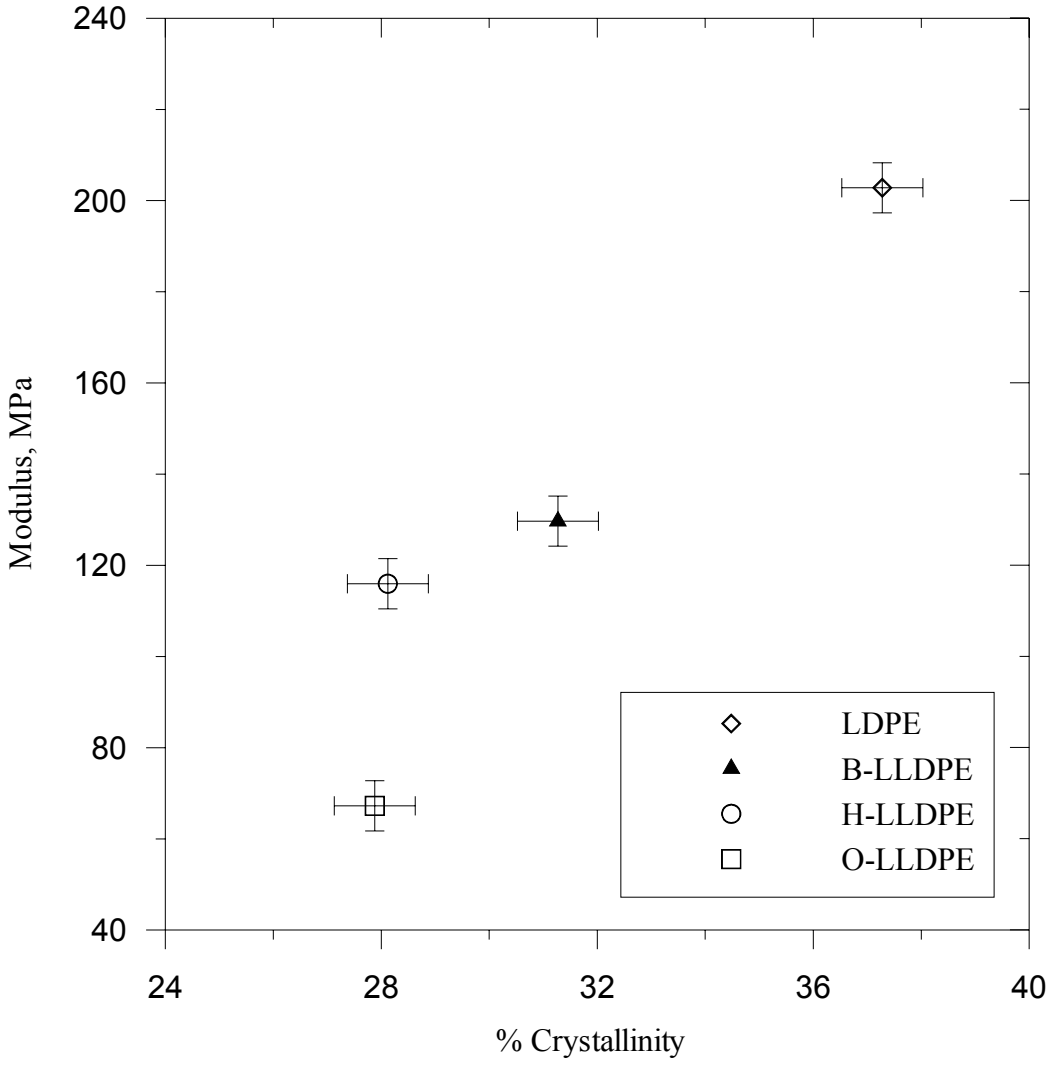

Figure 5.8: Initial modulus versus percent crystallinity of pure polymers

The effect of blend composition on the modulus of elasticity is shown in Figure 5.9. The modulus values of the B-type blends show linear variation for most of the blend ratios (Figure 5.9a). This indicates that B-LLDPE has good compatibility with LDPE. The effect of H-type blends on modulus of elasticity is presented in Figure 5.9b. It is evident that the addition of LDPE improves the modulus of the blends. For O-type blend system, most blend compositions have similar modulus values to that of pure O-LLDPE. It is observed that the addition of small amount of O-LLDPE to pure LDPE results in large decrease of its modulus (Figure 5.9c). The variation of initial modulus with percent crystallinity values is reported in the Figure 5.10. It can be seen that the initial modulus values were found to decrease with percent crystallinity values (DSC) for all the blends.

5.4.2 Variation of Yield Stress

The yield point of pure polymers versus crystallinity is presented in Figure 5.11. It can be inferred that pure m-LLDPE has lower yield stress value compared to pure LDPE. Besides the crystallinity, the branch type, branch content and the branch size in a polymer molecule significantly affect the yield stress. The compositional dependence of yield stress for all the blend systems is shown in Figure 5.12. For the B-Type (Figure 5.12a), a small addition of B-LLDPE to LDPE decreases its yield stress appreciably. For H-type blend system (Figure 5.12b), it is observed that the yield stress values remained quite close to that of pure H-LLDPE for LDPE $\leq$ 50%. The remaining blends have yield stress values similar to that of pure LDPE. Similar behavior of yield stress with blend composition results in O-type blend system (Figure 5.12c).

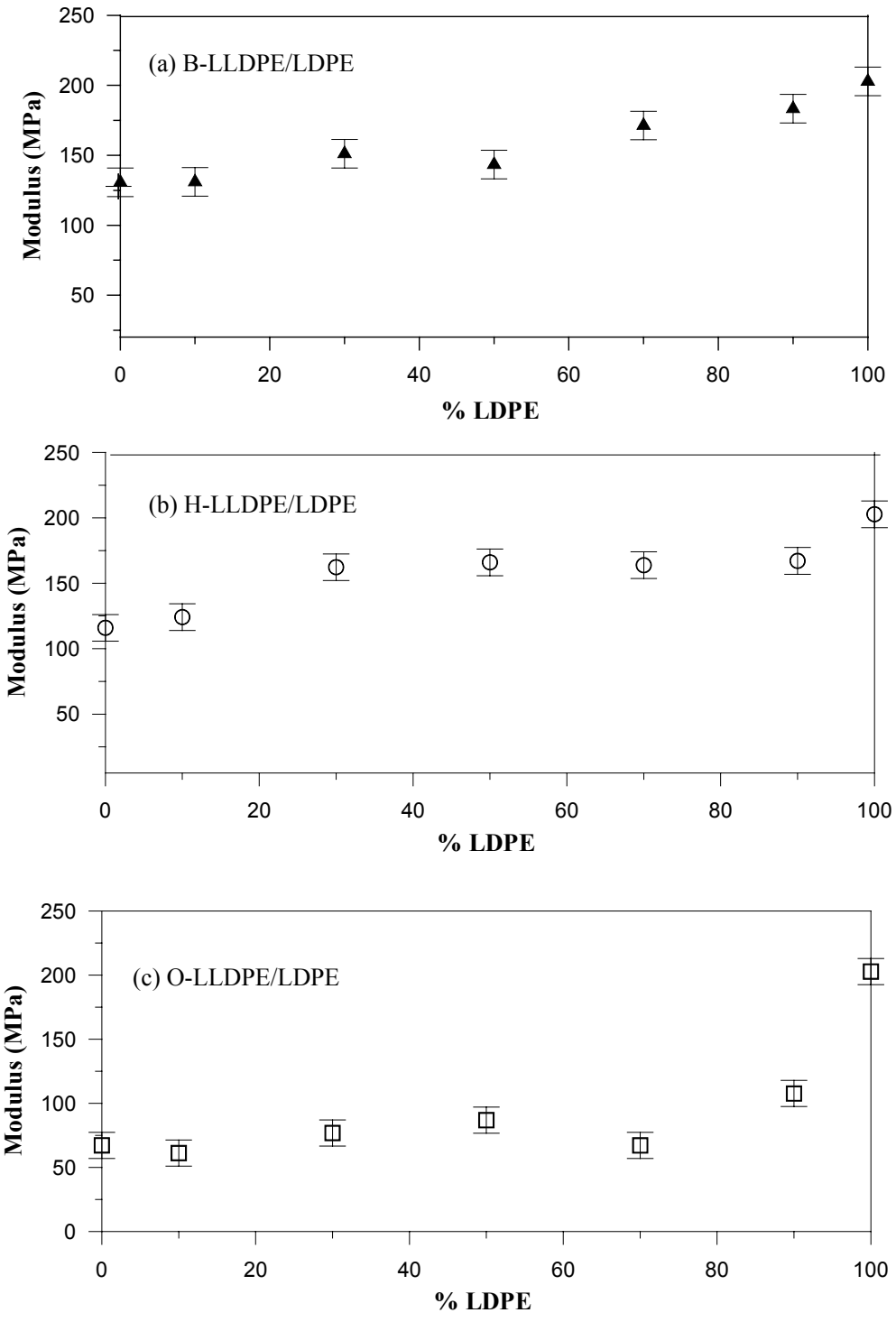

Figure 5.9: Initial modulus as a function of LDPE content for all the three blend systems (a) B-Type (b) H-Type (c) O-Type

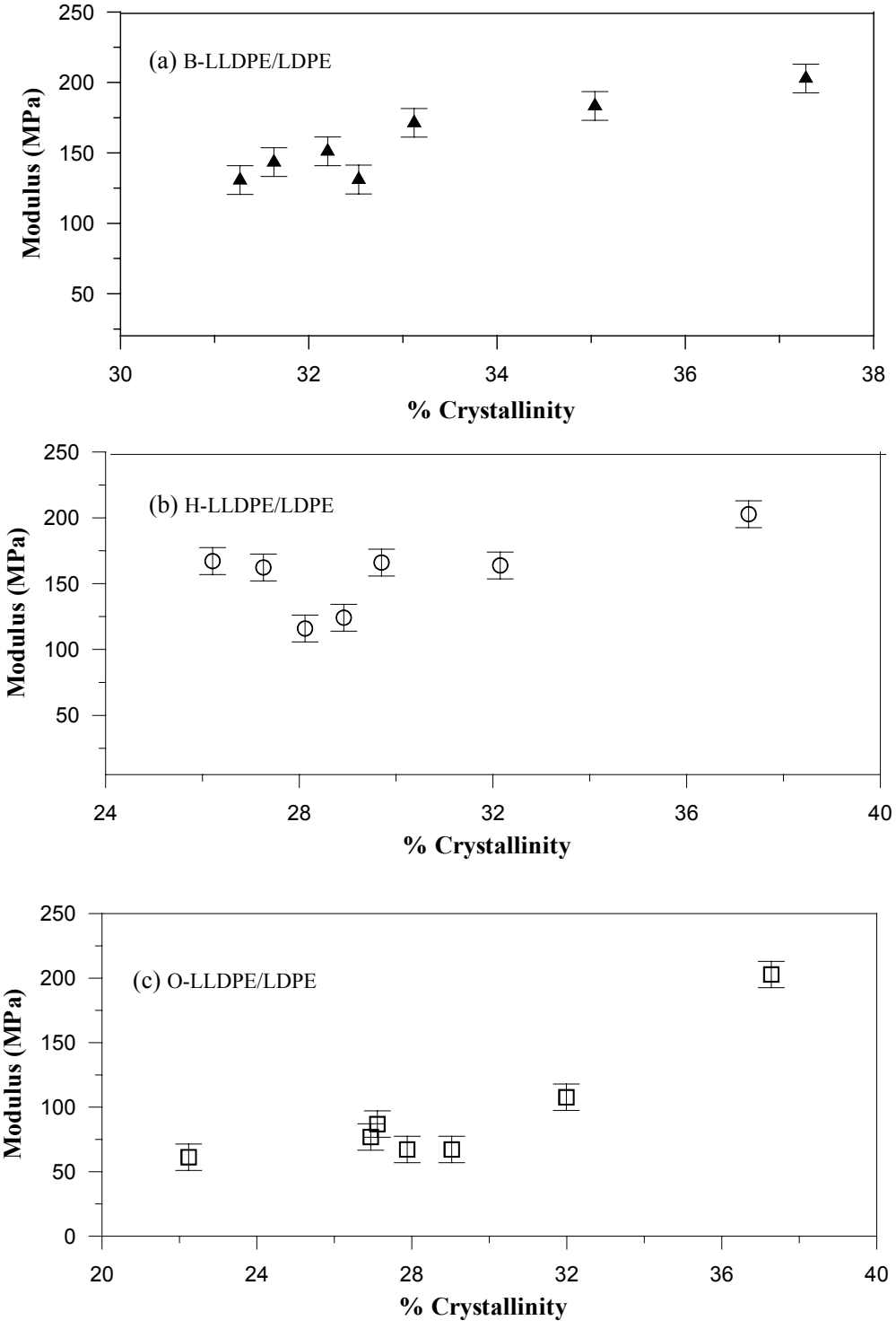

Figure 5.10: Variation of initial modulus versus percent crystallinity for the three blend systems

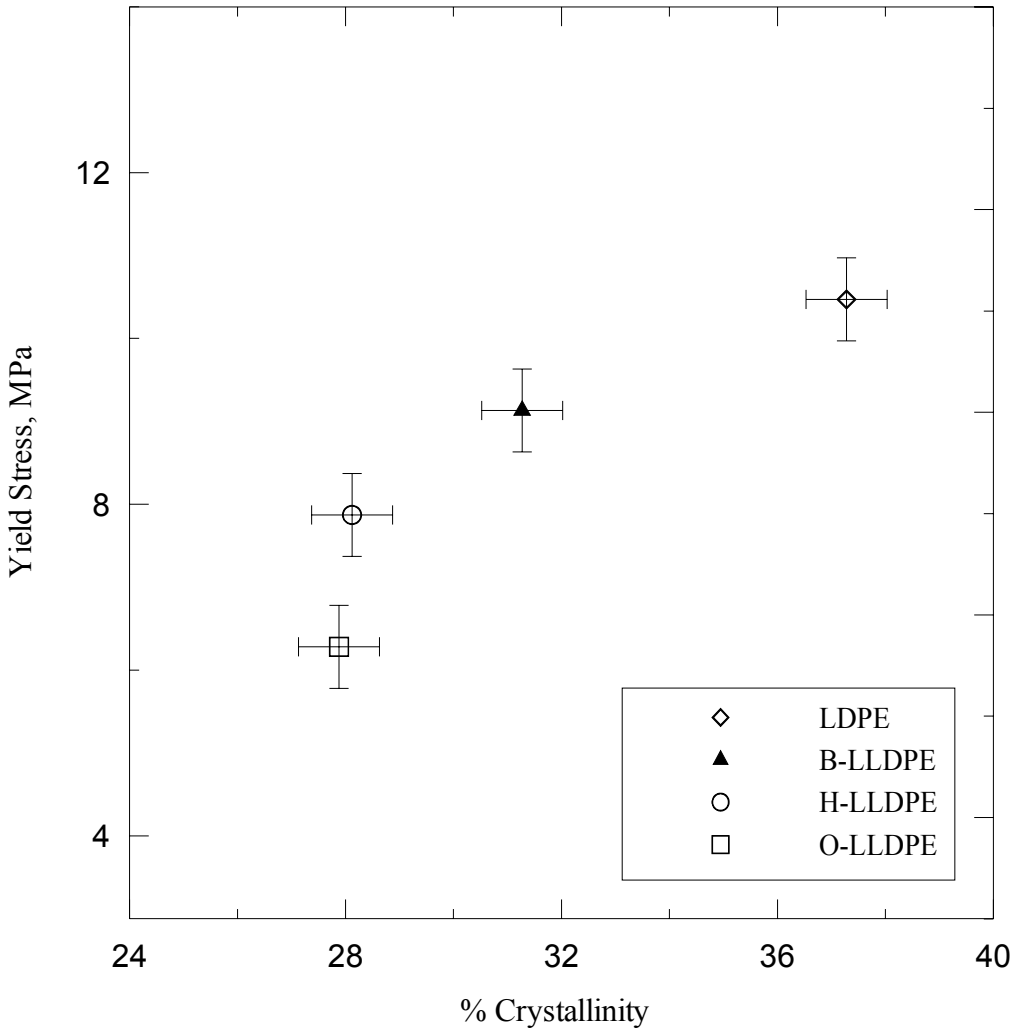

Figure 5.11: Yield stress versus percent crystallinity of pure polymers

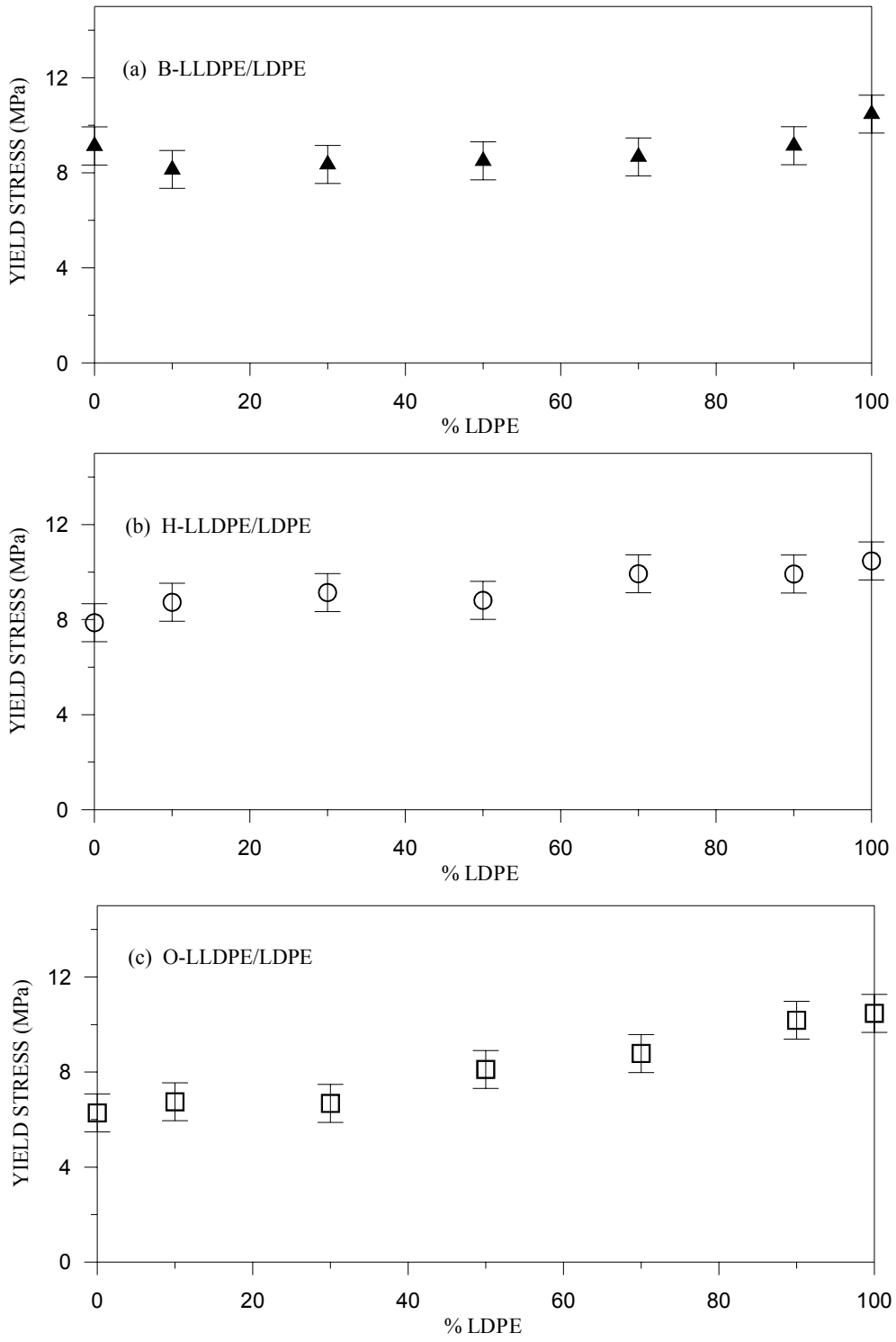

Figure 5.12: Yield stress as a function of LDPE content for all the three blend systems (a) B-Type (b) H-Type (c) O-Type

Figure 5.13 illustrates the variation of yield stress versus the percent crystallinity values. It can be seen that the yield stress values were found to decrease with percent crystallinity values (DSC). Yield stress has been reported to be a linear function of degree of crystallinity (DSC) [41]. They reported that this linear variation for a wide range of densities. In this study, polymers were chosen for similar densities, this linear variation is not so evident (Figures 5.13).

5.4.3 Variation of Tensile Strength

The tensile strength versus the crystallinity of the pure polymers is reported in Figure 5.14. LDPE has the lowest tensile strength (12 MPa) compared to other polymers used in this study. Pure H-LLDPE and O-LLDPE have nearly identical tensile strength values. The compositional dependence of tensile strength values is shown in Figure 5.15. For the B-Type blend system (Figure 5.15a), the tensile strength values for the entire blend ratios were found to be in between that of the parent polymers and are found to vary linearly for most of the blend ratios.A similar trend is followed for H-type blend system (Figure 5.15b) and O-type blend system (Figure 5.15c). Figure 5.16 shows the dependence of tensile strength values of all the blend systems with percent crystallinity values.

5.4.4 Variation of Strain at break

The variation of strain at break values with the crystallinity for the pure polymers is depicted in Figure 5.17. Pure LDPE has lowest strain at break compared to the other pure polymers. The compositional dependence of the strain at break values for all the three blend systems is shown in Figure 5.18.

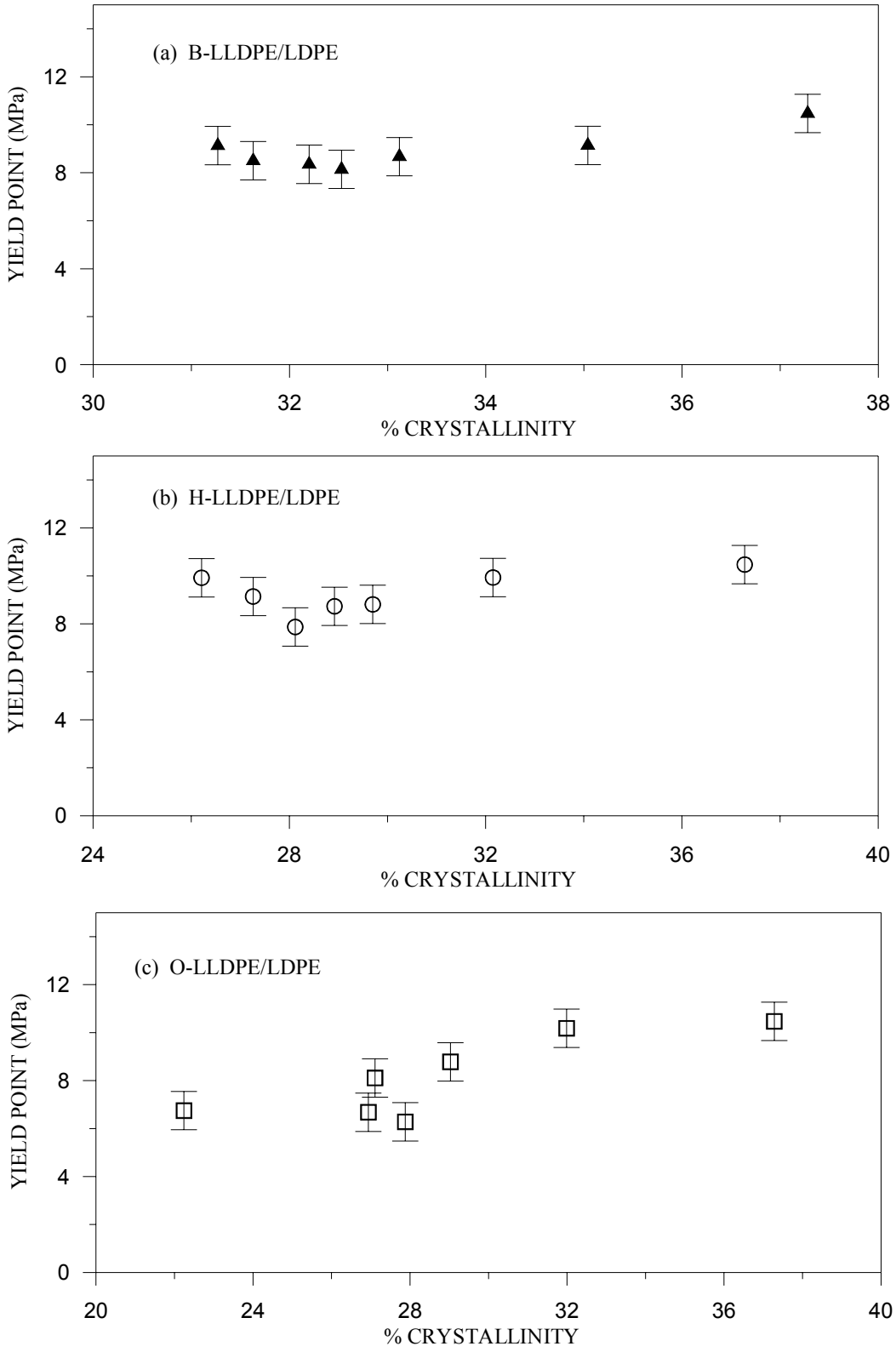

Figure 5.13: Variation of the yield point versus percent crystallinity values

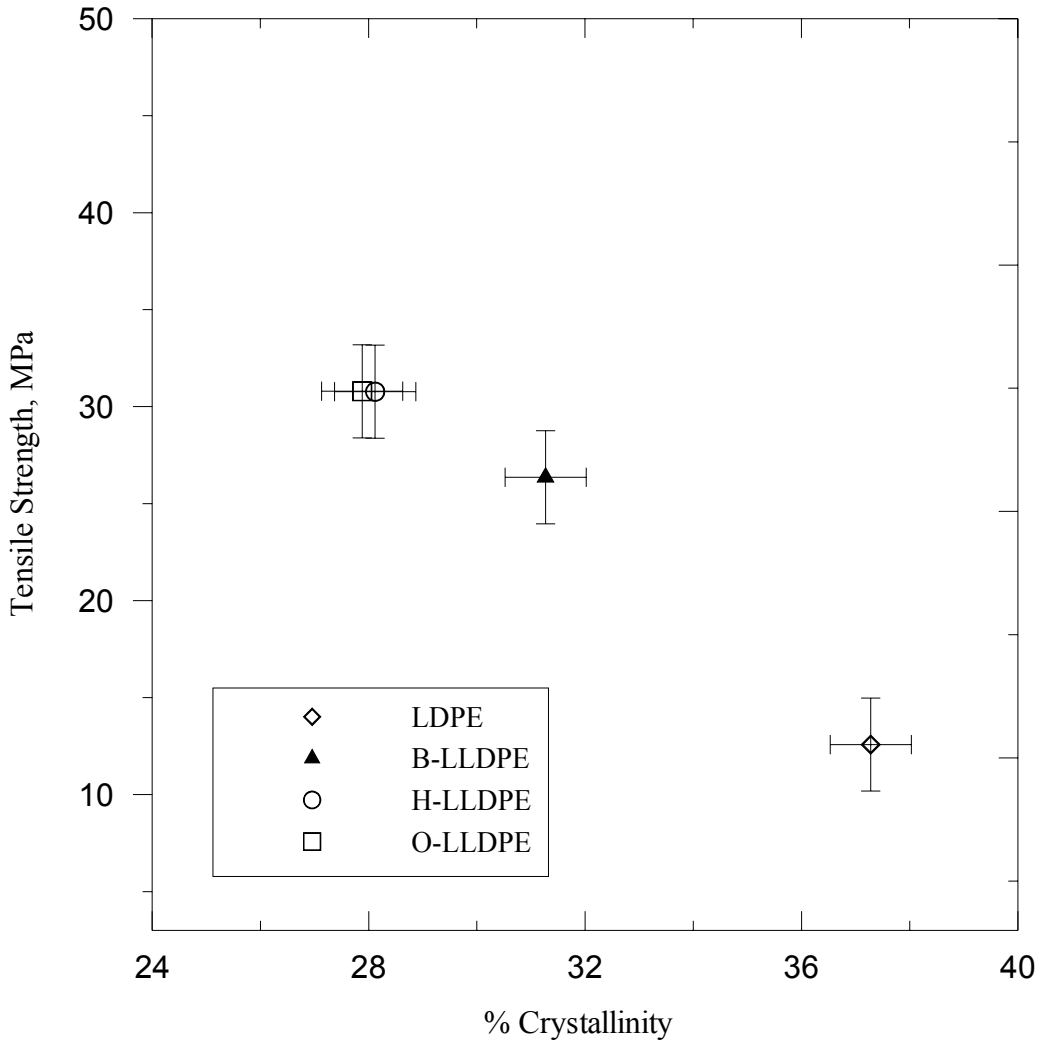

Figure 5.14: Tensile strength versus percent crystallinity of pure polymers

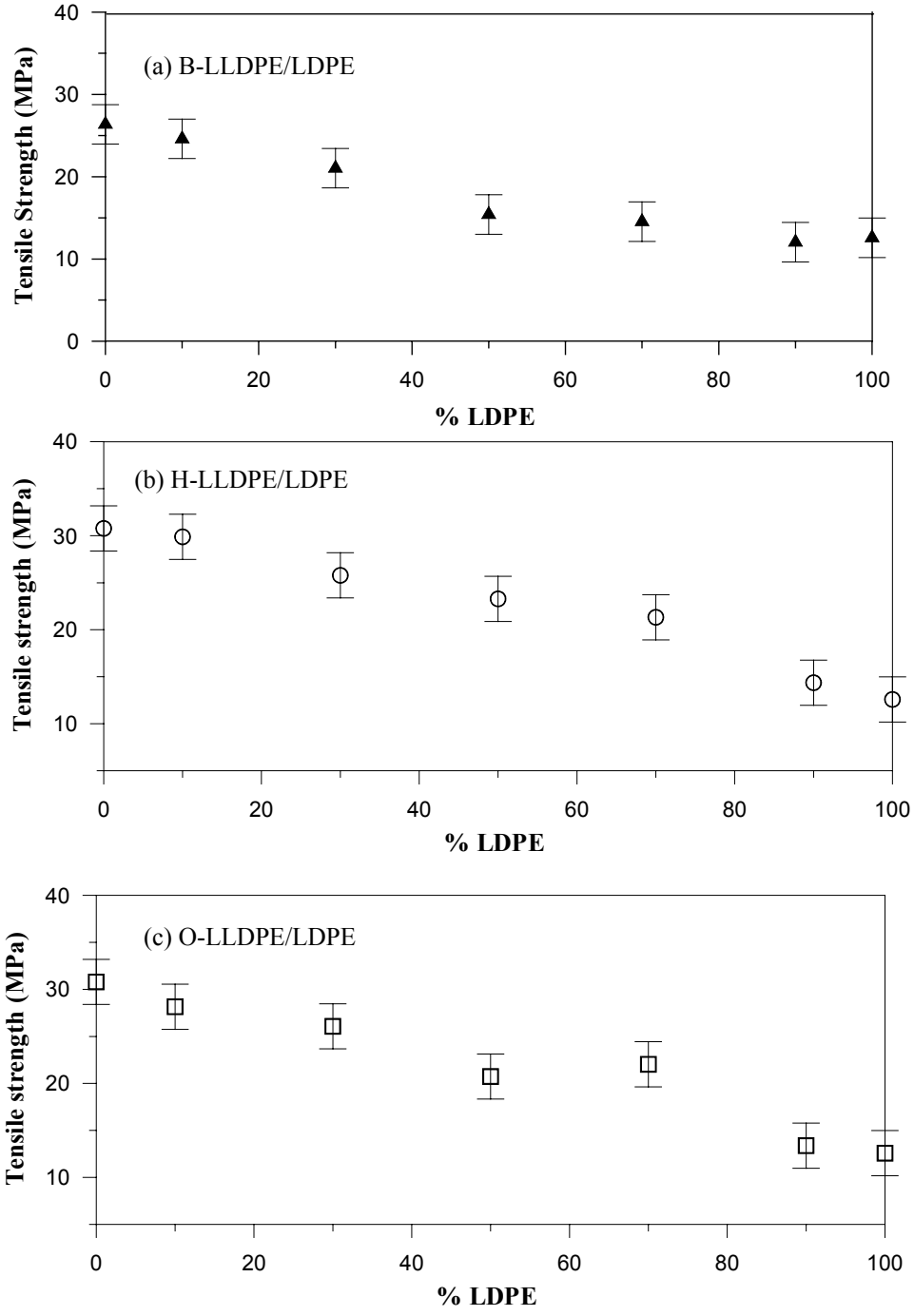

Figure 5.15: Tensile strength as a function of LDPE content for all the three blends (a).B-Type (b) H-Type (c) O-Type

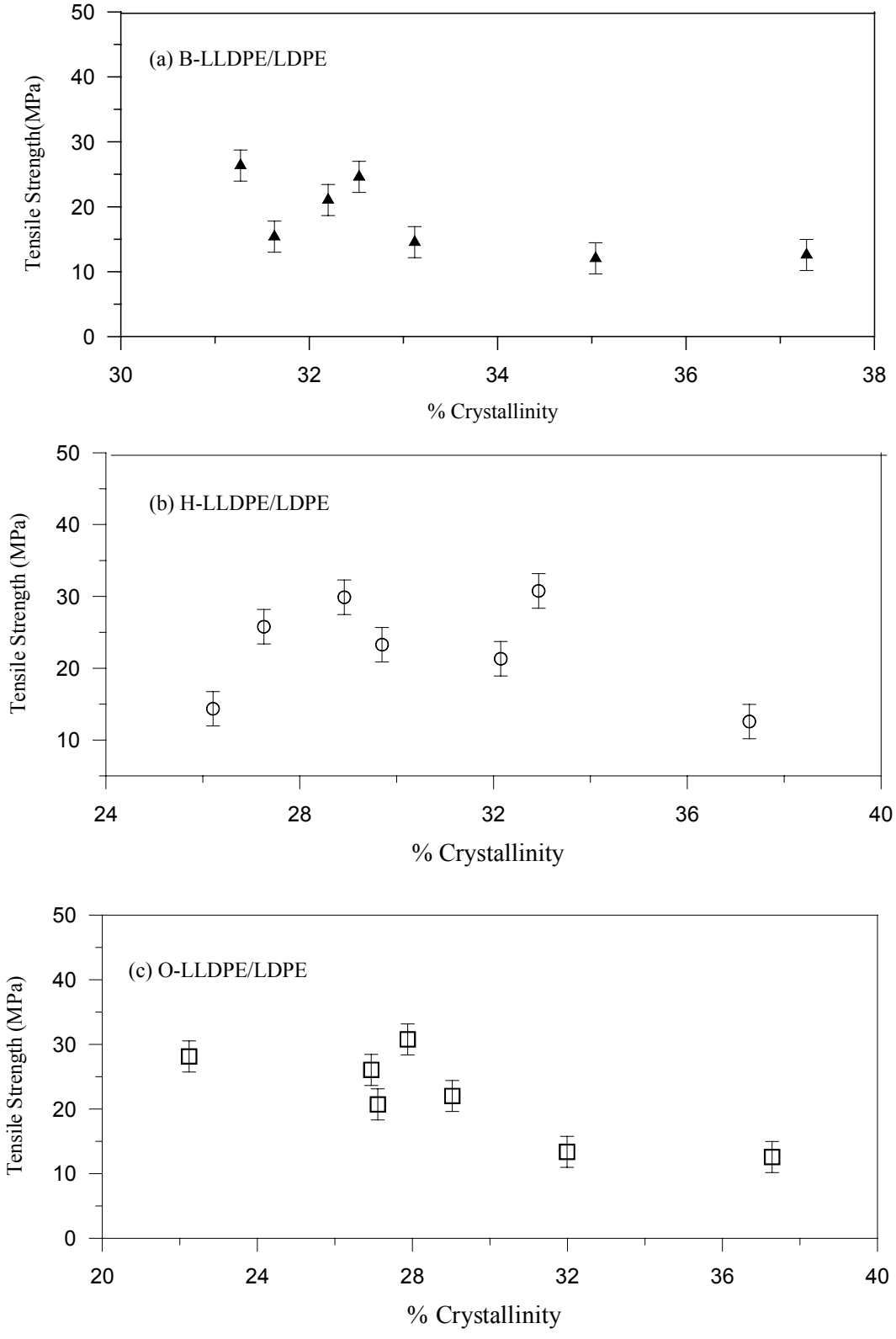

Figure 5.16: Variation of Tensile strength versus percent crystallinity values

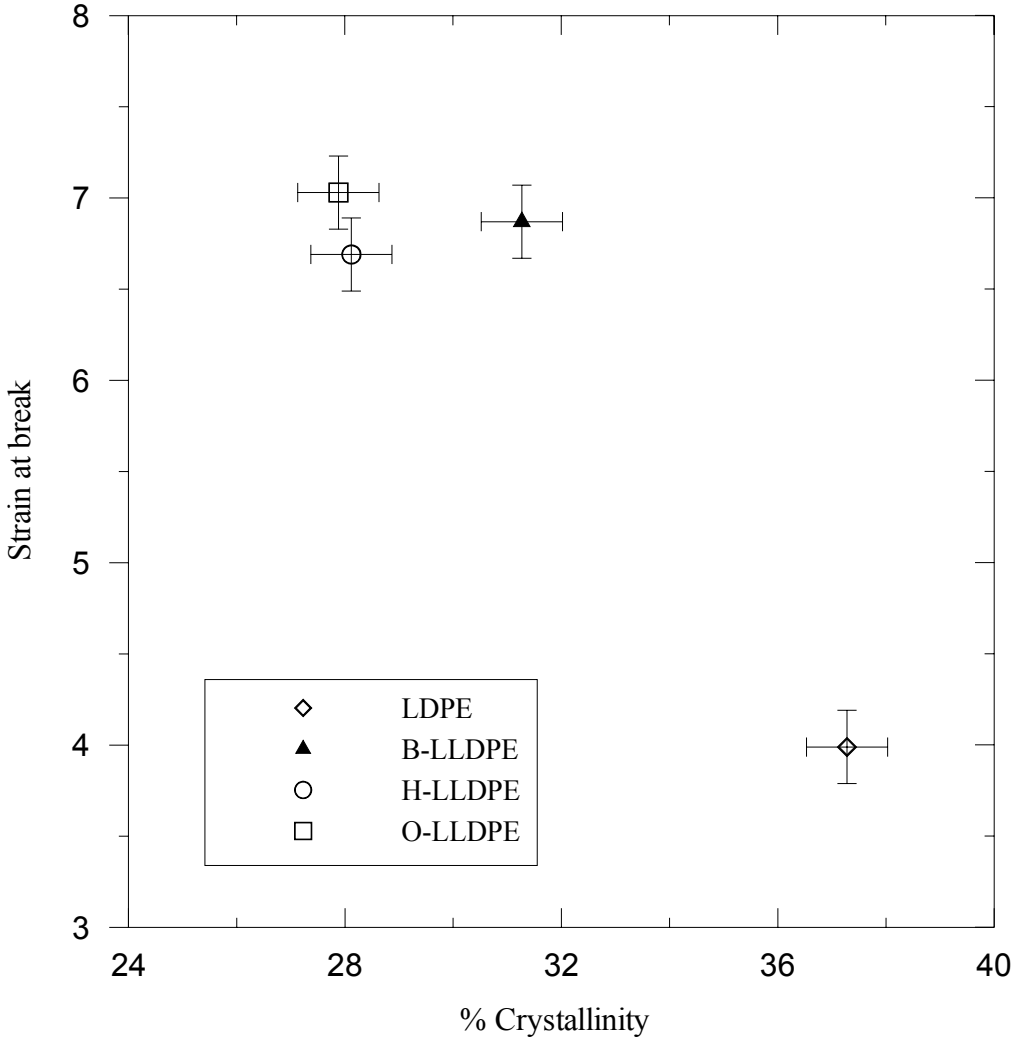

Figure 5.17: Strain at break versus percent crystallinity of pure polymers

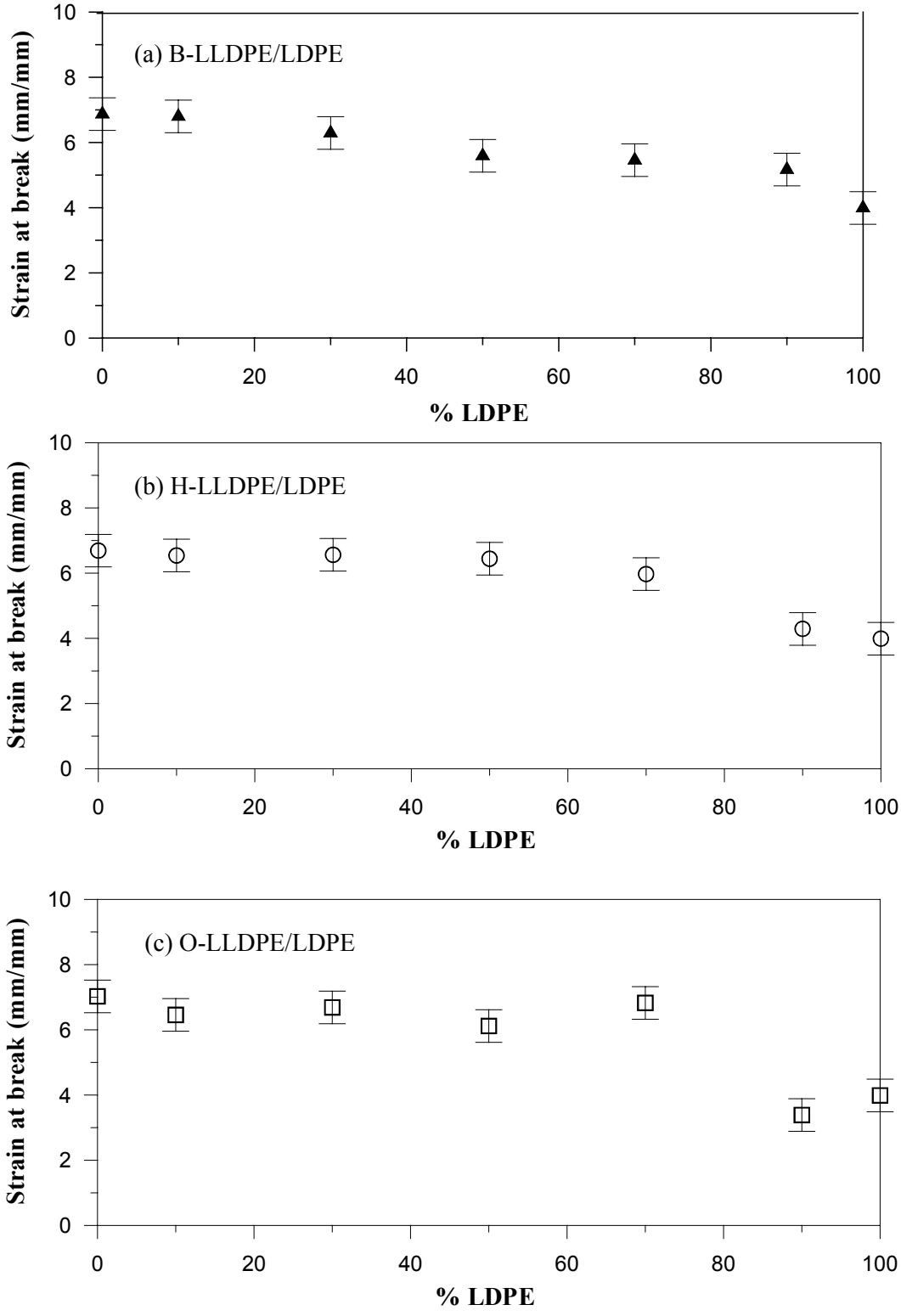

Figure 5.18: Strain at break as a function of LDPE content for all the three blends (a).B-Type (b) H-Type (c) O-Type

It can be inferred that the addition of m-LLDPE to LDPE improves the strain at break value and also the ultimate strength for all the blend systems. B-type blends showed a better compatibility than the other blend systems studied (Figure 5.18a). For H-type blend system (Figure 5.18b), the strain at break values remained closer to that of pure H-LLDPE for LDPE ≤ 70%. This trend can also be seen in O-type blend system (Figure 5.18c). Figure 5.19 shows the variation of strain at break values versus the percent crystallinity values for all the blends.

5.5 VICKER'S HARDNESS RESULTS

Vicker's pyramidal diamond indenter is used because of the fact that square indentation produced by the sharp diamond pyramid leads to an easy, accurate and above all optimal measurement of microhardness. To ensure reliable measurement of microhardness the volume of the material receiving the indenter must be free of external stresses and the surface must be parallel with the base of the tester. The variation of vicker's hardness number versus LDPE content is depicted in the Figure 5.20.

All the blends followed the linear rule for the most of the blend ratios. This indicates all the blends show better compatibility for microhardness values.

5.5.1 Variation of VHN with Percent Crystallinity

It is fundamental to know the influence of the structure on the microhardness values, by analyzing the variation of microhardness with crystallinity for all the samples. The VHN values correlated well with percent crystallinity values (Figure 5.21). It is evident that the VHN values increased with an increase in percent crystallinity (DSC).

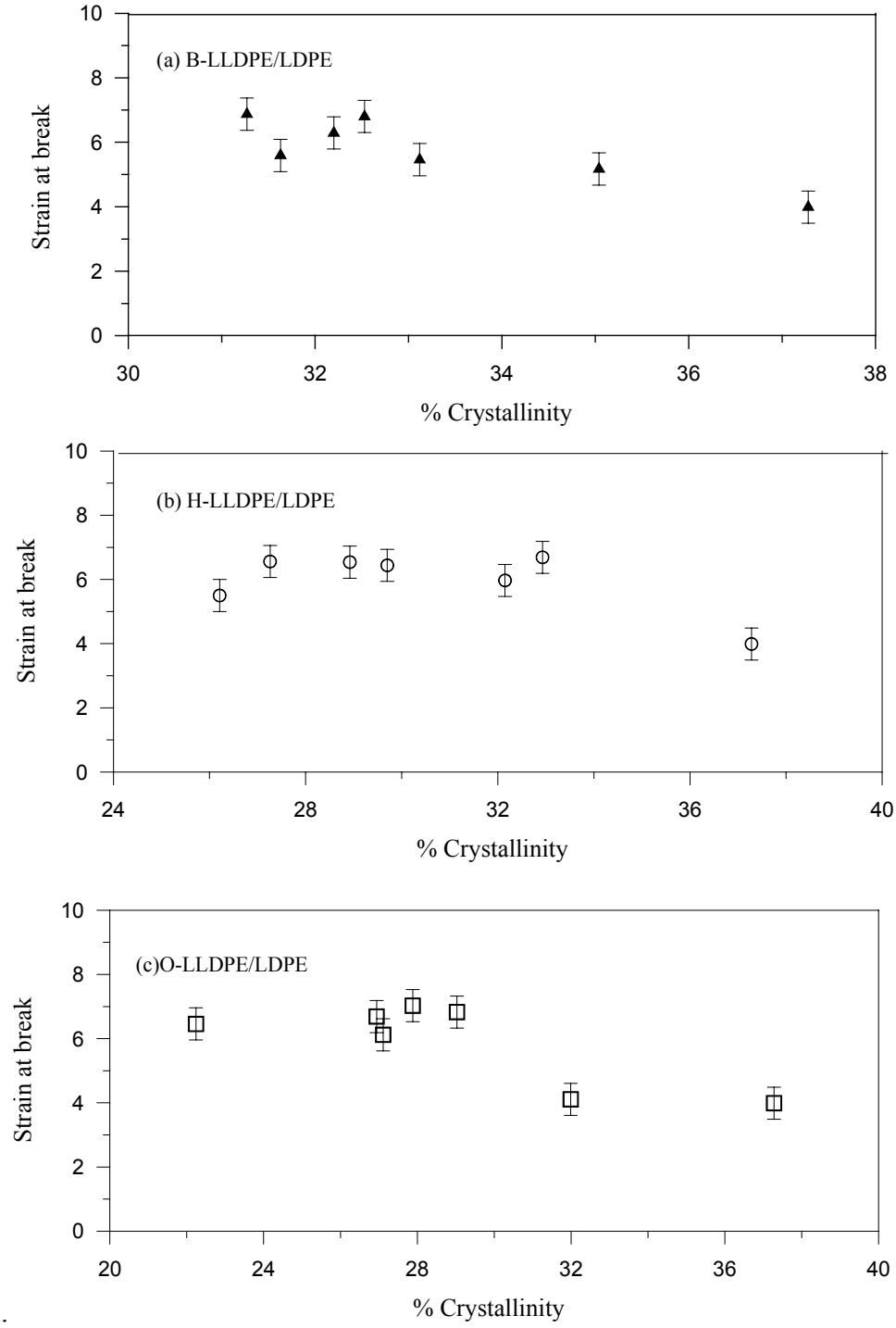

Figure 5.19: Variation of Strain at break versus percent crystallinity values

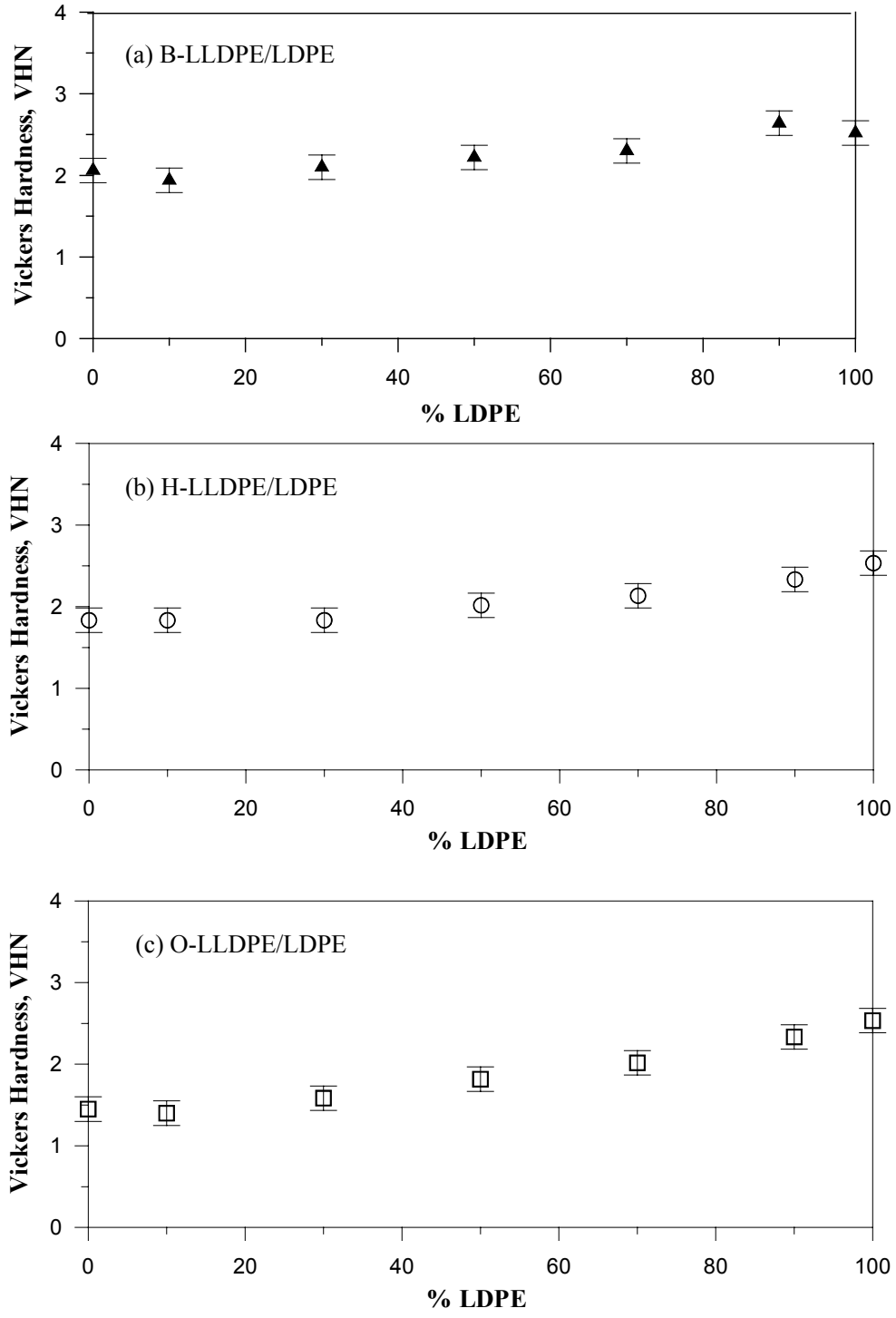

Figure 5.20: Variation of VHN versus % LDPE content for all the blend systems (a)B-type (b) H-type (c) O-type

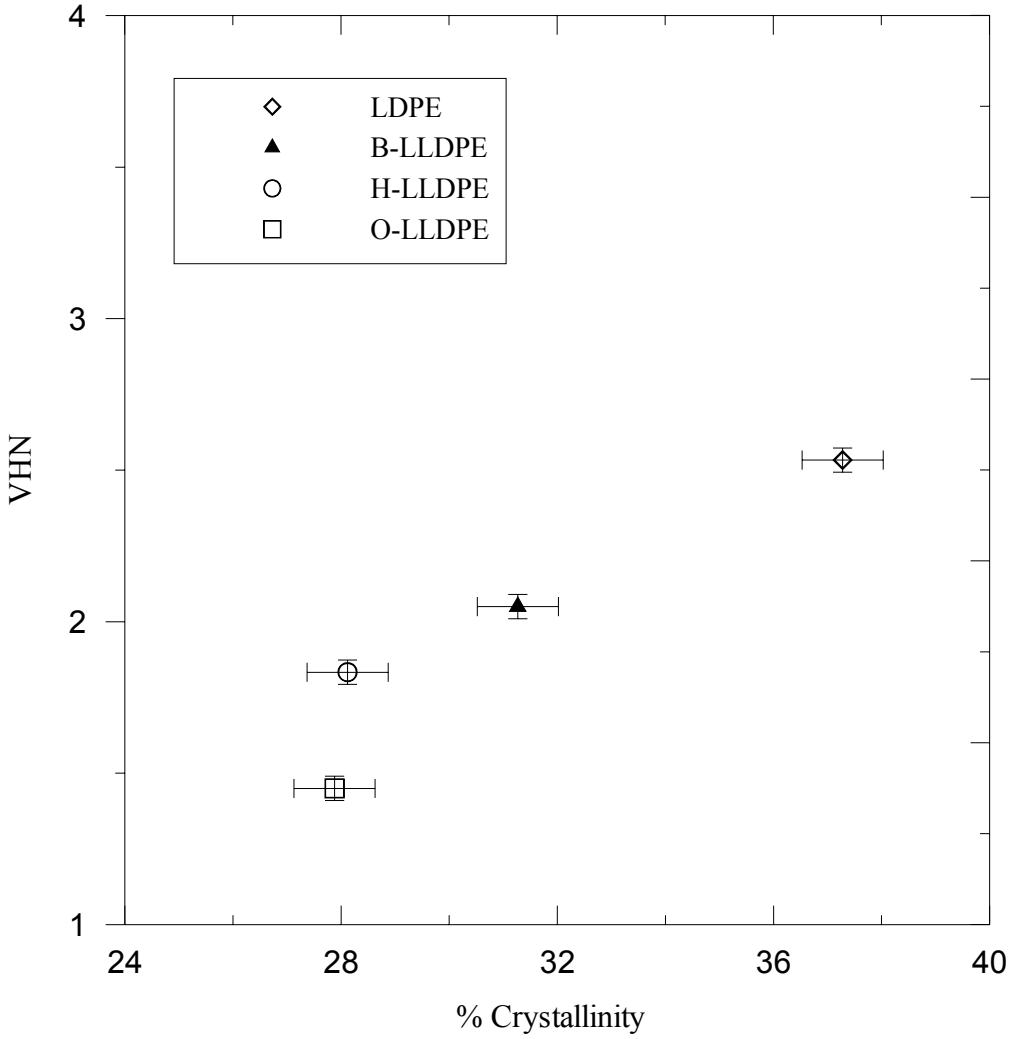

Figure 5.21: Variation of VHN with percent crystallinity (DSC)

5.5.2 Correlation with Initial Modulus

The variation of initial modulus for the polymers is shown in Figure 5.22. Vicker's hardness number (VHN) of pure LDPE is 2.53. The VHN for B-LLDPE, H-LLDPE and O-LLDPE are 2.05, 1.83 and 1.45 respectively. The higher value of pure LDPE can be attributed to its higher value of crystallinity compared to the other m-LLDPE. The influence of branch type and branch content on VHN is also evident. The correlation of yield stress values with VHN for all the blend systems is shown in the Figure 5.23

For B-type blend system,

$$E_t = 70.87 * H_v \tag{5.2}$$

Similarly for H-type and O-type blend systems is given by

$$E_t = 76.1 * H_v \tag{5.3}$$

$$E_t = 52.84 * H_v \tag{5.4}$$

Where 'a' and 'b' are constants and 'E' is the elastic modulus.

5.5.3 Correlation with Yield Stress

The variation of yield stress with VHN for the polymers is shown in Figure 5.24. The higher value of yield stress of pure LDPE can be attributed to its higher value of crystallinity compared to the other m-LLDPE. The correlation of yield stress values with VHN for all the blend systems is shown in the Figure 5.25.

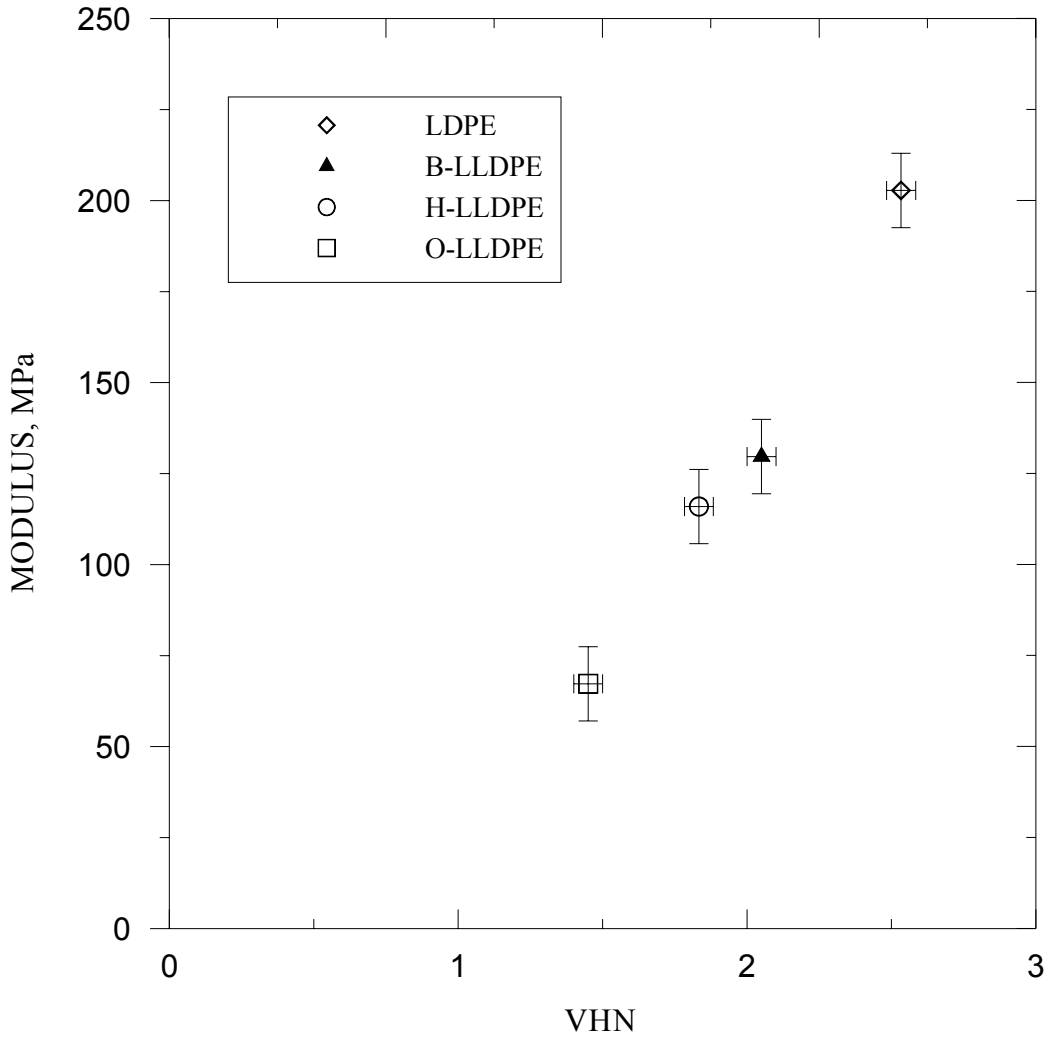

Figure 5.22: Variation of initial modulus with VHN for polymers

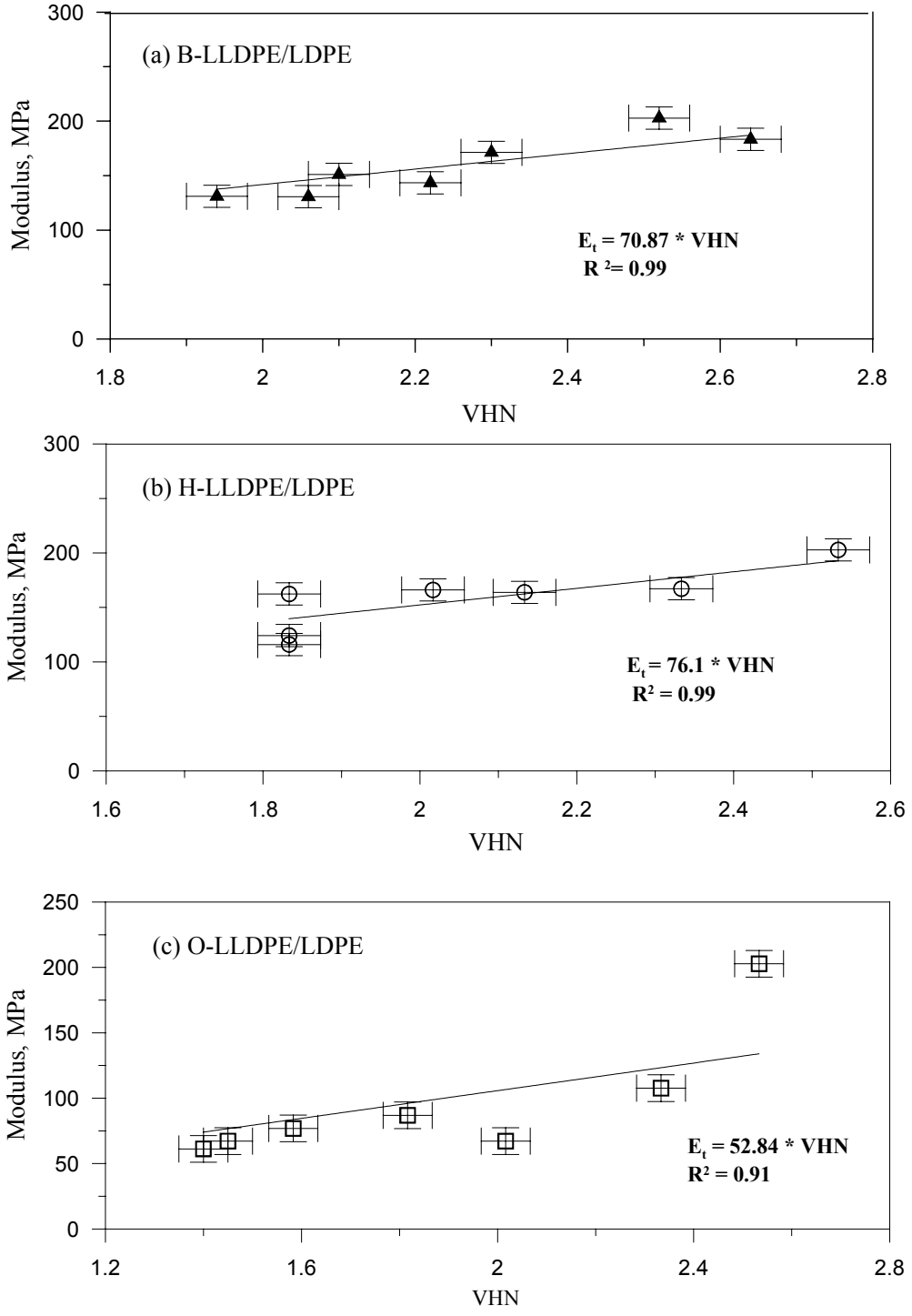

Figure 5.23: Correlation of initial modulus with VHN (a)B-type (b) H-type (c) O-type

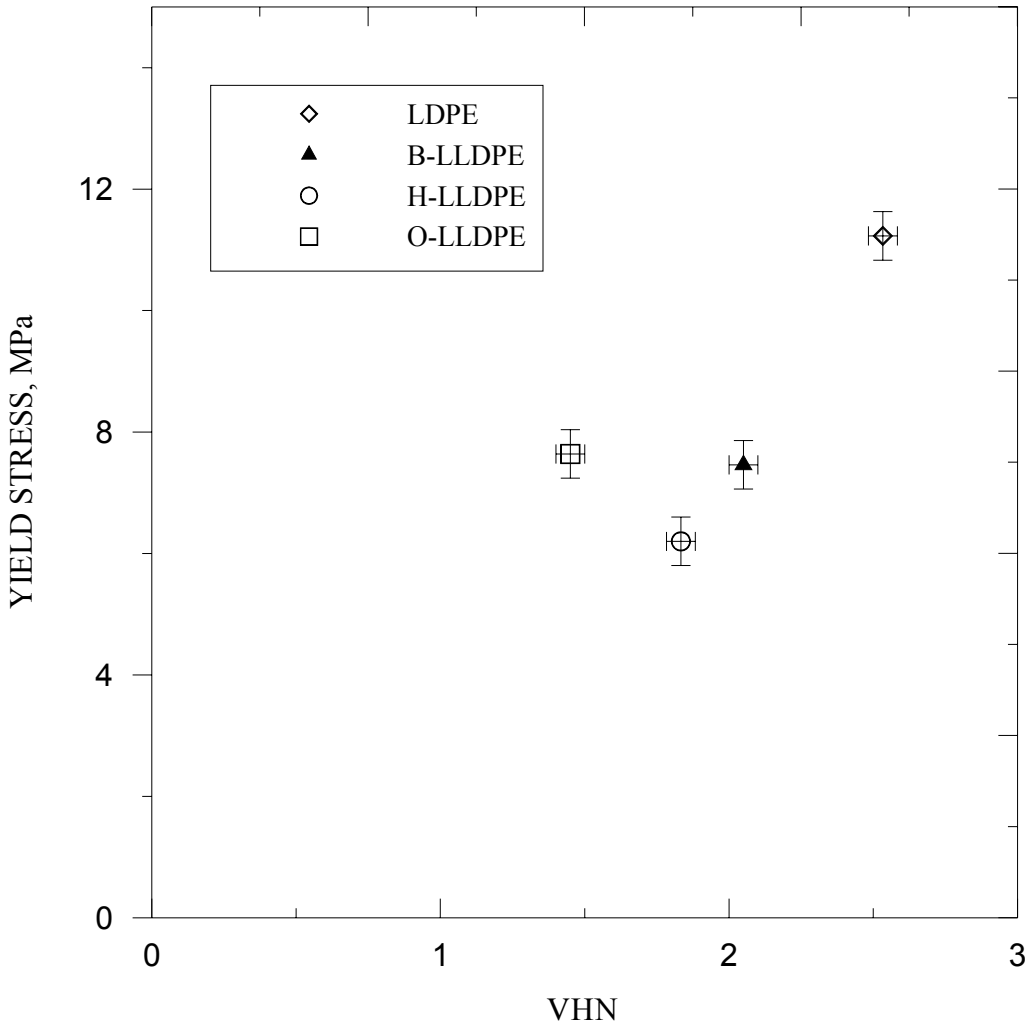

Figure 5.24: Variation of yield stress with VHN for polymers

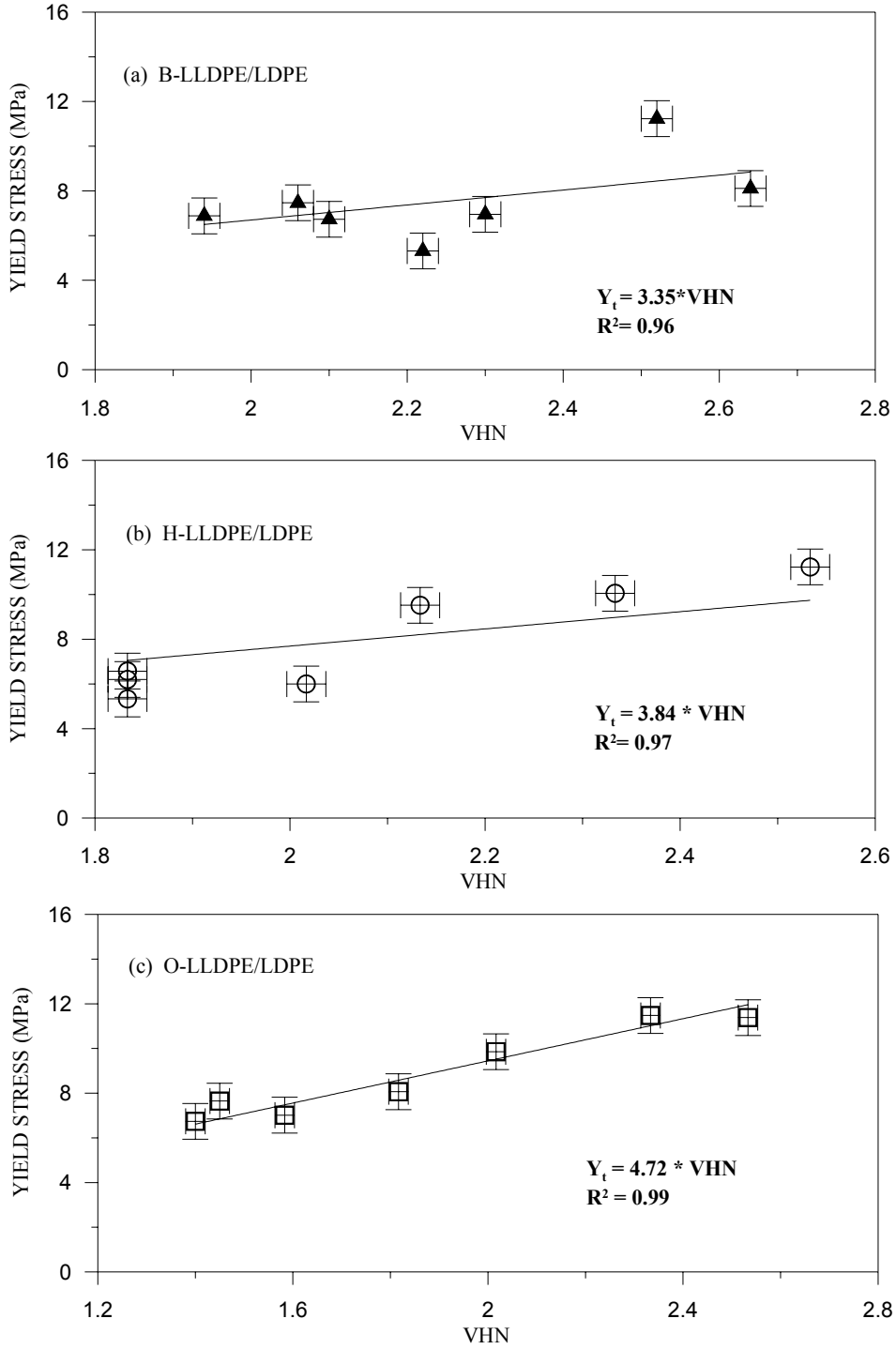

Figure 5.25: Variation of yield stress with VHN for all the blend systems (a) B-type (b) H-type (c) O-type

Correlation of yield stress with VHN for B-type blend system can be given as

$$Y = 3.35 * H_V \tag{5.5}$$

Similarly for H-type and O-type blend systems is given by

$$Y = 3.87 * H_v \tag{5.6}$$

$$Y = 4.72 * H_v \tag{5.7}$$

According to classical theory of plasticity, the expected indentation hardness value for a Vicker's indentor is approximately one-third the yield stress (Tabor's relationship). Equations 5.4 and 5.5 for B-type and H-type blend reveal that this relationship is well established. For O-type blend system, this relationship is not well established. This can be readily explained in the terms of crystallinity. It has already been established from the thermal analysis that O-type blends do have lower crystallinity values compared to other blend systems studied. However, systems of high crystallinity values will approximate to Tabor relationship that is evident from the above relationships.

5.5.4 Variation of VHN with Tensile Strength

The variation of tensile strength with VHN for the polymers is shown in Figure 5.26. Though LDPE has highest VHN, it displays lowest tensile strength on account of higher crystallinity. The variation of tensile strength values with VHN for all the blend systems is shown in the Figure 5.27. The tensile strength values decreases with VHN for all the blend systems.

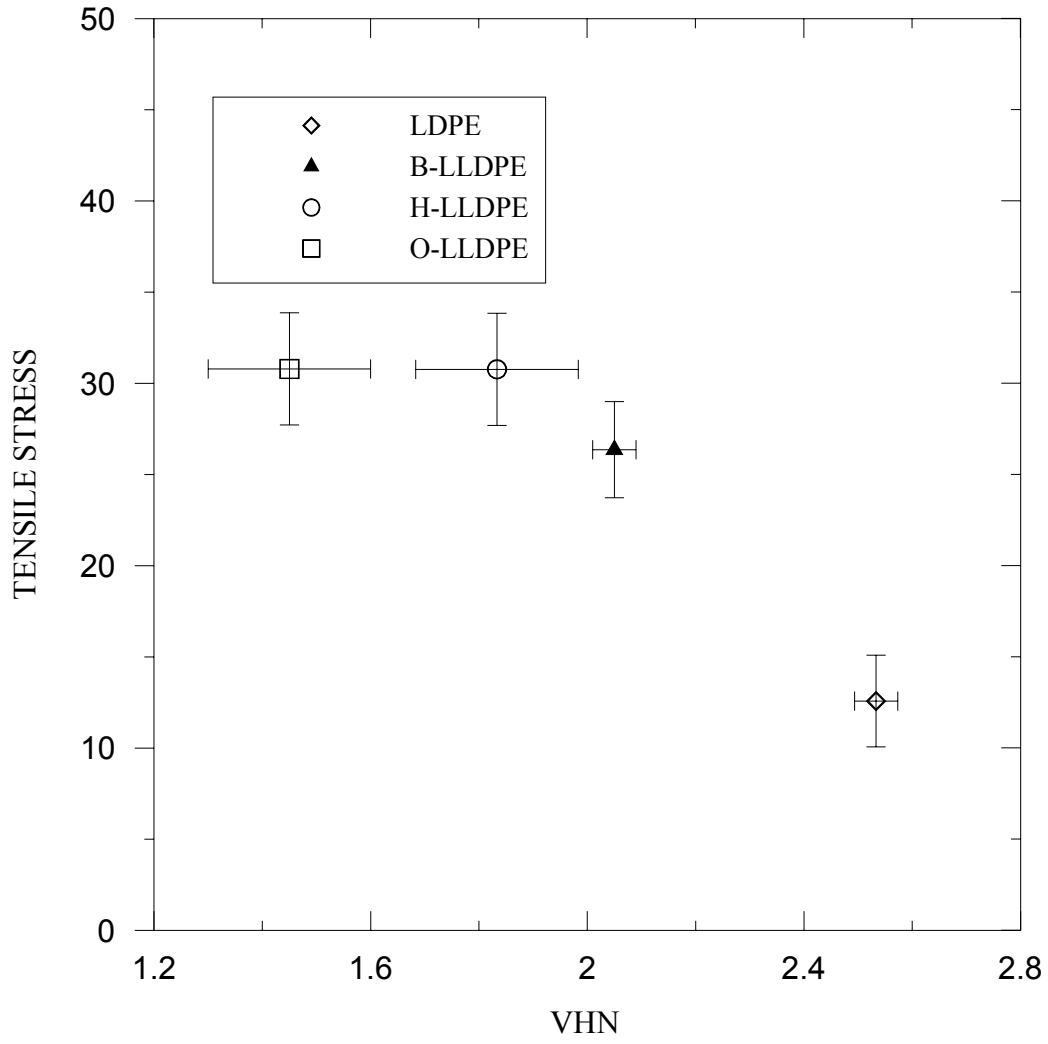

Figure 5.26: Variation of tensile strength versus VHN for polymers

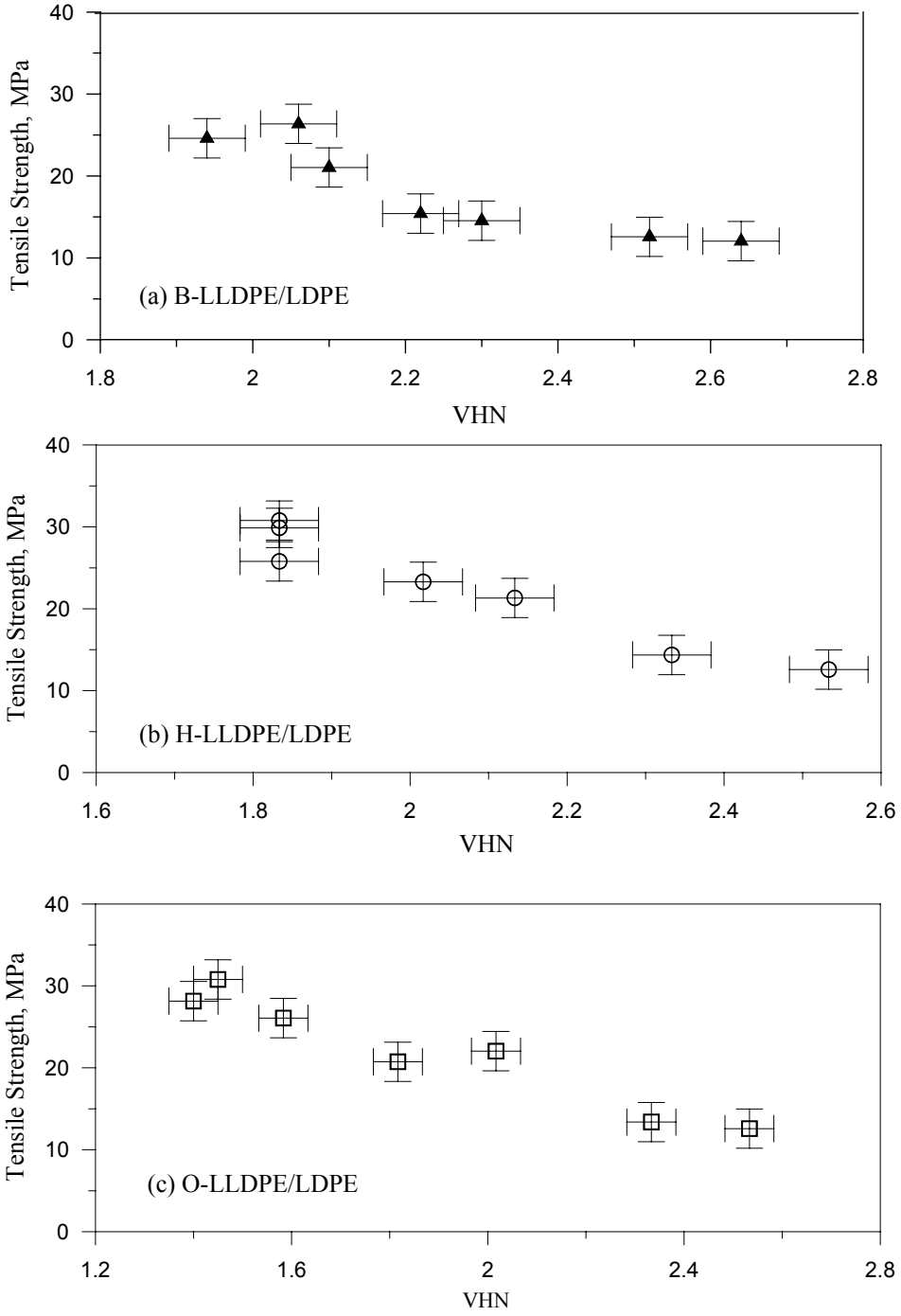

Figure 5.27: Variation of tensile strength versus VHN for all the blend systems (a) B-type (b) H-type (c) O-type

5.5.5 Variation of VHN with Strain at Break

The variation of tensile strength with VHN for the polymers is shown in Figure 5.28. Pure LDPE, which has highest VHN, has the lowest strain at break value. Pure m-LLDPE (B, H or O-type) has higher strain at break values on account of their lower crystallinity values. This reveals the importance of non-crystalline portions of the polymer. The variation of strain at break values with VHN for all the blend systems is shown in Figure 5.29. It is evident that the strain at break values decreased with increasing VHN for most of the blend ratios.

5.5.6 Effect of Indentation time

It is well known that most of the plastics exhibit visco-elastic behavior. Due to the creep effect, an increase in the dimensions of the impression with longer indentation time is observed and consequently a lower microhardness value is obtained. At different indentation times, hardness number is reported for pure LDPE and B-LLDPE (Figure 4.24).

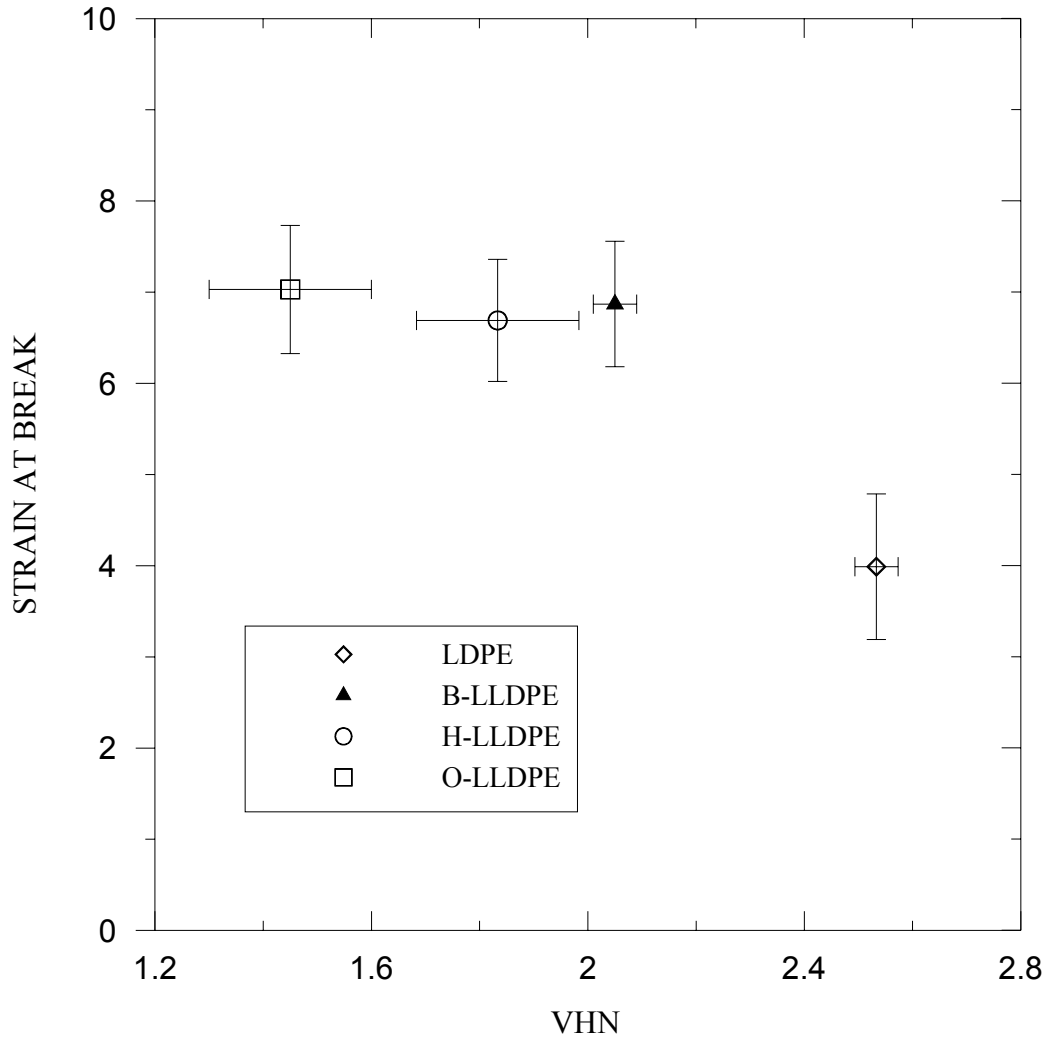

Figure 5.28: Variation of strain at break versus VHN for polymers

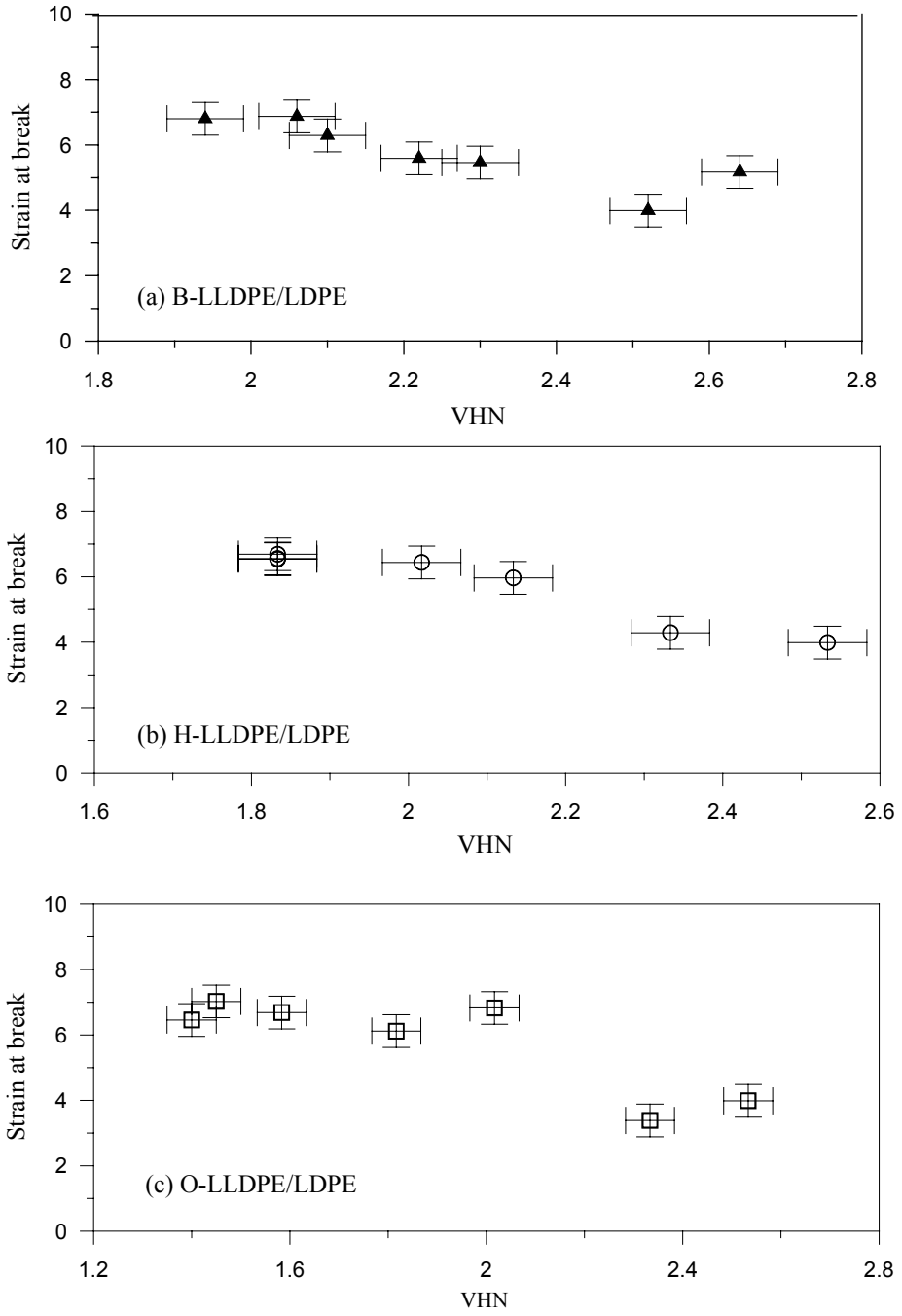

Figure 5.29: Variation of strain at break versus VHN for all the blend systems (a) B-type (b) H-type (c) O-type

CHAPTER 6

CONCLUSIONS AND RECOMMENDATIONS

6.1 CONCLUSIONS

In this work the effect of thermal history and the branch type of m-LLDPE on the thermal and mechanical properties of m-LLDPE/LDPE blends are investigated. Mechanical testing included both the tensile testing and microhardness testing of the prepared samples. Tensile tests were carried out at 125 mm/min at room temperature. Microhardness testing was carried out using Vickers hardness machine. Thermal analyses of the sample were carried out at a heating rate of 10°C/min.

For isothermal cooled samples, the occurrence of multi peaks in this DSC scan of pure H-LLDPE is attributed to the growth of different crystal populations from the melt. Pure LDPE and pure H-LLDPE had similar melting points indicating the growth of thicker lamellae microstructure. Though the branch content of H-LLDPE had lower branch content than LDPE, the similar melting temperature of former as that of latter is attributed to the existence of branch distributions in pure H-LLDPE. Pure O-LLDPE has lowest melting peak indicating the growth of thinner lamellar microstructure. For samples, the occurrence of high melting points for LDPE is attributed to the

growth of the thicker lamellar structure. DSC scans for B-LLDPE and O-LLDPE revealed similar behavior. The existence of two broad melting peaks in the case of pure H-LLDPE is most probably attributed to the bimodal distribution of the lamellae thickness. The diffuse nature of endset melting temperature of pure H-LLDPE also supported this observation.

All the studied polymer blends displayed ductile behavior accompanied with the neck formation at the yield point. Double yield points were evident in the Figure shown. The modulus of elasticity increased with the amount of crystallinity of pure polymers. At the molecular level, these results indicated the effect of branch content and the side chain length on the modulus of elasticity. An addition of small amount (10%) of LDPE to m-LLDPE results in a negligible effect on the modulus of elasticity, whereas; the addition of 10% m-LLDPE to LDPE results has a more pronounced effect. There are two competing factors that govern the molecular mobility and consequently the yield point. These factors are the branch size and the amount of crystallinity. It can be concluded that all the three blend systems studied showed better compatibility for tensile strength values. The addition of m-LLDPE to LDPE improves the strain at break values for all the blend systems. B-type blends showed a better compatibility than the other blend systems studied. The correlation of vicker's hardness numbers with yield strength values was found to follow Tabor's relationship for most of the blend systems. The correlation of Vickers hardness numbers with initial modulus values were found to follow a power law relation as discussed in the literature earlier.

6.2 RECOMMENDATIONS

Following are some of the recommendations for any future work to be carried out on m-LLDPE/LDPE blends.

- The effect of strain rate and temperature on the tensile properties of m-LLDPE/LDPE blends can be a useful extension to the present work. These results can be useful in predicting the mechanical behavior of the plastics at different working environments.

- The occurrence of double-yielding phenomenon for these blends needs further investigation.

- Wide-angle X-ray diffraction studies can be carried out for the samples to confirm the structure existing in the material.

- Microhardness testing of the samples at different indentations can be a useful contribution in understanding the elasto-plastic process.

- Useful correlations of Vickers hardness number with mechanical properties can be really productive for the practical applications such as the prediction of the service lifetime of prosthetic thermoplastics against a simulated human body environment.

- Impact testing of the m-LLDPE/LDPE blend samples can furnish useful information which can be really helpful in a successful design of PE pipe.

BIBLIOGRAPHY

1. Peacock AJ, Handbook of Polyethylene, Structures, Properties and Applications, Marcel Dekker Inc., New York. Basel.

2. Swallowe GM, "Mechanical Properties and Testing of Polymers: An A-Z Reference", Polymer Science and Technology, 1999.

3. Ward IM and Hadley DW, "An Introduction to the Mechanical properties of Solid Polymers", Wiley, Chichester, 1993.

4. Nielsen LE, "Mechanical Properties of Polymers", Van Nostrand Reinhod Co., New York, Cincinnati, London, Melbourne.

5. Arridge, "Mechanics of Polymers", Clarendon Press, Oxford.

6. Seymour RB and Charles EC, "Structure-Property Relationships in Polymers", Plenum Press, New York and London, 1984

7. Young RJ, "Introduction to Polymers", Chapman and Hill, London, New York, 1980.

8. Lue, Ching T, "Easy processing metallocene polyethylene", Journal of Plastic Film and Sheeting, vol 15, No 2, 1999, pp 131-139.

9. Chen F; Shanks R; Amarasinghe G, "Miscibility behavior of metallocene polyethylene blends", Journal of Applied Polymer Science, Vol 81, No 9, pp 2227-2236.

10. Junting Xu, Xurong Xu, Feng L, "Short chain branching distributions of metallocene based ethylene copolymers", European Polymer Journal, 1999, pp 685-693.

11. Hussein M, Davies GR, and Ward IM, "Preparation of ultra high modulus materials from metallocene based linear polyethylenes", Polymer, Vol 42, 2001, pp 3679-3686.

12. Beagan and Malleja C, "The extrusion, performance and characterization of metallocene-catalyzed polyethylene based packaging films", DAI-C 61/104, Winter 2000, p.1091.

13. Sierra, Juan D; Noriega P, Maria; Osswald, Tim A, " Effect of metallocene polyethylene on heat sealing properties of low-density polyethylene blends", Journal of Plastic film and Sheeting, 2000, Vol 16, No 1, pp 33-42.

14. Salazar JM and Calleja B, “Mechanical model on polyethylene blends as revealed by microhardness”, Journal of Material science letters, Vol 4, 1985, pp 324-326.

15. Flores A, Calleja B and Bassett DC, “Microhardness studies of chain-extended PE: I. Correlations to Microstructure”, Journal of Polymer Science: Part B: Polymer Physics, Vol 337, pp 3151-3158 (1999).

16. Rueda DR and Calleja B, “Study of blends based on recycled polyethylene wastes. Part I. Variation of mechanical properties with composition”, Journal of Materials science, Vol 29, pp 1109-1114(1994).

17. Zamfirova and Dimitrova A, “Some methodological contributions to the Vickers microhardness technique”, Polymer Testing, Vol 19, pp 533-542 (2000).

18. Calleja FJ, Santa Cruz, Bayer RK and Kilian HG, “Microhardness and surface free energy in linear polyethylene: The role of entanglements”, Colloid and Polymer Science, Vol 268, pp 440-446(1990).

19. Lopez J, “Microhardness Testing of Plastics: Literature Review”, Polymer Testing, Vol 12, pp 437-458(1993).

20. Fakirov S, Krumova M and Rueda DT, “Microhardness model studies on branched polyethylene”, Polymer, Vol 41, pp 3047-3056(2000).

21. Hartman B, Gilbert FL, and Richard FC, “Tensile yield in Polyethylene”, Polymer Engineering and Science, Vol 26, 1986, pp 554-559.

22. Shishesaz MR and Donatelli AA, “Tensile Properties of Polyethylene Blends”, Polymer Engineering and Science, Vol 21, No 13, pp 869-872(1981).

23. Seguela R and Reistch F, “Double-yield point in polyethylene under tensile loading”, J. Materials Science letters, Vol 9, pp 46-47 (1990).

24. Balsamo V and Muller AJ, “The phenomenon of double-yielding under tension in low-density polyethylene and their blends”, Journal of Materials science letters, Vol.12, pp 1457-1459(1993).

25. Yamada K and Takayanagi M, “Superstructural Description of Deformation Process in Uniaxial Extension of Preoriented Isotactic Polypropylene”, Journal of Applied Polymer Science, Vol 24, pp 781-799 (1979).

26. Lucas JC, Failla MD, Smith FL, Mandelkern L and Peacock AJ, “The Double Yield in the Tensile Deformation of the Polyethylenes”, Polymer Engineering and Science, Vol 35, No13, pp 1117-1123 (1995).

27. Muramatsu S, Lando JB, “Double yield points in Poly(tetramethylene terephthalate) and its copolymers under tensile loading”, Polymer Engineering and Science, Vol 35, No13, pp 1077-1085 (1995).

28. Plaza AR, Ramos E, Manzur A, Olayo T, and Escobar A, "Double-yield points in triblends of LDPE, LLDPE and EPDM", Journal of Materials science, Vol 32, pp 549-554(1997).

29. Seguela R and Darras O., "Phenomenological aspects of the double-yield of polyethylene and related copolymers under tensile loading", Journal of Materials science, Vol 29, pp 5342-5352(1994).

30. Rajendra K; Lamborn J, "Tensile properties of linear low-density polyethylene (LLDPE) blown films", Polymer Engineering and Science, Vol 40, No 11, 2000, pp 2385-2396.

31. Jafari S, Rana, Surya K., "Tensile fracture morphology/properties correlation of high-density/linear low-density polyethylene blends", Iranian Polymer journal, Vol 9, No 3, 2000, pp 133-142.

32. Cho K; Lee BH; Hwang K; Lee H; Soonja C, "Rheological and mechanical properties in PE blends", Polymer Engineering and Science, Vol 38, No 12, 1998, pp 1969-1975.

33. Muller AJ, Balsamo V and Rosales CM, "On the miscibility and mechanical Compatibility of Low density and Linear low density polyethylene blends", Polymer Networks and Blends, Vol 2, No 4, pp 215-223(1992).

34. La Mantia FP and Acierno D, "Mechanical properties of blends of low density with linear low-density polyethylene", European Polymer Journal, Vol 21, No 9, pp 811-813(1985).

35. Mantia FP, Valenza A and Acierno D, "Influence of the structure of linear density polyethylene on the rheological and mechanical properties of blends with low density polyethylene", European Polymer Journal, Vol 22, No 8, pp 647-652(1986).

36. Yamaguchi M, Shigehiko A, "LLDPE/LDPE Blends .I. Rheological, Thermal and Mechanical Properties", Journal of Applied Polymer Science, Vol 74, pp 3153-3159(1999).

37. Liu Y, and Truss R, "Tensile yielding and microstructures of blends of isotactic polypropylene and LLDPE", Journal of Polymer Physics: part B, Vol 33, 1995, pp 813-822.

38. Wilkes GL, Jordens K, Janzen J, Rohlfing DC, Welch MB, "The influence of molecular weight and thermal history on the thermal, rheological, and mechanical properties of metallocene catalysed linear polythylenes", Polymer, Vol 41, pp 7175-7192.

39. Tanem BS and Stori A, "Blends of single-site linear and branched polyethylene. I. Thermal characterization", Polymer, Vol 42, pp 5389-5399(2001).

40. Lee, Sang-Won; Kim, Jang-Yup; Hyun, Uk; Huh, Wansoo, "Crystallisation behavior and mechanical properties of low-density polyethylene and metallocene linear low-density polyethylene blend", American Chemical Society, Polymer preprints, Division of Polymer chemistry, Vol 40, No 2, 1999, pp 776-777.

41. Popli R, and Mandelkern L, "Influence of Structural and Morphological Factors on the Mechanical Properties of the Polyethylenes", J.Polym.Sci. Part B: Polym.Phys, Vol 25, pp 441-483(1987).

42. Kennedy MA, Peacock AJ and Mandelkern L, "Tensile Properties of Crystalline Polymers: Linear Polyethylene", Macromolecules, Vol 27, pp 5297-5310 (1994).

43. Alizadeh A, Escalona M, Lafuente P, Ramos G, Salazar JM, "Structure and melting of blends of linear and branched polyethyenes crystallized at high under cooling", Polymer, Vol 38, No 5, 1997, pp 1207-1214.

44. Morgan, RL; Hill, MJ; Barham, PJ; Kip, BJ, "Study of the phase behavior of PE blend using micro-Raman imaging", Polymer, Vol 42, No 5, 2001, pp 2121-2135.

45. Kristiansen PE; Hansen EW; Pedersen B, "Isothermal crystallization of PE by in situ NMR and analyzed within the Avrami' model framework", Polymer, Vol 42, No 5, 2001, pp 1969-1980.

46. Morgan RL; Hill, MJ; Barham, "Morphology, melting behavior and co-crystallisation in PE blends: the effect of cooling rate on two homogenously mixed blends", Polymer, Vol 40, No 2, 1999, pp 337-348.

47. Popli R, and Mandelkern L, "The transition in Ethylene copolymers: The β-transition", Polymer Bulletin, Vol9, pp 260-267 (1983).

48. Junting Xu; Xurong Xu; Chen L, "Effect of composition distribution on miscibility and co-crystallisation phenomena in the blends of LDPE with conventional and metallocene-based ethylene-butene copolymers", Polymer, Vol 42, No 8, 2001, pp 3867-3874.

49. Weignall GD.; Londono JD; Lin, JS, "Morphology of blends of linear and long chain branched polyethylenes in the solid state: a study by SANS, SAXS and DSC", Macromolecules, Vol 28, NO 9, 1995, pp 3156-3167.

50. Drummond, Kate M.; Hopewell, Jefferson l.; Shanks, Robert A., "Crystallisation of LDPE and LLDPE rich blends", Journal of Applied Polymer Science, Vol 78, No 5, 2000, pp 1009-1016.

51. Gupta AK, Rana SK and Deopura BL, "Crystallization behavior of HDPE/LLDPE blend", Journal of Applied Polymer Science, Vol 44, 1992, pp 719-726.

52. Utracki, Abdellah LA, “Compatibilisation of polymer blends”, Progress in Rubber and Plastics Technology, Vol 33, No 3, 1997, pp 153-188.

53. Stein K, Shi RH and Richard S, “Characterization and properties of PE blends”, Journal of polymer science part B: polymer physics, Vol 25, 1987, pp 89-103.

54. Prasad A, “Quantitative analysis of LDPE and LLDPE blends by DSC and Fourier transform infrared spectroscopy methods”, Polymer Engineering and Science, Vol 38, No 10, 1998, pp 1716-1728.

55. Datta NK, Birley AW, “Thermal Analysis of Polyethylene Blends”, Plastics and Rubber Processing and Applications, Vol.2, 237-245(1982).

56. Lee HS, and Denn MM, “Blends of linear and branched polyethylenes”, Polymer Engineering and Science, Vol 40, 2000, 1132-1142.

57. Rosario, Perena JM, Antonio B, and Perez E., “Influence of chemical composition distribution and thermal history on the mechanical properties and viscoelastic relaxations of ethylene-1-butene copolymers”, J. Mat. Science letters, Vol 25, pp 4162-4168 (1990).

58. Rana D, Cho K, Woo T, Lee BH and Choe S., “Blends of Ethylene 1-otene copolymer synthesized by Ziegler-Natta and Metallocene catalysts. I. Thermal and Mechanical Properties”, Journal of Applied Polymer Science, Vol 74, pp 1169-1177(1999).

59. Starck P, and Lofgren B, “Thermal Properties of ethylene/long chain α-olefin copolymers produced by metallocenes”, European Polymer Journal, Vol 38, pp 97-107(2002).

60. Mezghani K, Campbell RA, Phillips PJ, “Lamellar thickening and the equilibrium melting point of polypropylene”, Macromolecules, Vol 27, pp 997-1002(1994).

61. ASTM Handbook for Plastics, Vol. 8.01.

VITA

NAME: Mohammad Faheem

PLACE OF BIRTH: Warangal, INDIA.

ADDRESS: H No.5-2-28, Kothur Street,
Hanamkonda,
Warangal (AP) -506001,
INDIA.

E-MAIL: faheem567@yahoo.com
mohammadfaheem@hotmail.com

EDUCATIONAL QUALIFICATION:

M.S ***(Mechanical Engineering)***
June 2003
King Fahd University of Petroleum and Minerals
Dhahran, Saudi Arabia.

B.E ***(Mechanical Engineering)***
May 1999
Osmania University
Hyderabad, India.